In the IOCCG Report Series:

Reports and Monographs of the International Ocean-Colour Coordinating Group

An Affiliated Program of the Scientific Committee on Oceanic Research (SCOR)
An Associated Member of the (CEOS)

IOCCG Report Number 12, 2012

Ocean-Colour Observations from a Geostationary Orbit

Edited by:
David Antoine, Laboratoire d'Océanographie de Villefranche (LOV-CNRS),
Villefranche-sur-mer, France)

Report of an IOCCG working group on Ocean-Colour Observations from a Geo-
stationary Orbit, chaired by David Antoine, and based on contributions from (in
alphabetical order):

Yu-Hwan Ahn	Korea Institute of Ocean Science and Technology (KIOST)
David Antoine	Laboratoire d'Océanographie de Villefranche, France
Jean-Loup Bézy	ESA/ESTEC, The Netherlands
Prakash Chauhan	Indian Space Research Organisation (ISRO), India
Curtiss Davis	Oregon State University (OSU), USA
Paul DiGiacomo	National Oceanic and Atmospheric Administration, USA
Xianqiang He	State Key Lab of Satellite Ocean Environment Dynamics, China
Joji Ishizaka	Nagoya University, Japan
Hiroshi Kobayashi	University of Yamanashi, Japan
Anne Lifermann	Centre National d'Etudes Spatiales (CNES), France
Antonio Mannino	National Aeronautics and Space Administration (NASA), USA
Constant Mazeran	ACRI-ST, Sophia Antipolis, France
Kevin Ruddick	Management Unit of the North Sea Mathematical Models (MUMM), Belgium

Correct citation for this publication:

IOCCG (2012). Ocean-Colour Observations from a Geostationary Orbit. Antoine, D. (ed.), Reports of the International Ocean-Colour Coordinating Group, No. 12, IOCCG, Dartmouth, Canada.

The International Ocean-Colour Coordinating Group (IOCCG) is an international group of experts in the field of satellite ocean colour, acting as a liaison and communication channel between users, managers and agencies in the ocean-colour arena.

The IOCCG is sponsored by the Canadian Space Agency (CSA), Centre National d'Etudes Spatiales (CNES, France), Department of Fisheries and Oceans (Bedford Institute of Oceanography, Canada), European Space Agency (ESA), Helmholtz Center Geesthacht (Germany), National Institute for Space Research (INPE, Brazil), Indian Space Research Organisation (ISRO), Japan Aerospace Exploration Agency (JAXA), Joint Research Centre (JRC, EC), Korea Institute of Ocean Science and Technology (KIOST), National Aeronautics and Space Administration (NASA, USA), National Centre for Earth Observation (NCEO, UK), National Oceanic and Atmospheric Administration (NOAA, USA), and Second Institute of Oceanography (SIO), China.

http: //www.ioccg.org

Contents

Preface

In every decade since the 1960s satellite Earth remote sensing has achieved a major breakthrough. As far as ocean observations are concerned, major advances were the launch of the SEASAT mission in 1978, which was the first Earth-orbiting satellite designed for remote sensing of the Earth's oceans (Allan, 1983), the Nimbus-7/CZCS ocean-colour mission in 1978 (Clarke et al., 1970; Hovis et al., 1980), and the GeoSat altimetry mission in 1985 (Sandwell and Smith, 1997). The CZCS sensor totally renewed oceanographers' view of the functioning of the global ocean, by providing unprecedented observations of the ocean biomass (phytoplankton) at global and synoptic scales. Another major step was the launch of the SeaWiFS instrument in 1997 (Hooker et al., 1992), followed by the MODIS-Aqua (Salomonson et al., 1989) and MERIS (Rast and Bézy, 1995; Rast et al., 1999) instruments in 2002. These missions provide more systematic and accurate observations, and fostered new science and operational applications. Ocean-colour remote sensing now provides observations from which several tens of parameters of geophysical interest can be derived on a near-operational basis. The exponential increase in the use of ocean-colour data in peer-reviewed scientific journals as well as in operational services demonstrates the very high potential of this technique. Scientific and operational uses and societal benefits of ocean colour are numerous (see IOCCG Report 7, 2008).

It is believed that another dimension will be brought to ocean remote sensing, in particular remote sensing of ocean colour, with the launch of sensors on satellites operating in geostationary or geosynchronous orbits (hereafter referred to as "GEO observations"). Today, the question is no longer whether or not this is feasible, but rather, when it will become a reality. The preliminary results using SEVIRI on Meteosat Second Generation for mapping of total suspended matter (Neukermans et al., 2009) and early data from the South Korean Geostationary Ocean Colour Imager (GOCI) are encouraging. Elements that will make such missions a success are mature and can now be combined to design innovative mission concepts for the coming decade that will allow major advances for space oceanography. These missions have the capability to image the entire Earth disk from a geostationary position, providing multi-spectral ocean-colour observations with a high revisit frequency over the open ocean and coastal zones. They can also focus on more limited areas at higher spatial resolution (for example, the GOCI mission).

One of the major physical forcings, and the most obvious environmental signal, is the diel cycle of solar irradiance. This cycle is known to affect many physical and biogeochemical processes, the latter being observable through ocean-colour

remote sensing. This fundamental cycle is, however, inaccessible to present and planned satellite ocean-colour missions which sample once per day near noontime, at most. Technological advances now also allow sampling of the ocean *in situ* at high frequency, and this new data has revealed the transient nature of many phenomena. Again, with the exception of GOCI, none of the present and planned ocean-colour missions provide a revisit frequency adapted to sample rapidly changing environments such as the coastal areas.

Ocean-colour sensors on a geostationary orbit overcome these limitations. The sampling strategy that can be designed from such observations would allow a breakthrough in ocean sciences thanks to high-frequency repeated observations of ocean colour in coastal zones and the open ocean. Observations could be taken from about 30 minutes to 1 hour at a nadir resolution close to that of current low-Earth orbiting sensors (a few hundred meters) over the entire Earth's oceanic and coastal areas as seen from the GEO orbit (including the coastal land fringe).

The science domains that would benefit from GEO ocean-colour observations include the study of the diurnal variability of optical and biogeochemical properties of the ocean, the use of this diel variability to determine community particle production, the study of coupling at meso and sub-meso scales between physics and biology and the consequences on primary production and carbon fluxes, data assimilation into coupled ocean physical-ecosystem models, the study of dynamics of coastal ocean ecosystems and habitats, quantification of sediment and carbon transport and fluxes from land to ocean, and the study of aerosol transport from land to sea, including dust or volcanic aerosols. These observations would provide critical information to address many of the challenges identified by the oceanographic community.

The geophysical parameters of interest are the multi-spectral marine reflectances from the visible to the near-infrared, from which a variety of biogeophysical products can be derived, such as the chlorophyll concentration, the total suspended matters, the inherent optical properties that are proxies of the particle load and type, phytoplankton functional groups that determine the functioning of the ecosystem, phytoplankton fluorescence that reflects biomass and physiological status together, net primary production that partly sinks to the deep ocean (the "biological pump"), and aerosol loads and types (as by-products of the atmospheric correction of the top of atmosphere observations). Therefore, GEO ocean-colour observations by themselves can provide a large variety of products and applications that would contribute substantially towards the development of an "Earth system science approach", where the many compartments of the Earth's functioning are jointly investigated. Such missions also contribute complementarily to the international efforts in producing global and comprehensive status reports of our Planet, and in producing a number of essential climate variables that will eventually be incorporated into long-term, climate-quality data records.

In addition to these foreseen advantages of GEO observations, this new way of

observing the oceans is likely to generate unforeseen discoveries or entirely new ways of processing ocean-colour data. Just as the Coastal Zone Colour Scanner provided crucial first estimates of primary production for the world's oceans, far surpassing its planned one-year mission and coastal zone focus, geostationary ocean colour is likely to provide information on unimagined new processes. Similarly the processing of ocean-colour data is currently performed on pixels independently. With geostationary ocean-colour data it becomes possible to use very recent (e.g., hourly) information on target parameters such as chlorophyll-a concentration or auxiliary parameters such as aerosol type, in the data processing to either constrain retrieval algorithms or provide extra quality control. The paradigm of pixel-by-pixel processing may be significantly reconsidered.

Beyond the cutting-edge science that GEO ocean-colour observations will foster, data required to further develop user-driven applications and operational monitoring of coastal areas will also be delivered. Marine services in the coastal zones (e.g., the European GMES (Global Monitoring for Environment and Security) program) will expand rapidly when high-frequency observations become available, whereas they now have difficulty to respond appropriately to societal demands because of the relatively low temporal frequency of data available from today's low-Earth orbiting satellite missions.

Chapter 1

Introduction

The ocean is the largest ecosystem on Earth, and it contributes roughly half of the planetary net primary production (Field et al., 1998). This "biological pump" fuels the oceanic food web and affects CO_2 fixation, thereby playing a global role in climate and other issues relevant to international protocols as expressed by the International Geosphere-Biosphere Programme (IGBP) and the Global Ocean Observing System (GOOS). Global-ocean maps of phytoplankton pigment concentration are now generated routinely at a frequency of ~1 to 2 days from remotely-sensed ocean-colour radiometry (OCR). Phytoplankton biomass concentration and distribution is of interest for describing and understanding the changes in the oceanic biota at any time scale of interest, from weeks to decades (e.g., Behrenfeld et al., 2006). The longer the time scale, the better to resolve longer-term effects. The user community also evolves concomitantly with the time scale of interest, from fisheries (e.g., near real-time survey, 2-3 days), to local authorities (days to months), and to research organizations focused on biogeochemical cycles, as well as international councils on climate change (years to decades).

The ocean includes coastal zones which form critical environments for marine resources. Because of the population density inhabiting coastal areas, and numerous resources exploited in coastal waters, the impact of human activity upon these coastal ecosystems is particularly important. A comprehensive observational system has to be developed to understand the role, the mechanisms and response of the entire ocean at both the global and local scales. Indeed, the observational requirements, driven by the nature of the phenomena under study, lead to the requirement for covering a broad range of spatial and temporal scales. Satellite remote sensing of the oceans therefore has to tackle major challenges in the coming decades.

A first mandate is to build decade-long consistent time-series of parameters derived from space observations, for example OCR, altimetry or sea surface temperature (SST). Such long-term records, which are now referred to as "climate quality data records" (McClain et al., 2004), are needed to identify possible trends in key oceanic parameters, and to understand whether or not they are due to regional or global environmental changes of oceanic physical, chemical or biological processes. This can be called the "continuity challenge". The second challenge is the "knowledge challenge", which refers to the need for improved interpretation of the radiometric

signals collected from the top of the atmosphere. Practically, this relates to the development of advanced sensors, observing platforms and algorithms, allowing for the derivation of new parameters, and the creation of new applications, thus increasing our knowledge of the ocean.

The monitoring of coastal environments is a third challenge. These complex environments are under increasing stress, and the development of observing systems allowing early warning, impact assessment and reaction in the event of unexpected crises is another priority. These three aspects are relevant to the specific problem of ocean colour, which is the focus of the present report. It is also clear that diverging requirements are expected from these three focus areas of remote sensing data utilisation.

Global missions dealing with Case-1 open ocean waters require planetary coverage ideally within less than 2 days, which can be obtained from sun-synchronous low-Earth orbit (LEO) sensors operating with a wide swath (or several moderately wide swaths). With such a swath, a moderate ground resolution has to be accepted, and in effect, is fully acceptable for global studies. Along this line, defined in the IOCCG Report No. 1 (IOCCG, 1998), a reduced number of spectral channels (e.g., 7-8) can fulfil the requirements for an accurate atmospheric correction, and for a retrieval of phytoplankton abundance and distribution as accurately as allowed by current state-of-the-art algorithms. In contrast to Case-1 open ocean waters, coastal zone monitoring requires a dedicated, oriented coverage rather than a global coverage. High spatial (~0.5 km or less) resolution is needed. The optical complexity of coastal Case-2 waters entails more spectral channels and band combinations than needed when studying oceanic Case-1 waters (IOCCG, 2000). Over and above these spatial and spectral characteristics, the repetition rate of observations is another critical aspect. A high frequency rate is required for observing specific, and often transitory, events occurring in coastal zones (ideally < 1 day), which is currently lacking and out of reach using single LEO satellites. Many user communities are disappointed by the insufficient revisit capability of current LEO ocean-colour senors. For instance, this is the case for coastal zone monitoring in cloudy regions or data assimilation in operational ocean forecast models.

The situation can be improved by observing the Earth from the geostationary orbit, thus providing high revisit capabilities, and a chance to remedy the chronic under-sampling of the ocean. In combination with existing and planned LEO satellite missions, this would ensure, simultaneously, a permanent assessment of ocean colour at the global scale and will lead to a new range of scientific questions to be addressed and new applications to be developed, in particular for coastal zones. The advantages of a geostationary orbit for ocean-colour studies include a better temporal coverage, the possibility of following episodic events at the scale of hours (e.g., red tides, sediment transport), and the improvement of the match between the temporal scale of satellite observations and those of models. Other potential applications include examining the daily cycle of ocean properties, reducing the

effects of clouds from ocean-colour measurements, and improving observations of planetary waves. Finally, data processing for individual pixels may benefit from knowledge of marine or atmospheric parameters estimated from data acquired in the previously acquired image, now only tens of minutes away.

The advantages are, therefore, manifold; technical difficulties are numerous as well. Within this context, several space agencies have displayed a high level of interest in ocean-colour observations from a geostationary platform. CNES (France) currently performs R&D activities in this domain, ISRO (India) has plans for a High Resolution GEO Imager (HR-GEO), ESA (Europe) is in the early design phases of a high-resolution GEO mission (Geo-Oculus), NASA (USA) is in pre-phase formulation for a geostationary mission (GEO-CAPE), and KIOST/KARI (Korea) has started to develop GOCI-II, which is scheduled for launch in 2018 following the successful launch campaign and in-orbit tests of their Geostationary Ocean Colour Imager (GOCI) aboard the COMS-1 satellite in 2010. This list is surely not exhaustive. The role of IOCCG is to intervene at the inception of such parallel, sometimes diverging, projects, to advocate for collaboration and standardisation, which should eventually benefit the different user communities (science and operations). The IOCCG working group on "Ocean-Colour Observations from a Geostationary Orbit" was formed to review science questions that can be addressed via ocean-colour observations from a geostationary orbit, to prepare an inventory of the most significant proposed projects and existing GEO ocean-colour missions, to examine the complementarity of LEO and GEO orbits, and to list requirements. The working group was also mandated to promote inter-agency cooperation and help coordinate activities.

The Case for Ocean-Colour Observations from a Geostationary Orbit: Science Focus and Examples of Applications

2.1 High Spatio-Temporal Observations for Understanding Coastal Ocean Processes

Environmental agencies, either at the federal, state or regional levels, are responsible for management of fisheries, monitoring water quality, protection of marine sanctuaries and marine mammal habitats, assessing the effects of storm events and other issues related to the use and protection of the coastal ocean. Each of these management responsibilities requires an improved understanding of coastal ocean dynamics. Considerable progress has been made in our ability to monitor ocean colour and temperature in the open ocean using polar-orbiting satellites. Current and past ocean-colour sensors (e.g., ESA's MERIS, NASA's SeaWiFS and MODIS instruments, VIIRS on Suomi NPP and ISRO's OCM-2 sensor on Oceansat-2) as well as future missions (e.g., OLCI on Sentinel-3), are well suited for sampling the open ocean. However, coastal environments are spatially and optically more complex and require more frequent sampling and higher spatial resolution sensors with additional spectral channels. Coastal waters are highly dynamic. Tides, diurnal winds, river runoff, upwelling and storm winds drive currents from one to several knots.

The present once-a-day coverage from polar-orbiting satellites, which is further limited by cloud cover, is not sufficient to sample the dynamics of the coastal ocean. A geostationary imager would substantially improve our ability to obtain usable imagery several times a day to resolve, for example, the effects of tides and wind events on coastal currents, and to understand changes in coastal water features that occur over a daily cycle. A geostationary ocean-colour imager with the proper spatial and spectral sampling characteristics is ideal for sampling the coastal ocean. This capability will greatly improve our ability to manage coastal resources just as GOES imagery has improved our ability to monitor and forecast the weather. Compared to the polar orbiting ocean-colour sensors, a geostationary ocean-colour imager will have significantly improved temporal sampling, and may have improved spatial and spectral sampling that will greatly enhance our ability to monitor and assess the

dynamics of the coastal ocean. The following sections discuss the advantages of these key improvements.

2.1.1 Sediment transport

Monitoring and understanding the sediment dynamics and suspended sediment transport is an important issue related to coastal engineering and other coastal activities. A study of the transport mechanism of suspended sediments in a marine environment is essential not only for the safeguard of marine installations or navigational channels but also for assessing pollutants and other biological activities in the coastal zone. River inputs to the coastal ocean also play a key role in the carbon cycle. On a global scale, about half the organic matter buried in marine sediments could be of terrestrial origin, delivered by rivers. The monitoring of coastal zones at the margin of big rivers is necessary to confirm these assumptions. In contrast to Case-1 open ocean waters, coastal zone monitoring requires a dedicated region-oriented coverage rather than a global coverage, with high spatial and temporal resolution. Apart from high spatial resolution, monitoring coastal waters requires more spectral information than is required for Case-1 open ocean waters. On top of these spatial and spectral characteristics, repetition of the observations to monitor the changes is of paramount importance here. Two examples are provided in Boxes 1 and 2.

2.1.2 Monitoring of harmful algal blooms

Harmful algal blooms (HABs) are important phenomena in coastal environments and can be monitored by ocean-colour remote sensing. The formation of such massive phytoplankton blooms imparts a change in the colour of the ocean that can be detected by ocean-colour satellite sensors. These blooms are often caused by artificial or natural eutrophication. Harmful algal blooms, sometimes called red tide events, produce toxic compounds and/or anoxic conditions and frequently damage the ecosystem as well as human activities, such as aquaculture. Many HAB species are flagellates, which are known to migrate vertically within the water column, congregating at the surface near noon. High frequency ocean-colour observations from GEO may provide a means to detect the vertical migration of such flagellates. It would be very useful to detect the vertical migration, not only to predict the movement but also to discern the potentially harmful organisms. At the management level, prevention and/or mitigation of the impact of red tides and other HABs requires high frequency observations to monitor coastal conditions that may become favourable for the growth of HABs, to detect the presence of these organisms and to predict their movement. GEO sensors can provide the necessary monitoring capabilities during daytime.

Box 1: Suspended Sediment Dispersal and Tides in the Coastal Zone

The Indian Space Research Organisation (ISRO) launched Oceansat-1 OCM sensor in 1999 and algorithms were developed for atmospheric correction and the estimation of chlorophyll-a and total suspended mater (TSM) (Chauhan et al., 2002). OCM data has been used extensively for suspended sediment monitoring in various coastal regions of the Indian coast. Rajawat et al. (2005) have demonstrated many case studies on the use of OCM data to study various coastal processes for tide and wave dominated coasts as well as delta environments. The two day repeat cycle of OCM was found useful to understand sediment dynamics in tide dominated regions of the Gulf of Khambhat, the Gulf of Kachchh and Hoogly Estuary. Chauhan et al. (2007) used OCM derived TSM data to describe dispersal pathways and sources of total suspended matter (TSM) in the Gulf of Kachchh, a macrotidal system with insignificant freshwater input. In the Gulf of Kachchh strong alongshore currents are prevalent at the mouth, moving in and out during flood and ebb tides respectively, and undergoing cyclic, dynamic changes with the tidal phases. The Gulf, unlike other regions of the Indian coastline, has a highly dynamic turbidity that is zonal (very high in the outer Gulf and in the creeks of the Gulf), particularly during flooding, and reduced in the central region throughout the entire tidal cycle. In a recent study by Ramakrishnan and Rajawat (2008) they demonstrated a strong relationship between sediment dispersal and tidal currents in the Gulf of Kachchh region. The figure below shows the OCM derived TSM maps for the Gulf of Kachchh region. However, the two day repeat cycle of OCM data does not allow the construction of complete sequences of tide controlled sediment dispersal and its operational use in modelling of sediment transport using numerical models. More frequent observations of TSM dynamics, such as from a geostationary platform, will enhance the use of ocean-colour observation on TSM and applications such as tide controlled sediment dynamics for operational use in simulation models.
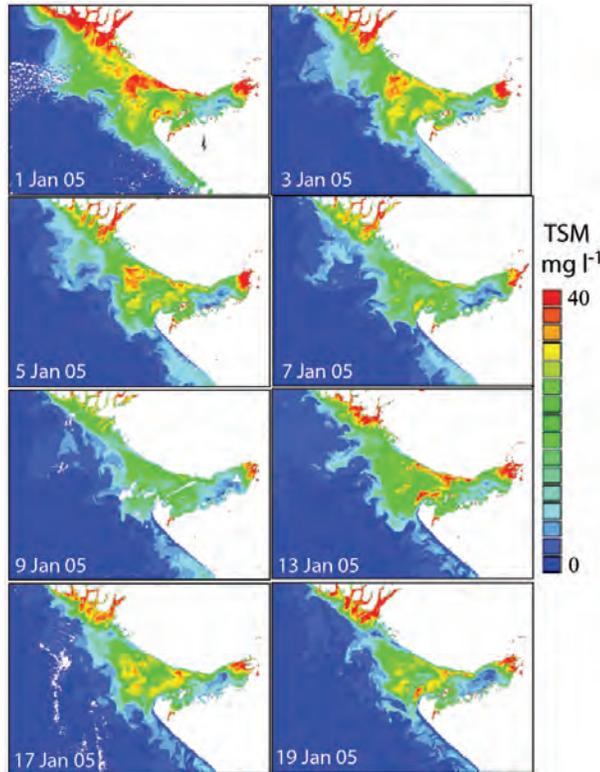
OCM derived TSM concentrations (mg l^{-1}) for different days during 1-19 January, 2005. Image credit: Prakash Chauhan, ISRO, India.

Box 2. An Example from SEVIRI on Meteosat Second Generation

A feasibility study for mapping Total Suspended Matter (TSM) from the Meteosat 2nd generation geostationary weather satellite platform was performed by Neukermans et al.(2009). The SEVIRI (Spinning Enhanced Visible and InfraRed Imager) sensor onboard provides images in near real-time every 15 minutes. Although SEVIRI lacks sufficient bands for chlorophyll remote sensing, its spectral resolution is sufficient for quantification of TSM in turbid waters, using a single broad red band, combined with a suitable near-infrared band. A test data set for mapping of TSM in the southern North Sea was obtained covering 35 consecutive days from 28 June to 31 July, 2006.

Atmospheric correction of SEVIRI images includes corrections for Rayleigh and aerosol scattering, absorption by atmospheric gases and atmospheric transmittances. The aerosol correction uses assumptions on the ratio of marine reflectances and aerosol reflectances in the red and near-infrared bands, based on the turbid water atmospheric correction approach of Ruddick et al. (2000). A single band TSM retrieval algorithm, calibrated by non-linear regression of seaborne measurements of TSM and marine reflectance, was applied. The effect of the above assumptions on the uncertainty of the marine reflectance and TSM products was analysed. Results show that mapping of TSM in the southern North Sea is feasible with SEVIRI for turbid waters (left panel below), though with considerable uncertainties in clearer waters. Moreover, TSM maps are well correlated with TSM maps obtained from MODIS-Aqua. During cloud-free days, high frequency dynamics of TSM are detected. The figure below shows high frequency variability of TSM concentration at three selected locations (P1-P3) on a cloud-free day (29 June, 2006). The error bars denote the estimated uncertainty on the TSM concentration introduced by the atmospheric correction assumptions.
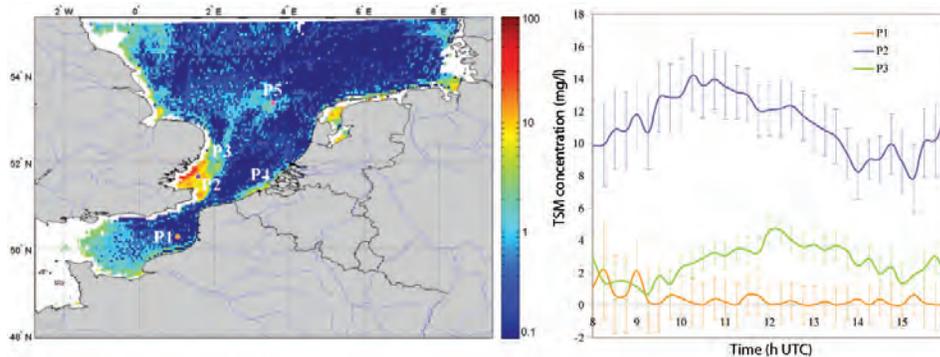
Left: TSM (mg l^{-1}) concentration in the southern North Sea from SEVIRI on 29 June, 2006 at 13:00 UTC. Right: High frequency variability of TSM concentration at locations P1-P3 on a cloud free day (29 June, 2006). The error bars denote the estimated uncertainty on the TSM concentration arising from the atmospheric correction assumptions.

2.1.3 Resolving tidal effects

Tides (Figure 2.1) drive coastal currents that can reach several knots and reverse approximately every six hours. A minimum sampling frequency of three hours is required to resolve these features, and to track water masses. Hourly sampling is recommended to compensate for data lost due to cloud cover and still resolve coastal dynamics. Sampling once per day, which is the best that can be expected from a single ocean-colour imager in low Earth orbit, is inadequate to sample these dynamics.
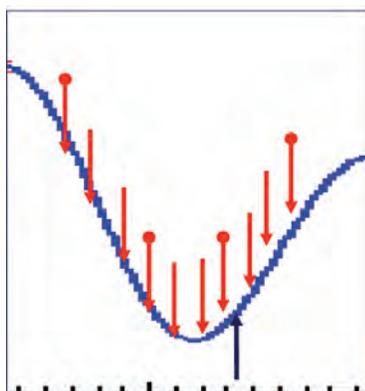
Figure 2.1 Example of a tidal cycle from Charleston, Oregon. The tidal range is more than 4 m and tidal currents on the Oregon coast can exceed 2 knots. Black arrow: VIIRS sampling at 1:30 PM local time; red arrows: hourly sampling. Red arrows with dots are once every three hours, i.e., the minimum sampling frequency needed to resolve a tidal cycle. Adapted from Davis et al. (2007), reprinted with permission from SPIE.

Tidal fluctuations are substantial through the course of a day in most coastal zones. According to *in situ* time series observations from Ariake Bay, Japan, which exhibits one of the largest tidal fluctuations in Japan, temperature, salinity, turbidity, and chlorophyll-a varied with the switch from flood tide to ebb tide. During low tide, high chlorophyll-a water spreads outside of the bay; moreover, inside the bay, complex patchy changes of chlorophyll-a are observed. The tidal movement is important for the transport of organisms such as red tides, and frequent observations from a GEO orbit can provide a means to follow these movements.

Tidal fluctuations of suspended particulate matter also induce corresponding fluctuations of light available for photosynthesis and related parameters such as euphotic depth. The present generation of marine ecosystem models generally does not account for such variations although it is clear that the daily average of photosynthetic rate may be significantly different from that based on an estimate of daily-averaged euphotic depth (averaging of a non-linear process).

2.1.4   Inland waters

For inland bodies of water, spatial resolution is often the prevailing driver for requirements in terms of space-based observations given that these regions and their attendant processes and phenomena are typically smaller in scale than for offshore coastal regions. That said, more frequent ocean-colour observations afforded by geostationary platform(s) will benefit various research and application efforts in inland waters, e.g., regional carbon cycle studies, lake ecosystem dynamics and water quality assessments and monitoring (Dekker et al., 1995; Simis et al., 2005). More frequent ocean-colour observations can help address frequent cloud coverage
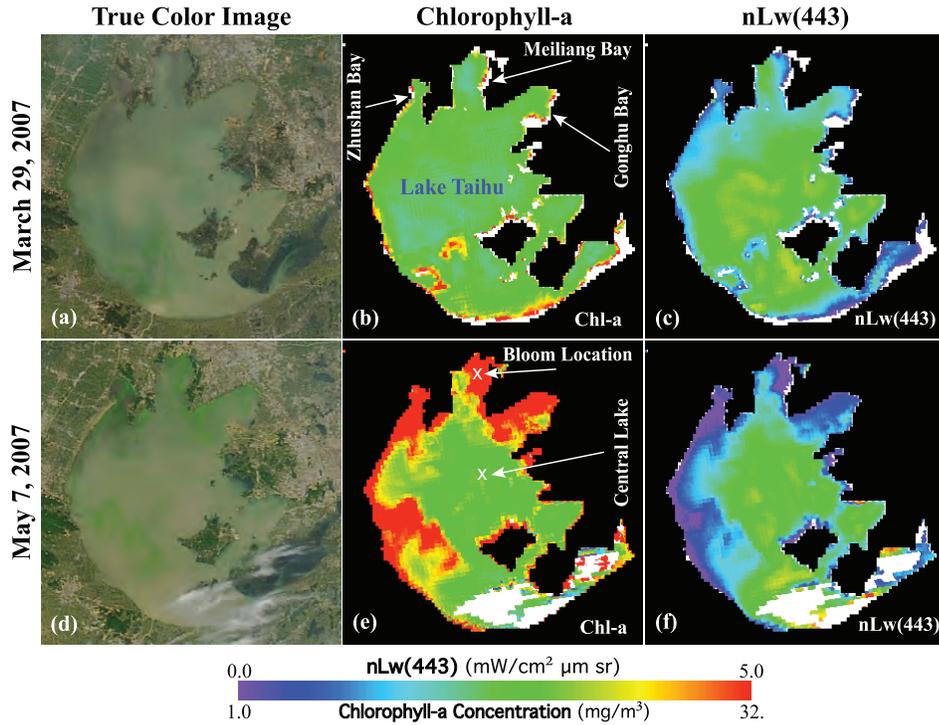
Figure 2.2 MODIS-Aqua true colour image, Chlorophyll-a concentration (as an index for bloom indication), and normalized water-leaving radiance at 443 nm (nL_w(443)) for Lake Taihu on 29 March 2007 (panels a-c) and 7 May 2007 (panels d-f) respectively. Results show the spatial variation of Lake Taihu's optical and biological properties before the algae bloom (29 March) and during the peak of the bloom (7 May). The major blue-green algae blooms occurred in Meiliang Bay, Gonghu Bay, and Zhushan Bay, as well as the west region of Lake Taihu, showing a significant drop of the nL_w(443) because of the strong algae absorption in the blue band (also considerably high Chlorophyll-a concentration). Image from Wang and Shi (2008), reproduced with permission of the American Geophysical Union.

over inland water bodies as well as better address dynamic, episodic lake properties and phenomena, e.g., blooms, runoff plumes, vertical migration and changes in ice cover. The variation of sun angle over the day may also help in the estimation of adjacency effects which can be particularly significant for inland waters.

Likewise, there are common as well as distinct remote sensing challenges in inland waters to be dealt with, including such issues as atmospheric corrections, adjacency effects, and water mass/optical characterizations that can be more effectively addressed using higher spatial, spectral and temporal resolution ocean-colour data.

Water quality is an issue of growing concern for inland water bodies due to increasing population growth and attendant changes in land cover and use, particularly development and urbanization of adjacent terrestrial regions. Loading of

nutrients, sediments and other pollutants and pathogens from terrestrial runoff is a significant concern in this context, as well as algal blooms (harmful and nuisance). Illustrating the latter, Wang and Shi (2008; 2011) described massive algal blooms in spring 2007 in China's Lake Taihu using MODIS-Aqua observations (see Figure 2.2). The waters of Lake Taihu are highly turbid, and Wang and Shi (2008) demonstrated the utility of the shortwave infrared (SWIR) atmospheric correction algorithm (Wang and Shi, 2007; Wang et al., 2009) for remote retrieval of optical and biological properties in such turbid regions. However, the lake was often obscured by cloud cover during this event and they indicated that there were only two MODIS-Aqua clear sky images, acquired one week apart, during the peak period of algal bloom contamination.

This application provides an excellent example of how geostationary platforms could better support water quality monitoring and management by providing more frequent water colour observations during episodic bloom and other events. The need for improved temporal, spatial and spectral water colour observations in inland waters is identified in the Group on Earth Observations Inland and Nearshore Coastal Water Quality Remote Sensing Workshop Report (GEO, 2007), and, more generally, for coastal waters in the Integrated Global Observing Strategy Coastal Theme Report (IGOS, 2006).

2.2 High Spatio-Temporal Observations for Studying the Open Ocean

2.2.1 Diurnal cycles of ocean properties

The diurnal cycle of optical properties is now a well established phenomenon, which is observed *in situ* (e.g., Siegel et al., 1989; Claustre et al., 1999; Figure 2.3), and can also be replicated in the laboratory (e.g., Claustre et al., 2002). These diurnal variations are mainly driven by the diel cycle of solar irradiance, and they are responsible for a part of the "natural noise" which is found in the databases from which a number of bio-optical algorithms have been developed (Stramski and Reynolds, 1993). The causes of these diurnal variations remain poorly understood. They can result from (1) the balance between daytime production and nighttime degradation of biogenic particles (phytoplankton, bacteria, small heterotrophs), (2) a change in particle size, or (3) a change of refractive index resulting from the internal concentration of organic compounds. From the diurnal variations of the beam attenuation coefficient (a proxy to the particulate organic carbon), a method has recently been proposed for estimating basic biogeochemical quantities, such as gross and net community production (Claustre et al., 2008).

Diurnal variations in the concentration of coloured dissolved organic matter (CDOM) that would result from a balance between processes of photo-production
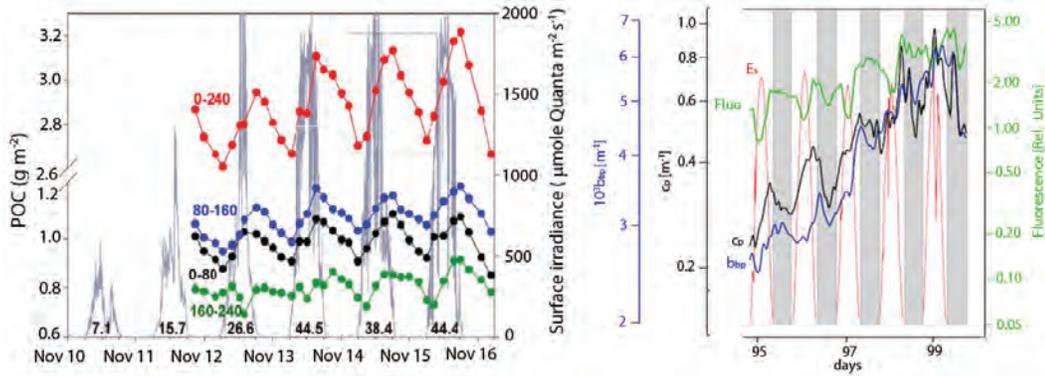
Figure 2.3 Left: Daily variations in integrated particulate organic carbon content, derived from measurements of the beam attenuation coefficient, over various optical depth intervals. Black: 0 – 80 m (100% – 10%); Blue: 80-160 m (10% – 1%); Green: 160 – 240 m (1% – 0.1%); Red: 0 – 240 m (surface to 0.1% of surface irradiance). Grey curves are PAR at the surface (from Claustre et al., 2008). Right: 6-day record of the diurnal changes in the beam attenuation (black), particulate backscattering (blue) and phytoplankton fluorescence (green) at the BOUSSOLE site in the Mediterranean Sea during a bloom in spring of 2007 (grey bars indicate night-time). Data collected near the surface.

and photo-degradation are also possible, although these changes have not been observed, for lack of appropriate technology. Analysis of these variations could infer quantitative changes of dissolved organic carbon (DOC), a significant proportion of which (up to ~50% of production) is known to be excreted by primary producers (Karl et al., 1998). It is therefore becoming increasingly clear that the acquisition of bio-optical and biogeochemical data at high frequency, through new acquisition platforms fitted with *ad hoc* sensors is an essential prerequisite for understanding the diurnal signal and interpreting it in a biogeochemical context (e.g., estimate of production, new production). With GEO observations, we can achieve large-scale observations of the daytime signal of the optical properties.

Documenting these phenomena is interesting from a scientific point of view, yet it also has a practical importance, which is to assess the possible bias in the LEO satellite observations, which are nearly always performed at the same time of the day for a given satellite. This may represent a perturbation in the observations from different LEO satellites passing over a given area at different times of the day (this may be an issue for merging of data from different missions).

In continuation of recent analysis of the diel cycle of the particulate beam attenuation coefficient (c_p) (Claustre et al., 2008; Gernez et al., 2011), it is also expected that the diurnal variability in the particulate backscattering coefficient (b_{bp}) is usable to estimate the particle growth rate and net community production, as well as their underlying parameters (i.e., maximum growth rate, growth efficiency and saturation irradiance). The capability of estimating these parameters over vast oceanic areas would be a breakthrough in marine science.
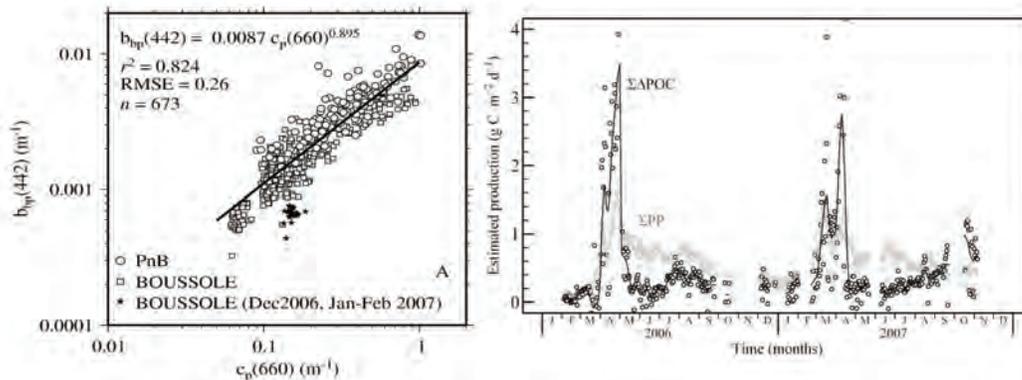
Figure 2.4 Left: Relationship between c_p and b_{bp} (from Antoine et al., 2011; data from the BOUSSOLE site and the "Plumes & Blooms" program). Right: Seasonal variation of net community production ($\Sigma \triangle$POC, derived from the diel change of c_p) and net primary production (ΣPP, derived from a light-photosynthesis model). The points indicate daily values; the lines show a 3-day running mean (from Gernez et al., 2011).

The logic here is to go from the diel changes of c_p or b_{bp} in the surface layer to an estimate of the daily change in particulate organic carbon ($\triangle$POC), and then to the integrated POC change within the productive layer (e.g., Duforêt-Gaurier, 2010).

An example is provided in Figure 2.4 (right panel), where a 2-year cycle of primary production at a fixed site in the Mediterranean Sea (BOUSSOLE site; Antoine et al., 2006) has been derived through two different methods. The first one (indicated by light grey symbols and ΣPP) corresponds to the classical use of a light-photosynthesis model (Morel, 1991) fed with daily surface chlorophyll concentrations, SST and above-surface irradiation (PAR). The second one (dark grey symbols; $\Sigma \triangle$POC) is from a new model (Gernez et al., 2011) that estimates the daily community production from the diel change of the beam attenuation coefficient (c_p). This is applicable to satellite observations provided that a relationship exists between c_p (desired but not measured) and b_{bp} (derivable from inversion of the marine reflectances and K_d). This relationship actually holds and is now documented in various environments (see Figure 2.4 left; see also Dall'Ollmo et al., 2009).

2.2.2 Biological-physical coupling at meso and sub-meso scale

Recent theoretical studies have suggested that ocean biogeochemistry is extremely sensitive to sub-mesoscale physics (see Lévy, 2008 for a review). The fingerprint of sub-mesoscale physics on phytoplankton distribution has emerged as a recurrent feature in ocean-colour observations since the beginning of OCR observations. These observations clearly reveal that the ocean is a turbulent fluid, populated by numerous interactive, mesoscale eddies. These interactive eddies generate very energetic dynamic phenomena, that can act to change the ocean stratification, to
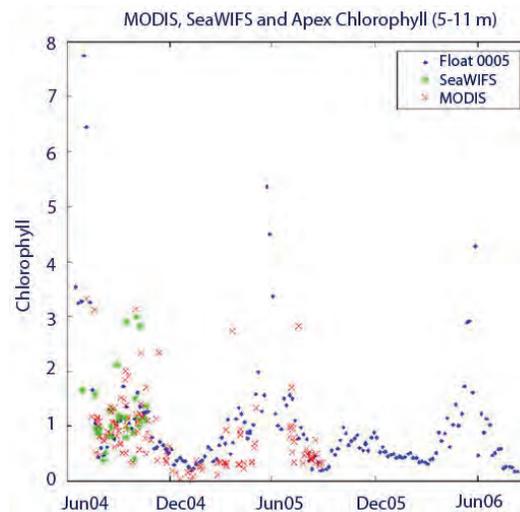
Figure 2.5 Surface Chlorophyll-a concentration (mg m^{-3}) in the North Atlantic, as derived by a profiling float (blue points), onto which remote sensing data (red MODIS, green SeaWiFS) extracted along the track of the profiling float are superimposed. In spring 2005 (late May, early June), satellite data from the current LEO missions were unable to detect the blooming event in this highly cloudy area (from Taylor et al., 2006).

stir water masses and to enhance vertical movements, with dramatic consequences on phytoplankton growth and distribution.

Given the space (1 – 10 km) and time (1 – 10 days) scales associated with sub-mesoscale dynamics, their impact on phytoplankton can hardly be examined *in situ* on a regional scale. A regional characterization of the processes is needed, however, to quantify the importance of the small scale structures (e.g., filaments) on global primary production budgets. Such a regional approach at high resolution will hopefully reduce the errors in global estimates of primary production due to the misrepresentation of the sub-mesoscale processes, both from models and from observation networks.

Bio-physical coupling at sub-mesoscale is not yet accounted for in global ocean biogeochemical models because it requires horizontal grid resolutions that are still out of reach. However, sub-mesoscale resolving regional models are emerging. These high-resolution models are still in their infancy, and, due to the scarcity of high-resolution observations, can only be validated at the large scale. In the next decade, such high-resolution models will become common practice, and there will be a corresponding demand for high-resolution observations to validate them.

High-resolution models are indicating that phytoplankton blooms are not continuous phenomena. They reveal an intricate entangling between the rapidly-evolving filaments, the seasonal variations, and the shorter-term variations of the wind. This entangling induces important bias when biogeochemical budgets are evaluated from a limited set of local observations. For instance, the spring phytoplankton bloom

can be interrupted locally, either by the passage of an atmospheric depression, or by the passage of a downwelling filament. These two phenomena have contrasting consequences on the larger scale budget. Synoptic, high-frequency observations are the only way to decipher these various phenomena, which will help reduce current bias in regional budgets.

A geostationary ocean-colour sensor will ensure an enhanced temporal resolution of observations, which will compensate for the loss of data due to cloud cover. GEO observations are thus expected to allow a better determination of the time evolution of blooms (Figure 2.5). Additionally, they will improve characterization of phenomena at small temporal scales, related to the fluctuations of the upper layer ocean dynamics.

2.2.3   Coupled physical-biogeochemical models

The steady increase of computational power available for numerical simulations of coupled physical-biological systems has drastically broadened the spectrum of spatial and temporal scales explicitly captured by ocean models. Results of studies addressing the existence of distinctive types of variability and interactions between dynamics and biological activity within the mesoscale and sub-mesoscale (tens to hundreds of kms; hours to days) have begun to emerge. However, the ocean variability in currents and material distribution is severely under-sampled by the observing systems in place today. Ocean-colour images from a geostationary orbit will contribute to reduce the measurement under-sampling and improve the match between the scales resolved by the models and those resolved by observations. The higher spatio-temporal resolution will also improve model evaluation. This will open new perspectives for synergistic approaches between models, *in situ* and satellite observations, especially through data assimilation. This "integrated approach" is expected to make substantial progress in the future, in terms of scientific, technological and operational applications (Brasseur et al., 2009).

Although ocean-colour data assimilation into coupled models is still in its infancy, innovative approaches are being developed using variational or sequential methods (Carmillet et al., 2001; Faugeras et al., 2003; Natvik and Evensen, 2003; Nerger and Gregg, 2008; Simon and Bertino, 2009) to reconcile data of different types (e.g., ocean colour in combination with altimetry, SST, *in situ* temperature and salinity profiles) with models, to improve the realism of coupled physical-biogeochemical simulations, analyses and re-analyses, and to develop an effective capacity to estimate routinely the biogeochemical state of the ocean and regional seas.

The accumulation of ocean-colour measurements at high spatial and temporal scales as anticipated from GEO missions will first be required to improve the characterization of modelling errors prior to model-data synthesis through assimilation. For computational reasons, many coupled physical-biogeochemical models will remain limited to eddy-permitting resolution in the foreseeable future. The
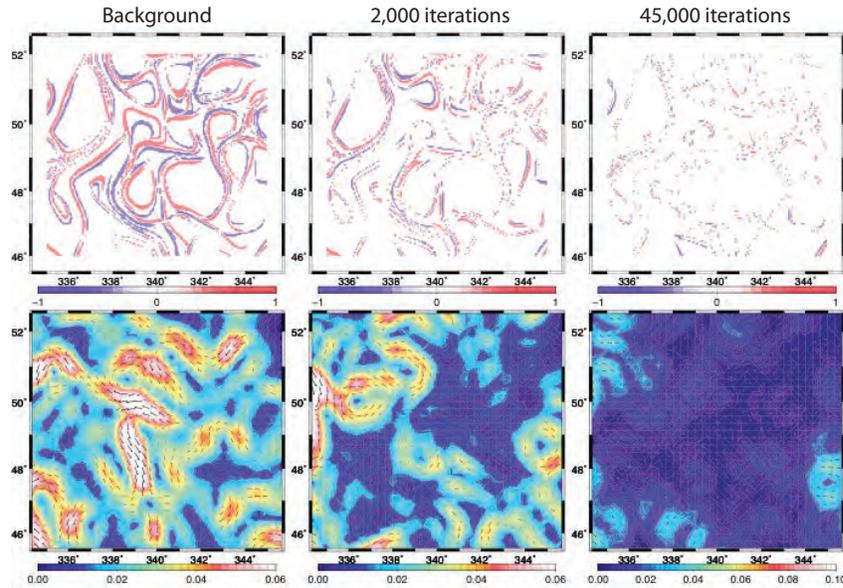
Figure 2.6 FSLE (Finite Size Lyapounov Exponent) pattern misfit (top panels) and velocity errors (m s^{-1}, bottom panels) at three stages of the assimilation process: background state (left panels), after 2,000 iterations (middle panels), after 45,000 iterations (right panels). Image courtesy of Jacques Verron (CNRS, France).

spatial resolution offered by geostationary ocean-colour sensors will be critical to estimate the representativeness errors in biological models due to sub-grid sampling. Until now however, most ocean-colour assimilative systems rely on the use of "low-frequency" data sets (e.g., weekly or monthly composite data products), which may be a source of bias when high-frequency processes are not taken into account properly. Therefore, sequential assimilation methods will be tuned to make optimal use of (almost) time-continuous data streams and to better understand how the average effect of diurnal scales can be represented in coupled physical-biological models.

The assimilation of image-type information is another perspective opened by the geostationary orbit. Recent studies have shown that the structures contained in sub-mesoscale images can be inverted to control the ocean circulation at larger scales (Verron pers com.). This can be achieved through the use of an intermediate quantity, the Finite Size Lyapunov Exponent (FSLE), which has the ability to provide structural information from ocean-colour images for assimilation into larger scale ocean circulation models (Figure 2.6). Ocean colour from a geostationary orbit will offer an excellent opportunity to further explore this assimilation concept, and undertake implementations in various dynamically contrasted regions.
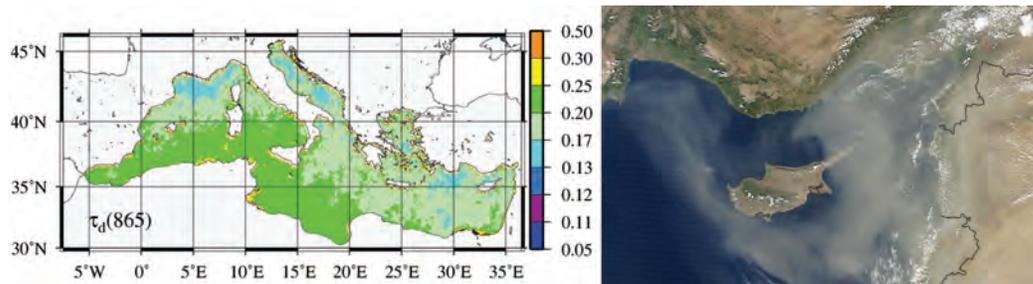
Figure 2.7 Left: Average (1998-2004) dust optical thickness over the Mediterranean Sea, as derived from SeaWiFS observations (after Antoine and Nobileau, 2006). Right: Dust storm over the eastern Mediterranean Sea, captured by MODIS-Terra on 29 September 2011 (NASA image credit: Jeff Schmaltz, MODIS Rapid Response Team, NASA GSFC).

2.3   Aerosols

A wide range of techniques has been developed over the past 20 years for the remote sensing of aerosols, using different types of sensors and various parts of the electromagnetic spectrum (see reviews in Kaufman et al., 1997; King et al., 1999; Kaufman et al., 2002). Quite recently, ocean colour arose into the panoply of methods considered as capable of providing reliable information about the amounts and types of aerosols (e.g., Wang et al., 2000; Moulin et al., 2001). The main focus of ocean-colour science with respect to aerosols is to remove their effect on the recorded signal, i.e., atmospheric correction, rather than studying aerosols themselves, which explains this situation.

Ocean colour is extremely demanding in terms of accuracy of the retrieved water-leaving reflectances, in particular in the blue (Gordon, 1997). For modern sensors, atmospheric correction schemes have been drastically improved compared to what was done in the 1980's with the CZCS (Coastal Zone Color Scanner). This was achieved (amongst other things) by using aerosol models to describe the spectral dependence of the atmospheric signal, and in particular the multiple scattering effects. It is through this process that the by-products of the atmospheric correction of ocean-colour observations were improved and became relevant to aerosol science.

Regional to large-scale quantitative assessment of aerosols over the ocean, and in particular of desert dust, is now within reach either using historical data sets such as CZCS (Stegman and Tindale, 1999) or using the new generation of ocean-colour sensors such as SeaWiFS (Jamet et al., 2004; Stegman, 2004a,b; Wang et al., 2005), MODIS (Kaufman et al., 2005; Remer et al., 2005), MERIS (Antoine and Nobileau, 2006) or POLDER-I and -II (Boucher and Tanré, 2000; Chiapello et al., 2000; Deuzé et al., 1999, 2000) (see Figure 2.7).

The LEO satellites are not adapted, however, to monitoring specific aerosol events, such as desert dust outbreaks, volcanic eruptions or pollution clouds. The

transient character of these structures makes their description hardly feasible via sparse observations. In addition, it cannot be excluded that the average description that is built from LEO observations is sometimes biased by this insufficient sampling;

Box 3. Desert Dust Aerosol Detection Using Geostationary INSAT-3A CCD Data over the Arabian Sea

Sand and dust blown into the atmosphere by sustained winds can trigger huge dust storms and cause conditions of near-zero visibility. The local climatic conditions become altered by airborne particles from dust storms by intercepting sunlight and modifying the energy budget through their ensuing behaviour of cooling and heating of the atmosphere. For ocean-colour remote sensing the absorbing aerosols are one of the major sources of error in the atmospheric correction procedure. Many studies using SeaWiFS, MODIS and other satellite data sets have shown the importance of satellite imagery to detect and monitor dust storms. However, the geostationary platform is much more suitable to studying the dynamic behaviour of such events. In the figure below, we demonstrate the use of INSAT-3A (Indian National Satellite) data to characterize a massive dust storm event that occurred during 15-16 October, 2008 over the northern Arabian Sea. The INSAT-3A sensor has a spatial resolution of 1 km and observations are made at hourly intervals.
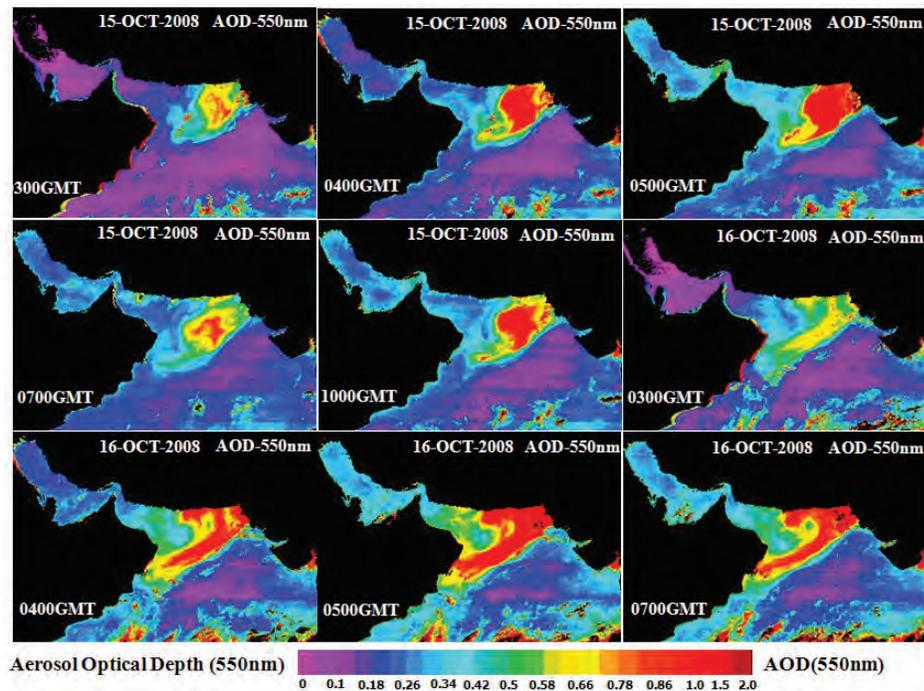
INSAT-3A CCD derived aerosol optical depth over the Arabian Sea from a geostationary platform (image courtesy of Prakash Chauhan, ISRO, India).

The dust storm generated by strong winds lifts particles of dust or sand into the air and is characterized by high aerosol optical depth (AOD), lower Angström exponent (α) along with near zero visibility conditions. Multi-temporal INSAT-3A data for every hour have been used to study the characteristics and transport of these dust storm events. AOD and α estimation were also compared with MODIS-derived AOD at 550nm and α (550/865).

this may be the case for the desert dust transport, while it is likely not a problem for background aerosols.

GEO observations of aerosols are already available through a new generation of Meteosat satellites (e.g., the SEVIRI sensor). Near real-time products over the ocean are routinely provided, for instance, by the ICARE Data and Services Centre (`http://www.icare.univ-lille1.fr/browse/`). A quick look at aerosol browse images highlights the essential benefit from GEO observation, namely the significant improvement of coverage. Future GEO ocean-colour observations would complete the description with a much better spectral resolution, leading to the possibility to better discriminate different aerosol types. A second benefit will arise from the capability to derive aerosols over land as well as over oceans. Other techniques are required due to the additional unknown surface as a boundary condition for the aerosol inversion.

Such GEO aerosol products with high spatial and temporal resolution will also open new perspectives in the area of air quality monitoring. Even if the vertical information critical to air quality applications is not provided by radiometry in the visible, the high-resolution aerosol images will contribute the global picture required by the models used for the assimilation of the *in-situ* measurements. With the growing concern over air quality and climate change, such aerosol products will be very useful for the development of air quality operational services in the near future.

2.4   Land-Ocean Interactions

At the interface between land and ocean, river outflows are a major source of erosion and consequently, of sediment-bound carbon and pollutants transfer. Although these events are still poorly understood due to a lack of experimental sites and long-term hydro-meteorological data with adequate space-time resolution (Beusen et al., 2005), they are believed to represent a large proportion (around 80%) of particulate input to the ocean (Schlunz and Schneider, 2000). Rivers transport ~0.8 x 10^{15} g C per year to the coastal ocean (~0.4 x 10^{15} g of dissolved inorganic carbon [DIC], ~0.5 x 10^{15} of dissolved [DOC] and particulate organic carbon [POC]) (Sabine et al., 2004). While particles from terrestrial ecosystems are primarily deposited in the coastal region (Hedges, 1992), DOC is considered the main conduit for transporting terrestrial organic carbon into the deep ocean. Historically, coastal ocean waters have been a source of CO_2 to the atmosphere because of river contributions of DIC and land-derived organic carbon that is subsequently degraded to CO_2 by microbes in the coastal ocean (Sabine et al., 2004). However, human population growth, agriculture and other activities along coastal regions have resulted in the export of higher levels of nutrients to the ocean, which support more extensive phytoplankton blooms in coastal waters and potentially greater sequestration of

carbon into sediments. Furthermore, recent evidence demonstrates the importance of CO_2 outgassing from rivers to the atmosphere with tropical rivers of greatest significance due to microbial degradation of large inputs of land vegetation and soil derived organic matter into these rivers (Sabine et al. 2004). Combining field data and geostationary satellite measurements would greatly help to quantify the trapping efficiency of estuarine environments (Beusen et al., 2005; Doxaran et al. 2009) and the net emission of carbon from estuaries and deltas to the atmosphere (Frankignoulle et al., 1998) and carbon fluxes to the coastal ocean (Del Castillo et al. 2008) and open ocean. There is also a need to follow formation and evolution of cross-shelf filaments forced by upwelling or fresh water run-off (e.g., Wang et al., 1988; Bignami et al., 2008).

2.5   Operational Services for the Coastal Zone

In this section, examples of existing pre-operational services using ocean-colour observations are briefly presented. One of the main reasons for these services not being truly operational at the moment is the insufficient revisit of the LEO systems. The advent of GEO observations would allow these "demonstration activities" to evolve towards truly operational services.

2.5.1   Algae blooms, in particular harmful algal blooms

Algal blooms are rapid local increases in the abundance of phytoplankton. Harmful algal blooms (HABs) are special cases of the former, which are known to cause deleterious effects either on human health (e.g., paralytic or neurotoxic shell fish poisoning) or on natural or cultured marine resources (mass mortality of fish). Besides this generic term there is, however, a complex reality (some species may be harmful at low density, for instance). Algal blooms are well detected by ocean-colour remote sensing, due to their strong influence on the optics of water. Conversely, the identification of their possible toxicity from space is far from being achieved; currently the exact distinction of the causative organisms in the bloom is only realized through *in situ* measurements. The key role of ocean colour thus lies in:

❖ visualizing the bloom extent;
❖ launching advanced warnings, through combination of models and Earth observation data;
❖ deploying opportune *in situ* campaigns to analyse the potential toxicity of the bloom;
❖ if phytoplankton functional type algorithms can be extended to the coastal ocean in the future, they might help determine the type of bloom under consideration.

2.5.2 Turbidity and eutrophication

The concentration of human population near the shore confronts many governments with the problem of monitoring, predicting and managing the coastal environment. To be effective, the assessment of the impact of urbanization, tourism, harbour development, agriculture, etc. on coastal ecosystems requires an integrated approach including databases, models and monitoring programs at regional scales, which could benefit greatly from high frequency geostationary ocean-colour observations. In this way, the European Environment Agency has expressed its needs for simple and robust indicators for annual analyses of the state of European coastal water, which are partly estimated by remotely-sensed data.

In many coastal waters, disastrous changes in water composition result mainly from non-natural loads of sediments that have three different detrimental effects:

- ❖ an increase in turbidity, that shades the water and impacts benthic habitats;
- ❖ a rich supply in nutrients, that increases algal biomass (eutrophication) and replaces the natural ecosystem, possibly leading to HAB development; and
- ❖ a load of heavy metals trapped in the sediments.

Water clarity is a critical parameter for navy, professional and sport divers, as well as aquaculture and commercial and recreational fisheries. Estimates of water clarity are derivable from ocean-colour observations, including suspended particulate matter (SPM), chlorophyll-a, transparency (Secchi depth), K_d (diffuse attenuation coefficient), and turbidity indices. For all of these applications the step forward with GEO observations essentially lies in the dramatic increase in the capability to study the dynamics of the relevant phenomena. For example, in areas with strong tides or diurnal winds, water clarity changes dramatically on an hourly basis as tidal currents resuspend sediments from the bottom.

2.5.3 Front detection for internal waves and localisation of fish stocks

Front detection is an advanced processing of ocean colour corresponding to the spatial variation of a product, generally chlorophyll or transparency. It is based on horizontal gradient calculation and, in even more advanced versions, the contour detection by hystereris method (Figure 2.8). This product enlightens the fronts of the image and provides information about oceanic structures; it is thus a key element for tracking dynamics features of the ocean (like internal waves) as well as fisheries resources. While the Navy requests the former application for operation support, the latter is obviously interesting for the fishing industry and fisheries management.

Observations from the GEO orbit would dramatically increase the temporal frequency of such mappings, with an obvious impact on the understanding of the dynamics of fronts and filaments, and on the quality of the service that can be provided to many users.
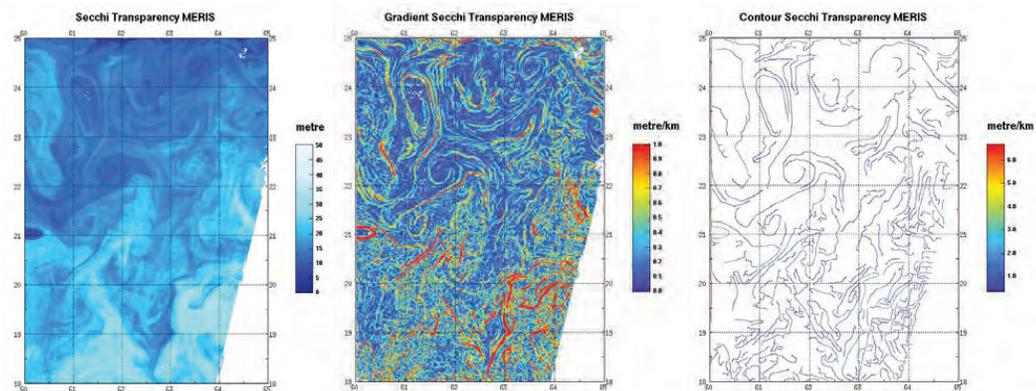
Figure 2.8 Example of structure detection for a MERIS scene (9 April 2003 in Indian Ocean). From left to right: transparency map, gradient map, contour map. Spatial resolution is 1 km. Illustration of a service delivery to the French "Service Hydrographique de la Marine" (image courtesy of ACRI-ST).

2.6   Societal Benefits

The societal benefits of ocean colour have been detailed extensively in IOCCG Report 7 (2008), "Why Ocean Colour? The Societal Benefits of Ocean-Colour Technology", as well as in IOCCG Report 8 (2009), "Remote Sensing in Fisheries and Aquaculture". As addressed in those reports, as well as in this current report, ocean colour can be utilized to support a number of important research and applied/operational efforts including: assessments of climate variability and change through improved understanding of biogeochemical cycles (e.g., carbon pools and fluxes) and food web impacts; integrated ecosystem assessments and living marine resource management (e.g., marine protected areas, fisheries, aquaculture and threatened/endangered species); monitoring of coastal and inland water quality (e.g., pollutant and pathogen-laden runoff plumes and spills); assessments of natural and anthropogenic hazards (e.g., harmful algal blooms, oil and sewage spills, sediment resuspension events); improved understanding of ocean and coastal dynamics (e.g., eddies and blooms); development of robust indicators of the state of the ocean ecosystem, and, ecological modelling and forecasting activities.

In support of these efforts, ocean-colour observations from a geostationary plat-form will provide significantly improved temporal coverage of near shore coastal, adjacent offshore and inland waters, and likely improved spatial and spectral cov-erage relative to current LEO sensors, which are generally more focused on global observations of Case-1 open ocean waters. The higher frequency observations from GEO will help mitigate the effects of cloud cover, as well as better resolve the dynamic, episodic, and/or ephemeral processes, phenomena and conditions commonly observed in coastal regions. This will result in a denser and more compre-hensive ocean-colour data set, leading to further development, use and operational
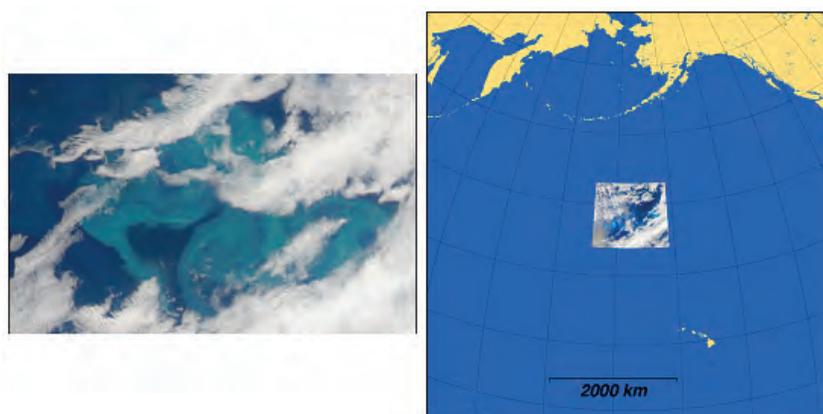
Figure 2.9 A break in the clouds over the central North Pacific revealed a large patch of bright aquamarine water on June 6, 2007. Other ocean patches of a similar colour have been identified as coccolithophore blooms in the past. The location and timing of this bloom is what one might expect for such phytoplankton, but surface water samples would be needed to confirm the identification. Credit: Ocean Biology Processing Group, NASA/GSFC, reproduced from http://oceancolor.gsfc.nasa.gov/cgi/image_archive.cgi?c=CHLOROPHYLL

implementation of more timely and accurate products, e.g., harmful algal bloom forecasts, which in turn will provide better information to users in support of their management and decision-making needs.

2.7 Future Geostationary Ocean-Colour Applications

The previous sections show how existing scientific and operational activities would benefit from GEO observations, starting from the state of the art ocean-colour observations. It is important to emphasize that in the future, new scientific discoveries or operational uses will likely emerge after GEO ocean-colour observations become available, although it is currently not possible to anticipate all the future domains of GEO ocean-colour applications.

To illustrate this exploratory nature of the GEO ocean-colour observations, Figure 2.9 shows a bloom in the north Pacific, presumably composed of coccolithophorids, as detected by the MODIS-Aqua sensor, and occurring in an unexpected location, in principle. Although one MODIS image of this bloom was obtained, no possibility existed to follow its development. This should become feasible with more frequent GEO ocean-colour observations. It is anticipated that many such unexpected and transient structures will be identified and tracked with GEO ocean-colour observations providing insight into their causes and fate.

General Requirements for a GEO Ocean-Colour Sensor

3.1 Spectral Requirements

Spectral resolution requirements derive from the need to effectively remove atmospheric components of the total signal acquired by a satellite sensor, as well as the need to derive accurate values for geophysical products from the spectral radiances emanating from the ocean. The three sections below are not specific to ocean colour from the GEO orbit. In conditions where a compromise is necessary between spatial and spectral resolution it may be interesting to consider one or more broader bands for a GEO sensor, similar to the approach of the higher resolution panchromatic bands on sensors designed for meteorological or terrestrial applications such as SEVIRI and SPOT.

3.1.1 Spectral requirements for atmospheric correction

For the atmospheric correction, theoretical and empirical analyses of ocean colour have shown that at least two bands located in the near-infrared region of the solar spectrum are required to provide the aerosol radiative properties necessary for ocean-colour retrievals. For typical ocean waters the water-leaving radiance is 0 in the near infrared (NIR) and the measured radiances in the NIR are used to estimate the aerosol properties over the ocean. A band located between 855 and 890 nm, and another band located between 744 and 757 nm are considered the minimum for atmospheric correction (IOCCG, 1998). However, in waters with high particulates there is still measurable water leaving radiance at 750 nm and sometimes at 865 nm, so additional spectral bands are required for aerosol correction for these turbid coastal waters.

Recently, an approach similar to the one used for open ocean waters has been developed for coastal regions by Wang and Shi (2007) and Wang et al. (2009). The method uses short wave infrared (SWIR) bands instead of the NIR bands. The approach has been tested for, and applied to, various coastal regions (e.g., the U.S. and east coastal regions of China) using MODIS data. Because of the much stronger water absorption, the ocean is generally still black at the SWIR bands even for very turbid waters. The spectral extrapolation to the visible is performed over a larger
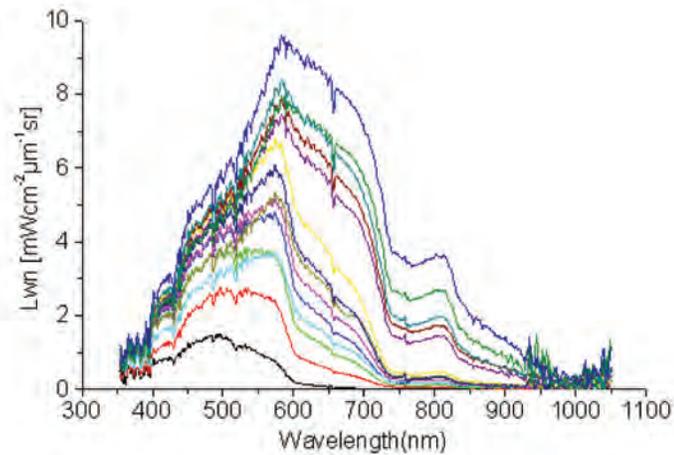
Figure 3.1 Normalized water-leaving radiances in the East China Sea. The total suspended particle matter concentration varied from 1.1 g m^{-3} to 184.1 g m^{-3} with large values of water-leaving radiances corresponding to high concentrations of particulate matter. Adapted from He et al. (2004).

range, however, which introduces an additional difficulty.

Using near-UV bands is another possibility for the atmospheric correction over turbid coastal waters (He et al., 2004). Figure 3.1 displays the variation of normalized water-leaving radiances measured in the East China Sea. With increasing turbidity caused by higher suspended particle matter concentrations, water-leaving radiances at UV bands increase very little as compared to the NIR bands. In coastal waters, suspended sediments and CDOM significantly influence the water optical properties. High values in water-leaving radiances in the VIS and NIR may result from scattering by high concentrations of suspended particle matter, meanwhile, the strong absorption of detritus and CDOM causes a rapid decrease in the blue part of the spectrum, and still more in the near-UV. Therefore, in some turbid coastal waters, UV bands are better than NIR bands to obtain more accurate atmospheric correction. The transparency of the atmosphere at near-UV wavelengths is another advantage of using this part of the spectrum.

In addition, the quality of ancillary data, i.e., atmospheric total column ozone amount, sea surface wind speed, atmospheric pressure, total column water vapour, and atmospheric NO_2, which are required inputs for satellite ocean-colour data processing, also significantly impact the data quality of satellite-derived ocean-colour products (Ahmad et al., 2007; Ramachandran and Wang 2011). In coastal waters, in addition to aerosols, atmospheric correction is needed for the presence of tropospheric trace gases such as nitrogen dioxide (NO_2), which has a strong absorption spectrum in the range 330 to 500 nm that varies rapidly with wavelength. A NO_2 correction algorithm using climatology NO_2 data (Ahmad et al., 2007) has already been implemented in the current SeaWiFS and MODIS ocean-colour data

processing (R2009 and R2010). However, the high temporal (diurnal) and horizontal spatial (< 1 km) variability in tropospheric NO_2 concentrations caused by natural and anthropogenic emissions can result in significant errors in normalized water-leaving radiances in coastal waters on the order of 7-20% for high solar zenith angles and view angles (Herman et al., 2009).

Ozone has an even greater impact on water-leaving reflectances if not taken into account in atmospheric corrections. The dilemma is that current sensors provide total column ozone and NO_2 measurements at coarse spatial (12 x 24 km for the Ozone Monitoring Instrument, OMI) and temporal resolution (once per day), which may be inadequate for application of atmospheric corrections to retrieve water-leaving radiances in coastal waters, particularly adjacent to urban areas where NO_2 variability is most significant.

In summary a minimum of 5 channels are recommended for atmospheric correction of open ocean and coastal waters: one UV channel in the 350-380 nm range, the two standard channels between 744 and 757 nm and between 855 and 890 nm, and two SWIR channels at 1240 and 1640 nm.

3.1.2   Spectral requirements for in-water properties

For the purpose of retrieval of bio-geochemical parameters in the highly diverse and dynamical coastal water, hyperspectral imaging is an option for geostationary ocean-colour sensors in the next decade. In particular, hyperspectral imaging with 10 nm or better spectral sampling has proven to be essential when imaging optically-shallow waters where reflectance from the bottom adds to the complexity (Lee and Carder, 2002). The minimum spectral requirements for ocean-colour measurements in the open ocean are discussed in IOCCG Report No. 1 (1998) and are briefly summarized in IOCCG Report No. 2 (1999), providing a starting point for assessing the basic requirements. A minimum set of three bands (e.g., 443nm, 490nm, 555nm) is necessary to retrieve the key oceanic biological parameters, primarily the concentration of chlorophyll-a (IOCCG, 1998). Bandwidths of 20-nm are the minimum requirement for visible bands, but 10 nm is desirable to gather specific information about pigment composition (IOCCG, 1998). However, the minimum spectral set cannot be applied to the coastal water for biogeochemical algorithms. IOCCG Report No. 1 (1998) recommends adding a spectral band in the blue (around 410 nm) to separate the effects of CDOM absorption (with a possible addition of near-UV bands in the 340 – 380nm range), and adding channels to monitor the height of the fluorescence signal above a baseline determined using two channels on either side of the emission peak or relative to a nearby single band (e.g., 667 nm for MODIS). IOCCG Report No. 2 (1999) recommends adding a spectral band around 620 nm to quantify water turbidity and adding either additional channels in the near-infrared (NIR), and/or the use of inverse techniques to estimate in-water constituents and aerosols simultaneously. These spectral requirements are also
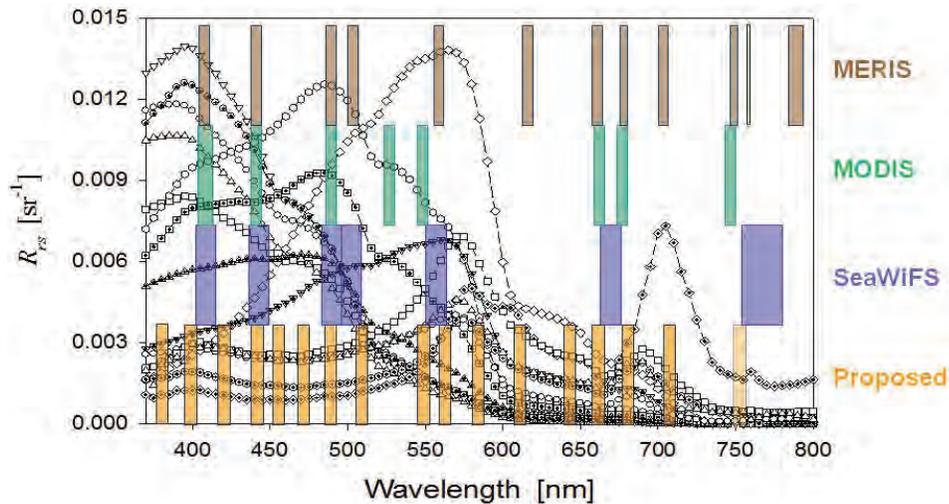
Figure 3.2 Spectral bands proposed by Lee et al. (2007a) with spectral bands of SeaWiFS, MODIS and MERIS overlaid. The 750 nm band is mainly used for atmospheric correction.

suitable as minimum requirements for geostationary ocean-colour observations.

Lee and Carder (2002) demonstrated that ~15 bands are required in the 400 – 800 nm range for adequate derivation of major properties (phytoplankton biomass, coloured dissolved organic matter, suspended sediments, and bottom properties) in both oceanic and coastal environments. Of the current sensors in orbit, the authors concluded that the MERIS band set performed the best and was closest to meeting this requirement. More recently Lee et al. (2007a) demonstrated that the primary bands (in the 380 – 800 nm range) that optimally capture the spectral signatures of R_{rs}, can be determined by analysis of the first- and second-order derivatives of water-leaving radiance spectra for a representative range of water types (Figure 3.2). In general these bands cover the operational bands of SeaWiFS, MODIS and MERIS, and provide important and useful suggestions and guidance for extra bands for future multi-band sensors, which will provide improved results for remote sensing of oceanic and coastal waters. However, these bands are optimized for general observation of the majority (99% or more) of global aquatic environments and are derived based on available measurements. As pointed out by Lee and Carder (2002), sensors with discrete spectral bands always face the possibility of missing important spectral features of special cases, such as found in coral reefs and/or seagrass beds (e.g., Holden and LeDrew, 1998). Sensors with higher spectral resolution (along with high spatial resolution) or specially placed bands could be more helpful for remote sensing in such challenging waters.

In summary hyperspectral imaging with 10 nm or better spectral sampling is useful particularly when imaging optically-shallow waters where reflectance from the bottom adds to the complexity (Lee and Carder, 2002). However when the

bottom is not imaged, a band set similar to the one of MERIS has proven to be as good as 10 nm hyperspectral data for water column properties. For example, the 620 nm channel on MERIS is useful for mapping suspended sediments and the 705 nm channel for detecting phytoplankton blooms. Although hyperspectral imaging is not required, following the MERIS design, the instrument could be a hyperspectral imager with the order of 1 nm spectral resolution and the ocean bands binned on the spacecraft. There are a number of advantages to this approach. One key advantage is that the binned spectral bands have a Gaussian (or better) shape, so filter stray light issues do not have to be dealt with, nor the possibility of the filters ageing in space. Mission specific trade-offs are needed to decide between a filter imaging radiometer (filter wheel or other design) and an imaging spectrometer. Preliminary studies have shown that the latter might actually be difficult to accommodate on a GEO orbit.

3.1.3   Summary table of useful spectral bands

Table 3.1 summarizes useful spectral bands that could be accommodated in a sensor on a geostationary orbit, along with typical signals expected from the ocean or other targets that such a sensor would view (e.g., clouds). This table is not exhaustive, and the radiance levels and signal-to-noise ratios (SNR) are rough estimates.

3.1.3.1   Some explanations for the selection of spectral bands

The individual band justification in Table 3.1 sometimes refers to algorithms, as examples. It should be noted that some algorithms, specifically neural networks, might use the full visible band set to determine several quantities simultaneously.

3.1.3.1.1   *Visible domain (VIS)*

395 nm: this band can be used to discriminate between absorption by phytoplankton (negligible here) and CDOM (maximum because it increases exponentially towards short wavelengths). CDOM is an important contribution to light absorption in this spectral domain, and often interferes with the determination of chlorophyll-a concentration. CDOM can have a significant effect on biological activity in aquatic systems so it is essential to determine accurately its contribution to total phytoplankton absorption.

412 nm: currently this band is used to discriminate between absorption by phytoplankton and CDOM. The combination of both a 395 nm and 412 nm band would better elucidate the role of CDOM in the optical budget.

442 nm: this is the main absorption peak for phytoplankton chlorophyll-a, used in all chlorophyll algorithms and, in particular, maximum band ratio (MBR) algorithms (OC4V4, O'Reilly et al., 1998; 2000).

470 nm: The relatively large gap between the usual 442 and 490 nm bands in the blue could be filled by a band at 470 nm. This band could prove to be useful when analysing the 2nd order variability of reflectance, in search of specific features due to the presence of typical phytoplankton groups. It could also be used in the MBR algorithm.

490 nm: this is the second band used to determine phytoplankton chlorophyll-a through MBR algorithms.

510 nm: this is the third band used to determine phytoplankton chlorophyll-a through the MBR algorithms. This band is also a "switching point" for the reflectance in Case-1 waters and can be used, for instance, to detect the presence of absorbing aerosols (Nobileau and Antoine, 2005).

560 nm: this is the reference band used to determine phytoplankton chlorophyll-a through the MBR algorithms. It is near the maximum reflectance in turbid Case-2 waters.

590 nm: there are at least two reasons for proposing this band, which does not exist on current or planned ocean-colour sensors. Firstly, the maximum reflectance in Case-2 turbid waters is often at this wavelength, so that the traditional band centered at 560 nm cannot capture this maximum. Secondly, it could be useful to better determine the spectral slope of the particulate backscattering coefficient in open ocean Case-1 waters.

620 nm: This band provides a capability for estimation of the sediment load and might be useful for chlorophyll-a determination in turbid waters.

660 nm: current ocean-colour sensor have bands at either 665 nm (MERIS) or 670 (SeaWiFS/MODIS). Such bands are still affected by phytoplankton fluorescence to some extent, which makes them sub-optimal as a baseline to determine fluorescence line height (FLH). A band at 660 nm would fall outside of the phytoplankton fluorescence peak, so that it can be used optimally as one of the fixed points for the FLH baseline (the second point being the 709 band).

681 nm: this band corresponds to the peak of the natural sun-induced phytoplankton fluorescence. It has a high potential for coastal waters.

709 nm: This band is used as the second point for the FLH baseline. It can also be used to check the atmospheric correction based on NIR bands with $\lambda > 750$ nm, although it is slightly contaminated by water absorption.

Band	λ (nm)	△λ (nm)	L_{min}	L_{ref}	L_{max}	$L_{max,ocean}$	SNR at 250 m[1] & L_{ref}	Use
			W m^{-2} sr^{-1} μm^{-1}					
1	395	10	12	65	580	180	400	Chl-CDOM separation
2	412	20	12	70	550	190	400	CDOM, possibly atmospheric correction above "black waters"
3	442	20	12	65	650	185	400	Chlorophyll, TSM, CDOM
4	470	20	11	60	650	175	400	Specific anomalies of the reflectance spectrum
5	490	20	10	50	665	165	400	Chlorophyll, TSM, CDOM, diffuse attenuation coefficient, Secchi transparency
6	510	20	8	45	620	155	400	Chlorophyll, TSM, CDOM, detection of blue-absorbing dust-like aerosols
7	560	20	6	30	580	132	300	Chlorophyll, TSM, turbidity index, Secchi transparency
8	590	20	5	25	550	120	300	Spectral slope b_{bp}, maximum R in Case-2 waters
9	620	20	4	20	550	95	300	Chlorophyll, TSM
10	660	20	3	15	500	86	300	Chlorophyll, TSM, Chl fluorescence (baseline)
11	681	7.5	3	15	500	82	200	Chl fluorescence (peak)
12	709	10	3	13	450	75	200	Chlorophyll, TSM, Secchi transparency, Chl fluorescence (baseline)
13	750	15	3	11	450	65	150	Atmospheric corrections
14	754	7.5	2	10	400	65	150	Reference for O$_2$ A-band
15	761	2.5	2	6	400	63	30	O$_2$ A-Band (aerosol scale height, clouds)
16	779	15	2	9	380	60	150	Atmospheric corrections
17	865	35	1	6	300	45	150	Atmospheric corrections
18	1020	40	1	4	220	45	150	Atmospheric corrections (turbid waters), cirrus clouds
19	1240	20	0.2	0.88	158	5	65	Atmospheric corrections (turbid waters)
20	1640	40	0.08	0.29	82	2	45	Atmospheric corrections (turbid waters)

1. These values lead to SNR > 1500 in the visible for 1-km resolution (i.e., 4 x 4 250 m pixels)

Table 3.1 Useful spectral bands for ocean colour from a geostationary orbit, including radiometric information and band use. IOCCG minimum requirements includes bands # 2, 3, 5, 7, 12, 13 and 17 (IOCCG, 1998). L_{min} are minimum radiance values that should be measured over the ocean, L_{ref} are typical ocean radiances, L_{max} are maximum radiances corresponding to non-ocean bright targets (clouds), and $L_{max,ocean}$ is the maximum radiance that should be measured above the ocean. The radiance values are indicative and may change slightly as a function of the assumptions used for their derivation.

Other considerations: the "red" bands (590 to 709) can be used as an alternative to determine chlorophyll in high-chlorophyll environments. In such circumstances, the signal in the blue bands vanishes, and the red bands are less affected by atmospheric correction errors.

3.1.3.1.2   Near infrared domain (NIR)

The role of NIR bands is essentially to perform atmospheric correction. Four of the NIR bands listed in Table 3.1 (709, 750, 778 and 865 nm) can be devoted to this task. This is two more bands than on current ocean-colour sensors (which essentially use 778 nm or similar, and 865 nm), which is noteworthy because improvements in the accuracy of atmospheric corrections are one of the most important steps towards improving ocean-colour products in coastal Case-2 waters, as well as many open ocean Case-1 waters. The optimal procedure for using the four bands, instead of only two bands, for atmospheric correction is still being investigated.

The band couple 754nm and 761nm (O_2 A-band plus reference band) can be used to determine the aerosol scale height (Dubuisson et al., 2009) or cloud top height (Preusker et al., 2007). The latter could be used to identify cloud shadows.

3.1.3.1.3   Short-wave infrared domain (SWIR)

In the Short Wave Infrared (SWIR: 1-3μm) there are atmospheric transmittance windows around wavelengths 1040 nm, 1240 nm, 1640 nm and 2130 nm. Historically these have been used only for terrestrial remote sensing applications, because of the very high pure water absorption and consequently very low marine reflectance. The potential of the SWIR range for ocean-colour remote sensing of very turbid waters was first noted by (Wang and Shi, 2005), who used an assumption of zero SWIR marine reflectance for atmospheric correction over waters with non-zero NIR marine reflectance. This idea was extended by (Shi and Wang, 2009), for atmospheric correction of extremely turbid waters where even the SWIR marine reflectance, e.g., at 1240 nm, is not negligible. *In situ* measurements by Knaeps et al. (2012) confirmed that marine reflectance at 1020 nm is not negligible for waters with high suspended particulate matter (e.g., SPM > 100 g m^{-3}) and showed that the 1020 – 1080 nm range can be used for SPM retrieval in such waters. However, there is still considerable uncertainty in the SWIR range for both aerosol and marine properties (including particulate backscatter spectral variation and possible salinity variation of pure water optical properties).

Provided that the engineering challenge of achieving sufficient signal:noise ratio can be met, future ocean-colour sensors could benefit from SWIR bands particularly for turbid water applications. This benefit must be set off against the extra cost of sensors with detectors capable of measuring at wavelengths longer than 1000 nm. This cost may be particularly severe for geostationary missions.

3.2   Radiometric Accuracy, Signal-to-Noise Ratio (SNR)

For clear, Case-1 waters (low pigment concentration) the marine reflectance should be derived with an uncertainty of 5% in the blue. This requirement was first expressed by Gordon (1987; 1988; 1997), and was then translated in terms of maximum reflectance errors in different bands, specifically within the framework of the development of the MERIS atmospheric corrections (Antoine and Morel, 1999). These requirements have been established to allow the discrimination of 10 classes of chlorophyll concentration (Chl) values within each of the 3 decades of Chl between 0.03 and 30 mg Chl m^{-3}, when using a band-ratio algorithm to derive Chl. These classes are distributed regularly according to a constant logarithmic increment of 0.1. Shifting from one class to the next corresponds to a change in Chl by a factor 10 ± 0.1 (i.e., +25% or -20%). In summary: atmospheric correction errors (in terms of reflectance) must be maintained within $\pm1 - 2 \times 10^{-3}$ at 443 nm, within $\pm5 \times 10^{-4}$ at 490 nm, and within $\pm2 \times 10^{-4}$ at 560 nm, in order to allow discrimination of 30 reflectance values. If it is assumed that atmospheric correction errors in the 440 – 500 nm domain are approximately twice the errors at 560 nm, the second requirement (discrimination of 30 Chl values) requires errors within $\pm1 \times 10^{-3}$ at 443 nm (then $\pm5 \times 10^{-4}$ at 560 nm), or within $\pm5 \times 10^{-4}$ at 490 nm (then $\pm2 \times 10^{-4}$ at 560 nm).

It must be stressed that there are no universal requirements in terms of the acceptable errors for atmospheric correction. These requirements are dependant on the subsequent use of the normalized water-leaving reflectances. The above-mentioned requirements remain valid here provided that the pigment algorithm for Case-1 waters is based on a ratio technique. If the ocean-colour products for Case-1 waters are derived using another technique, e.g., a neural network using all bands, these requirements might have to be modified. The minimum radiometric requirement for an ocean-colour sensor is that errors (noise equivalent reflectances) are kept within 2×10^{-4} for all visible bands. This is roughly equivalent to 2.5 $\times 10^{-2}$ and 1.5×10^{-2} W m^{-2} sr^{-1} μm^{-1} in terms of radiances in the blue and red, respectively (at a spatial resolution of ~1 km). These numbers are expressed in terms of the SNR in Table 3.1, for a 250 m nadir resolution and the reference radiance "L_{ref}". It is worth noting that reaching high SNR from the GEO orbit is easy because the integration time can be increased compared to what is feasible with a LEO configuration.

3.3   Calibration

Ocean-colour sensors require highly accurate calibration, in the order of 0.3%, if they are to provide suitably accurate ocean-colour radiances. This is because approximately 90% of the at-sensor radiance is derived from the atmosphere. Typically, a

well calibrated sensor is calibrated to an accuracy of 3 – 5% in the laboratory and this level of accuracy is maintained on orbit by frequent calibration using a solar diffuser or imaging the Moon. However, a 5% calibration error in the at-sensor radiance can equate to a 50% error in the water-leaving radiance after the signal from the atmosphere and reflectances from the sea surface (typically 90% of the at-sensor radiance; Gordon and Wang, 1994; Gao et al., 2000) are subtracted from the signal. To address this issue, some form of vicarious calibration is performed (e.g., Franz et al., 2007). Vicarious calibration is a system calibration where known water-leaving radiances are propagated through the atmospheric correction algorithm to produce at-sensor radiances, and these are compared with the measured at-sensor radiances. Known water-leaving radiances are typically derived from three sources: measurements from a highly calibrated optical mooring, such as the Marine Optical Buoy (MOBY), in uniform low chlorophyll waters with a clear and stable atmosphere (Brown et al., 2007), observations of very clear central gyre waters in the South Pacific and Indian Oceans (Franz et al., 2007) or satellite ocean-colour data from other well calibrated sensors. A geostationary ocean-colour imager should be designed to view these open ocean sites.

A coordinated plan for calibration of a geostationary ocean-colour imager should include pre-launch calibration and characterization, on-orbit calibration using a solar diffuser or on-board lamp calibrator, lunar calibration, cross calibration with LEO ocean-colour sensors, and vicarious calibration. All of these have implications for the design and construction of the imager. The following sections give a more complete overview of each of these requirements. Most of these are identical to requirements for LEO ocean-colour sensors but are included here for completeness.

3.3.1   Pre-launch calibration and characterization

Calibration and characterization of an instrument involves pre- and post-launch measuring of the response of the instrument's sub-systems to controlled, well-characterized stimuli. Most of the pre-launch instrument calibration and characterization is performed under ambient conditions, although specific tests should be performed under environmental conditions which simulate on-orbit conditions as closely as possible (e.g., the thermal vacuum tests).

Absolute radiometric calibration and associated uncertainties/ instabilities should be verified by analysis, modelling, and/or simulation. The process of satisfying the radiometric calibration requirements against both uniform and structured backgrounds will be accomplished through instrument characterization using radiometric traceable standards (e.g., NIST, NPL). The radiance levels applied to the calibration process should be representative of the mission top-of-the-atmosphere radiance levels. The characterization and calibration process should follow well-defined protocols and guidelines established within the international space agencies, for example, as used by NASA for MODIS or ESA for MERIS/OLCI. The geostationary

ocean-colour sensor calibration should incorporate onboard radiometric calibration, for example a solar diffuser. The in-flight calibration plan should include solar diffuser, the monitoring of its Bidirectional Reflectance Distribution Function (BRDF) change due to the space environment, deep space, and lunar radiometric calibration opportunities. Instrument characterization enables the determination of the quantitative performance of the various sub-systems and the overall instrument system-level performance. Tests should include:

- ❖ Radiometric response: At the component level of assembly, the response of focal plane elements and sub-assemblies are characterized for linearity, dynamic range, noise, various cross-talk sources, and dead and marginal performing detector channels. At the sub-system level of assembly, tests with digital electronics determine analog-to-digital-conversion characteristics and anomalies. In the case of scanning instruments, mirror scan angle variations have to be characterized. At the instrument level of assembly, response is characterized with static and active scans. Sensitivity to polarization is also be measured.

- ❖ Stray light performance: Instrument spectral and spatial stray light is characterized on ground. Tests should include simulations of the most challenging target cases (clouds over the ocean and littoral waters). A stray light model should be established and validated to be used in the Level-1B ground processing. This is of particular importance for instruments that feature a large field of view (FOV).

- ❖ Spectral response: spectral characterization of optical elements, sub-assembly, and the instrument includes centre wavelength, band-pass, out-of-band response, cross-talk from other spectral regions, signal level dependent out-of-band response, and others as identified. The instrument slit function, in the case of the spectrometer concept, should be characterized with high accuracy for both the partly-filled or fully-filled slit illumination conditions.

- ❖ Spatial response: Knowledge of point source and edge response, centre of pixel position, edge of pixel position, relative alignment of spectral bands with respect to each other, knowledge of the line-of-sight variations with field-of-regard, and others that may be specific to the instrument design.

Special care should be taken to decide which characterization test should be performed in the ambient environment, or in both the ambient and vacuum environments. In addition to these tests, the pre-launch and on-board calibrations should be characterized to ensure the required on-orbit calibration performance. Specifically, the BRDF of the solar diffuser should be analyzed. Its variation as a function of elevation (instrument finite FOV) and azimuth (seasonal effect), and its stability should be well characterised. Also, there needs to be a careful analysis of the solar diffuser field-of-regard to assure that it is never partially blocked or impacted by stray light from other parts of the spacecraft.

**Box 4: Example of the GOCI Radiometric Calibration Technique**

A 3rd order, nonlinear function was chosen as the GOCI instrument radiometric model, to define the relationship between the digital instrument output (DN, digital number) and input radiance for each pixel, as follows:

$$S(B,i,j) = G(B,i,j) x T_{int}(B) x L(B,i,j) + b(B,i,j,t) x T_{int}^3(B) x L^3(B,i,j) + [T_{int}(B) x O(i,j,t) + F(i,j,t)]$$

where: *L(B,i,j)* is the radiance at instrument input (at-sensor radiance); *S(B,i,j)* is the output digital signal for pixel (i, j) for each spectral band, *B*; $T_{int}(B)$ is the integration time for each spectral band; *G(B,i,j,t)* is the linear pixel gain (including optics transmission, detector response, amplifier gain and analog to digital converter); *b(i,j,t)* is the non-linear pixel gain (3rd order approximation) modelled as a function of time; *O(i,j,t)* is the dark signal offset (including amplifier gain and ADC) modelled as a function of time; and *F(i,j,t)* is the fixed offset (not a function of integration time) modelled as a function of time.

GOCI radiometric calibration strives to calculate the linear gain [*G(B,i,j,t)*] and non-linear gain [*b(i,j,t)*] from the given instrument input radiance [*L(B,i,j)*] and output DN [*S(B,i,j)*]. GOCI is equipped with a solar diffuser for the solar calibration and a diffuser aging monitoring device to monitor the diffusion factor (transmittance) degradation of the solar diffuser due to the space environment (cosmic rays, space debris etc.). Characterization of the solar diffuser aims to find the best fitted function to explain the solar diffuser transmittance with respect to the incident angle of the light. Because the sun is the reference light source, an accurate solar irradiance model and diffuser characterization is very important for GOCI radiometric calibration.

During in-orbit operations, GOCI solar calibration is performed at different radiance levels on the focal plane using different integration times, and different solar incident angles on the solar diffuser with respect to variation of the Sun-Earth distance. The solar diffuser is used to correct non-uniform pixel response over the detector array. The apparent radiance transmitted by the solar diffuser is computed according to the on-ground diffuser bi-directional transmission characterization results, and corrected by calculating the actual solar incident angle during the calibration. Detailed GOCI instrument level solar diffuser bi-directional transmittance characterization has been performed in the on-ground GOCI calibration tests.
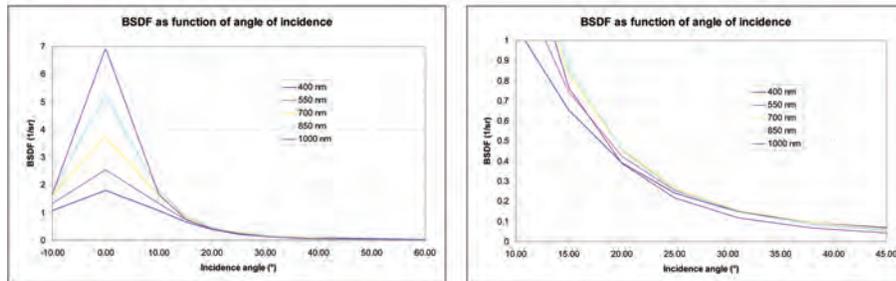
Bidirectional scattering distribution function (BSDF) characteristics of the GOCI solar diffuser with respect to the incident angle.

In the case of SeaWiFS, the additional correction for the azimuth angle of the solar diffuser is necessary. A major contributor of noise in solar calibration comes from the partial solar diffuser azimuth angle characterization during on-ground testing (McClain et al., 2000). For this reason GOCI underwent on-ground characterization with respect to the full range of incident and output angles. Lunar calibration, which does not require a diffuser, is useful as a reference on-orbit calibration to monitor the changes of the instrument's radiometric response. Due to technical and operational difficulties, lunar calibration is not available for GOCI, so the instrument's radiometric response variation is calculated based on the diffuser aging factor derived from radiometric gains between the solar diffuser and the diffuser aging monitoring device. The measured absolute radiometric calibration error in on-ground tests, including measurement uncertainty, is below 4%.

3.3.2 On board calibration system

An on-board accurate calibration system is essential for monitoring the performance of the sensor in space. The preferred on-board calibration system is a solar diffuser, or other system, that allows frequent measurement of the solar signal. The sun is the light source for the remote sensing reflectances that we measure from the ocean, and therefore calibration relative to the sun is optimal. There are two main issues with solar diffusers. Firstly, they age as they are exposed to the sun. Secondly, because they are diffusers they present a different image field than the normal sensor field-of-view when imaging the ocean. Means to monitor in-orbit degradation of the solar diffusers should be considered, such as incorporating a redundant diffuser, as implemented in MERIS and GOCI. The diffuser must be protected from exposure to contamination and UV radiation when not used for the radiometric calibration. Great care must be taken to assure that the solar diffuser does not receive a signal from other parts of the spacecraft when doing calibrations. For example, part of its field-of-view may be obscured under certain conditions, or reflections of sunlight bouncing off parts of the spacecraft could give a false signal.

3.3.3 On-orbit stability monitoring using lunar calibration

From the vantage point of a geostationary ocean-colour imager, the Moon will appear behind the Earth several times each month. Stone et al. (2005) built on their experience using lunar calibration for SeaWiFS, and suggested a technique for using Moon imaging for the on-orbit stability monitoring of a geostationary imager. Stone et al. (2005) use the NOAA GOES-12 imager as an example system (Figure 3.3). The field of regard for full-disk imaging is 20.8° E-W x 19° N-S, while the Earth disk diameter is about 17.4° from geostationary orbit, resulting in margins of 1.7° and 0.8° respectively. From a geostationary orbit the Moon's diameter ranges between 0.44° and 0.51°, thus for the GOES visible imagers with 1-km ground sample distance (GSD) the full Moon at perigee will be imaged in 318 N-S lines by 556 E-W pixels. The Moon appears skewed in high-resolution images, primarily due to satellite orbital motion during acquisition. However, geometric correction is straightforward.

By integrating the lunar disk image to an equivalent irradiance and using knowledge of the sensor's spectral response, a calibration can be developed through comparison against the USGS Robotic Lunar Observatory (ROLO) model (Kieffer and Stone, 2005). With this approach Stone et al. (2005) note that calibration precision similar to those achieved for SeaWiFS (±0.3% stability, Barnes et al., 2004) should be possible for a geostationary ocean-colour imager. Because the Moon is an inherently stable source, the lunar calibration technique is a good way to cross calibrate with other sensors that also use Moon imaging, including low Earth orbit ocean-colour sensors and other geostationary ocean-colour sensors.

Advantages of using the Moon as a stable target for monitoring the sensor
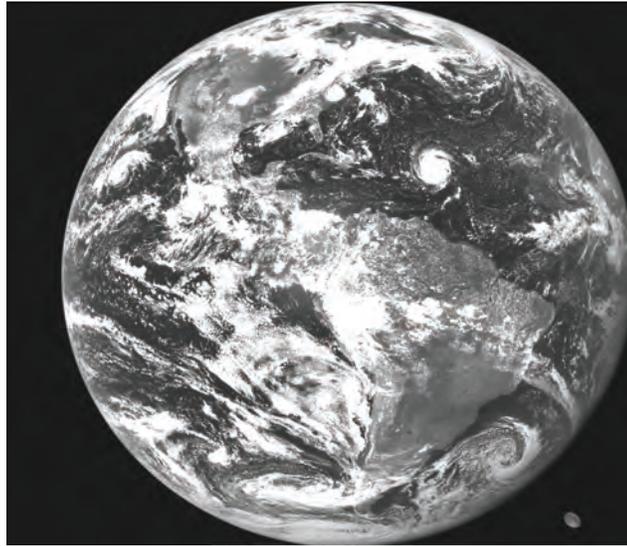
Figure 3.3 GOES-12 visible channel full disk image acquired on 30 August 2004, 17:45:14 UTC. The nearly full Moon is captured in the lower right corner. Image courtesy of Thomas C. Stone, US Geological Survey.

throughout its life are its reflectance stability (less than one part in 10^8 per year, Kieffer, 1997), low cost and the fact that it is available for all ocean-colour wavelengths. Disadvantages are that it is a small source (FOV only partially illuminated in some sensor designs), the uncertainties of absolute calibration are rather high (> 5%) and manoeuvres are required for nadir-viewing LEO sensors.

3.3.4   Cross calibration with LEO ocean-colour sensors

For a GEO sensor there are many advantages to using cross-calibration with low Earth orbit (LEO) ocean-colour sensors. It is possible to match data collection closely with LEO sensors and a GEO imager. Unlike vicarious calibration, which is done by comparison to a single point or area on the ground, comparisons between two sensors makes it possible to match a full scene covering a variety of environments and sea truth locations (within the limits that comparison is only possible for identical geometries). Several LEO sensors are very well calibrated and use vicarious calibration; cross-calibration can transfer that advantage to the GEO imager even if it cannot image the vicarious calibration site.

The challenge is to address the specific sensor characteristics for match-up with the GEO imager. First, it is essential to match spectral channels to GEO imager channels. If both sensors are filter radiometers, then it can be difficult to match the specific filter functions of the two sensors which are always different, unless the filters for both sensors come from the same batch. For this application LEO spectrometers are easier to match to GEO imager filter channels than other filter

channel instruments. If the GEO sensor is a spectrometer, then in theory it should be able to match the spectral channels of any LEO sensor. The second issue is to match ground sample distance and sampling locations for the two sensors. The geometries are different, but data mapped to the same Earth projection and then binned to a common pixel size will be good for comparisons. This method may require modelling the BRDF depending on the site and imaging geometries for the different sensors.

All sensors have unique artefacts in the data. For well calibrated sensors, these artefacts are removed in the calibration and processing so that they produce well geolocated and accurate remote sensing reflectances for the sea surface. For example, NASA's MODIS on Aqua continues to operate well and provide stable well calibrated data (http://modis.gsfc.nasa.gov/). However, MODIS has filter channels with specific shapes, thus if the GEO imager is a filter imager, the band passes will not match exactly unless the filters for both sensors are from the same filter fabrication run. Also, MODIS has a two sided scan mirror with some variable reflectance and polarization effects. NASA has developed good correction tables for these effects and can produce accurate at-sensor radiances. Additionally, MODIS is vicariously calibrated using MOBY to calibrate the combined sensor calibration and atmospheric correction to give accurate water leaving radiances. To cross calibrate a GEO sensor with MODIS it is best to use geolocated water-leaving radiances from both sensors. MODIS ocean-colour data has a 1000 m GSD, which is larger than the 300 m GSD anticipated for most GEO sensors. However the GEO sensor data can be binned to match the MODIS data for comparisons.

ESA's MERIS instrument is another well calibrated sensor that would have been a good choice for cross calibration with a GEO sensor. MERIS provided stable well calibrated data for over 10 years (http://envisat.esa.int/handbooks/meris/). Follow-on sensors of the same design (OLCI) are planned for the Sentinel-3 satellites to extend the ocean-colour time-series for decades. MERIS (and OLCI) are high resolution spectrometers binned to the selected channels. This approach gives regular channel shape and is more readily matched to GEO imager filter shapes. MERIS (and OLCI) full resolution data is 300 m GSD data which is close to the recommended GEO imager pixel size. MERIS vicarious calibration using MOBY and BOUSSOLE data has also been conducted. Like MODIS, OLCI will be a good choice for cross-calibration with a GEO sensor.

3.3.5   Ocean site vicarious calibration

Vicarious calibration is a system calibration where known water-leaving radiances are propagated through the atmospheric correction algorithm to produce at-sensor radiances and these are compared with the measured at-sensor radiances. Typically, the water leaving radiances measured at the sea surface are propagated to the sensor altitude by running the atmospheric correction model in reverse (atmospheric

correction models are an inversion of a forward radiative transfer model, so for this application the forward radiative transfer model is run). Note that when using buoy-based references, ocean site vicarious calibration is used to refine the combined calibration and atmospheric correction and only provides calibration data for the ocean channels. It is not a replacement for good pre-launch and on-orbit calibration of the sensor. On-orbit calibration includes all of the sensor channels and, using a solar diffuser or other on-board system, it can be done as frequently as several times a day. Possible vicarious calibration sites include:

❖ MOBY (Marine Optical Buoy), a U.S. optical buoy near the Hawaiian Islands. MOBY has provided accurate water leaving radiances for over a decade and has been used for the vicarious calibration of SeaWiFS, MODIS and other sensors (`http://data.moby.mlml.calstate.edu/moby248/index.html`).

❖ BOUSSOLE, a French Buoy providing accurate radiances in the Mediterranean Sea. BOUSSOLE was used in conjunction with MOBY for MERIS vicarious calibration (`http://www.obs-vlfr.fr/Boussole/html/project/introduction.php`).

❖ AERONET sites with SeaPRISM sensors can also be considered, which are located on towers or platforms in coastal waters. SeaPRISM data is good for validation of coastal products, but because of the highly variable nature of coastal waters, they are not recommended for vicarious calibration (`http://aeronet.gsfc.nasa.gov/new_web/ocean_levels_versions.html`).

Franz et al. (2007) have also used observations of very clear water sites in the South Pacific and Indian Ocean Gyres for vicarious calibration. The argument is that these sites have very stable biology and chemistry and based on years of observations with SeaWiFS, these sites have very consistent water-leaving radiances that can be modelled and used for calibration of other sensors. The geostationary orbit may offer advantages for vicarious calibration because the atmosphere is measured through different path lengths during the day. For a stable atmosphere this may enable improved corrections to be made in a similar way to use of Langley plots for calibration of sun photometers.

3.3.6   Calibration strategy

Like other ocean-colour sensors, a GEO imager should be well calibrated and characterized in the laboratory before launch. To provide well calibrated data over its lifetime the sensor should be designed to allow for regular on-orbit and vicarious calibration. A GEO imager should include a solar diffuser type on-board calibrator and the imager should be capable of full disk scanning. This will allow for monthly imaging of the Moon providing an independent check on the stability of the sensor. If possible it should image vicarious calibration sites (e.g., MOBY or BOUSSOLE) and the South Pacific or Indian Ocean central gyres. The best approach is to maintain the calibration with solar diffuser and Moon imaging, and then refine calibration coefficients with vicarious calibration. Additionally, it is preferable to cross calibrate

the GEO sensor with LEO imager. This approach makes it possible to check calibration over coastal and open sites, not just the vicarious calibration site. Also, LEO imagers can be used to cross calibrate between GEO imagers to provide a uniform global image from GEO.

## 3.4 Is the Technology Advanced Enough to Answer These Requirements?

The maturity of the technology required for a GEO-based ocean-colour instrument is very high. The most remarkable progress made in the last years is in the area of on-board calibration techniques based on solar diffusers, detectors and spectral filters.

On-board calibration of radiometric measurements in remote sensing is often achieved by observation of a sun-illuminated reflectance secondary standard using previously calibrated reflecting diffusers. Three types of diffuser materials have been used for ocean-colour instruments: surface diffuser (aluminum plate coated with YB71 paint, for SeaWIFS), volume diffuser (e.g., Spectralon, which is a proprietary thermoplastic formulation of polytetraflouroethylene for MERIS and MODIS) and Quasi Volume Diffuser (a piece of quartz which is roughened at two sides, used for GOCI). All these diffusers are known to age because of photochemical reactions of molecular contaminants under sun UV radiation in vacuum. A decrease of the diffuser reflectance properties has been experienced in all ocean-colour sensors with the largest effect in the blue channels. Several mitigation techniques can be implemented to minimize the ageing effect. A reduction of the outgassing of organic materials can be obtained by proper vacuum bake-out of the diffuser plate. Shielding from contamination sources during the on-ground assembly, integration and testing phases of the instrument and the satellite is possible with local purging with dry clean nitrogen. Furthermore the diffuser has to be systematically protected from contamination and Sun/Earth light exposure when not in operation for instrument calibration. The efficiency of these methods has been demonstrated for MERIS, whose nominal diffuser reflectance decreased by less than 2% in band B1 (412.5 nm) after 9 years in space. Two techniques have been successful: the ratioing radiometer (MODIS), and the secondary diffuser deployed at a low frequency to monitor the degradation of the frequently used diffuser (MERIS, GOCI). Despite these efforts, methods for monitoring on-orbit the diffuser bi-directional reflectance factor degradation in-flight need to be implemented to reach the high level of radiometric accuracy required for ocean colour.

Box 5: Example of the GOCI Instrument

   The baseline instrument concept of GOCI is a compact three-mirror anastigmat telescope with a 140 mm pupil diameter and a 1171 mm focal length, featuring a CMOS array of about 2 Mega-pixels. The 8 spectral channels are obtained by means of a filter wheel implemented close to the focal plane. The operating principle consists of imaging a portion of the specified image frame, termed a slot. A pointing mirror provides a bi-dimensional circular scanning on the Earth. By successively pointing 16 pre-defined directions, the array is moved in the field-of-view to cover the complete image area. Each slot is imaged over the 8 spectral channels, plus a dark position for offset monitoring and correction. The image is acquired for two gain levels, corresponding to sea and cloud radiance levels, respectively, and the image data are sent in real-time to the satellite. One single slot acquisition period takes about 90 seconds, leading to an overall image acquisition within less than 30 minutes. The following is a brief description of GOCI instrument subsystems and operation concept.

   The calibration/shutter mechanism contains the calibration devices. When GOCI is not operating, the shutter closes the instrument cavity, providing a stable thermal environment. The shutter is moved either to the open position for nominal Earth imaging, or to one of the calibration positions when the sun is available in the calibration field-of-view. For the protection of the diffuser aging monitoring device, additional radiation shield equipment is implemented under the shutter cover.
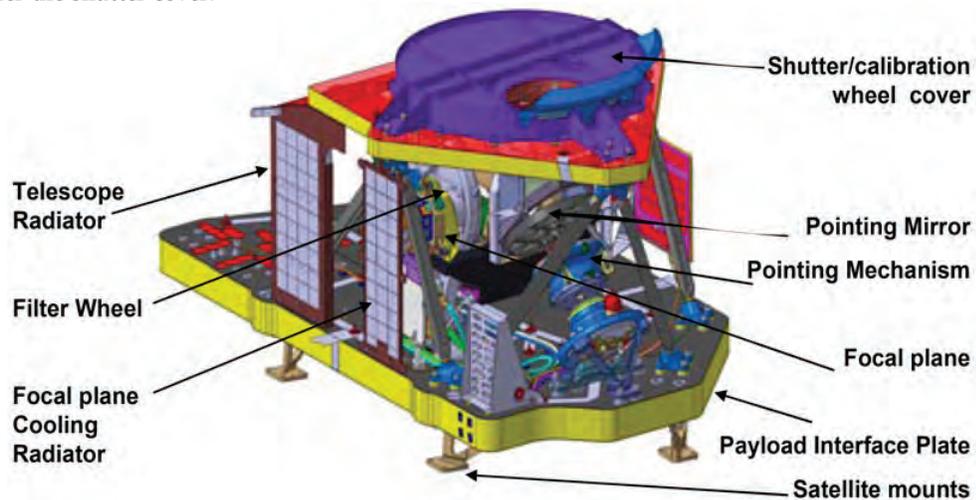
GOCI design with TMA telescope and 2D CMOS focal plane array

   The pointing mirror is supported by a 2-axis circular scanning mechanism; the beam is then folded by approximately 90°. All the optical components lie in a plane perpendicular to the incident beam. The pointing mirror and the three mirrors of the three-mirror anastigmat (TMA) telescope are all made of SiC. One folding mirror (about 90° fold angle, also made of SiC) simultaneously provides a compact instrument and compensates for the polarization generated by the pointing mirror, the folding plane being perpendicular to the pointing mirror folding plane. The filter wheel includes eight optical filters and a dark position allowing dark signal acquisition for offset compensation.

   The detection module is comprised of the detector array and front-end electronics. The array is a custom CMOS image sensor, featuring rectangular pixel size to compensate for the oblique projection over Korea, and electro-optical characteristics matched to the specified instrument operations. The Instrument Electronics Unit (IEU) includes image data processing, mechanism control, interface telemetry and housekeeping functions.

   All the equipment, except for the IEU, is mounted on a common structure (Main Unit), which is in turn mounted on the Earth face (+Zs) of the spacecraft. The primary structure, also made of

SiC, holds the TMA mirrors, the folding mirror and the focal plane assembly. It is mounted on the GOCI Payload Interface Plate (PIP) through bipods ensuring a high stability of the structure. The pointing assembly, the filter wheel assembly and the front end electronics are directly mounted on the GOCI PIP. The secondary structure, fixed to the PIP, surrounds the other equipment, supports the radiators and holds the shutter wheel. It is covered with Multi Layer Insulation (MLI) to guarantee the thermal stability of the main unit cavity. The Main Unit mounting is adjusted to provide the desired pointing direction towards Korea. The instrument electronics are gathered in a single unit (IEU), located inside the platform, close to the instrument main unit. The front-end electronics provides a first amplification and impedance adaptation to allow a safe transport of the signal to the processing electronics within the IEU. Heaters directly controlled by the spacecraft perform the thermal control of the instrument cavity.

CCD (Charge-Coupled Device) and CMOS (Complementary Metal Oxide Semi-conductor) image sensors are two different technologies that can offer excellent imaging performance when designed properly. While CCDs have a low noise and high dynamic range, CMOS features lower power consumption, better radiation tolerance, and high speed imaging capability. Moreover CMOS devices do not suffer from the undesired frame transfer smear signal that needs to be compensated in CCD sensors. Both sensors have been used for ocean-colour instruments (CCD for MERIS, CMOS for GOCI) and the choice depends on the application. Specific to geostationary-based instrument application is the need to develop large 2D arrays with small pixel pitch, to image the Earth disk in a step and stare mode with a minimum number of slots. Designing small detector pitch is now possible with the use of smaller lithography nodes (e.g., 0.18 μm). Improvement of the dynamic range and sensitivity of CMOS devices is in progress.

One of the issues to be addressed for a filter instrument such as GOCI is the stability of the filters. The optical coating community has greatly improved the environmental stability of interference filters through the incorporation of energetic processes into the deposition chamber. Hard-coated spectral filters manufactured with ion-assisted deposition or ion-beam sputtering feature remarkable stability with respect to pressure changes, as occurring during the launching phase in space applications (air/vacuum effect) or when exposed to space radiation. Shifts of the filter central wavelength lower than 0.1% have been demonstrated. These filters also have lower scattering and absorption properties.

Chapter 4

Elements of Geostationary Ocean-Colour Missions

4.1 Revisit Frequency

As for the temporal requirements, IOCCG Report No. 2 (1999) recommends one-day coverage as a minimum requirement for resolving events occurring every 2 to 10 days in continental shelf and slope waters (generally in response to wind forcing). In coastal regions, however, multiple observations during a single day are required to observe tidal and diurnal wind signals directly, which are difficult or impossible to observe with current single polar-orbiting satellites. Because semi-diurnal tides have a cycle of about 12 hours, a 3-hour temporal resolution is the minimum requirement for a good description of the sine wave. This requirement becomes twice as severe (1.5-hour) for tidal resuspension processes which have a period half that of the tidal cycle. Also, river runoff and wind-driven coastal currents can reach several knots. Therefore, the threshold requirement is to sample the coastal waters once every three hours with the goal of half an hour, similar to the sampling frequency of geostationary meteorological satellites.

The logic here is twofold: on the one hand having a high revisit frequency allows sampling of diel variability under appropriate conditions. On the other hand, at least one valid observation can be acquired per day when cloud cover, or the observation geometry, prevents resolving the diel cycle. Figure 4.1 provides an example of the density of observations that could be obtained by combining data from GEO and LEO satellites (Sentinel-3 in this example).

4.2 Spatial Sampling

Most coastlines are very complex with many sounds, bays and estuaries. In terms of area coverage, the 300 m spatial resolution (at nadir; this is implicit in all subsequent sections) recommended for a geostationary ocean-colour imager is approximately 10 times better than the ~1000 m resolution currently available from polar orbiting ocean-colour imagers (90,000 m^2 per pixel compared to 1,000,000 m^2). This higher spatial resolution will greatly enhance the ability to image and monitor complex areas. For example the higher spatial resolution will make it possible to image the Potomac River and other rivers feeding into the Chesapeake Bay that are missed at 1-km resolution (Figure 4.2).
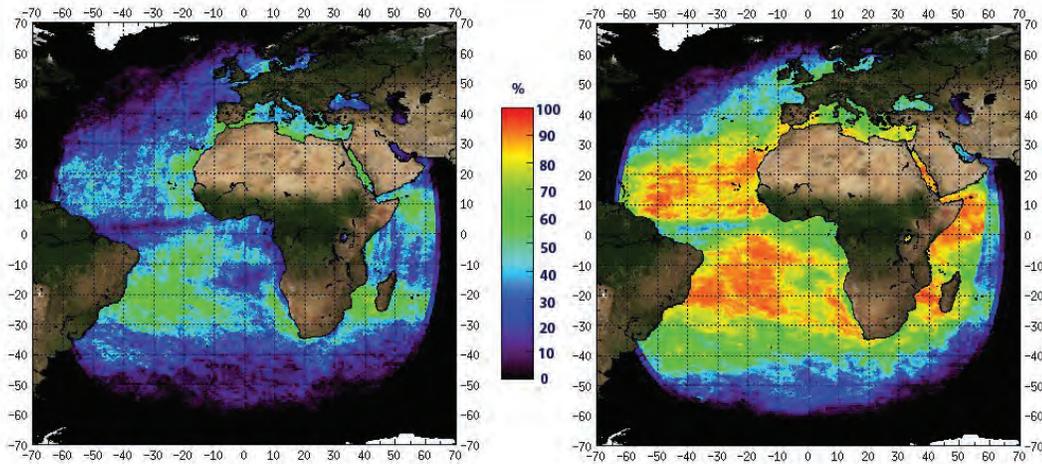
Figure 4.1 Example of monthly data availability in March for two mission configurations: a constellation of two Sentinel-3 satellites (left), and the same one complemented by a GEO with 1-h revisit (right). Data availability takes into account realistic cloud coverage (Meteosat Second Generation (MSG) data for year 2007) as well as geometrical constraints (air mass < 5, glint reflectance smaller than 5 x 10^{-4}). For a given pixel, availability implies at least one clear observation per day i.e., 50% means at least one useable clear observation for half of the days in the month. The observation area is constrained by the MSG observation area (MSG clouds used). Image courtesy of ACRI-ST, Sophia-Antipolis, France.
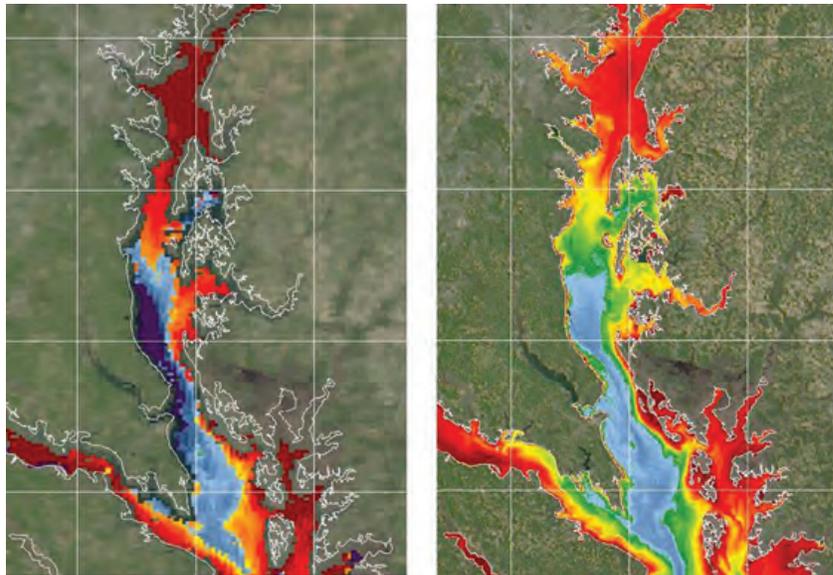
**Figure 4.2** Left, MODIS 1-km resolution image of water clarity for the Chesapeake Bay and the Potomac River (lower left corner of image) as it feeds into Chesapeake Bay. Right, 250-m resolution water clarity image simulated from the MODIS 1-km ocean-colour channels and the 250-m land channels. The land water interface is shown in white. Image reproduced from Davis et al. (2007), reprinted with permission from SPIE.

Outside of the bays and estuaries, the greatest impacts of HABs, as well as other features of interest in the near coastal ocean, such as sea grass beds and coral reefs, require a higher spatial sampling to resolve unique features of interest. Pixel contamination by land reflectance, and the inability to separate unique features, are just a few of the problems that are seen in the data from low spatial resolution ocean-colour sensors. A study by Bissett et al. (2004) to determine the optimal ground sample distance (GSD) for turbid coastal waters, suggests that variance in near shore colour requires a GSD of < 100 m to resolve the changes in high resolution reflectance measurements. In addition, many of the ocean-colour algorithms rely on non-linear equations to retrieve environmental data records (EDRs). In the coastal zone, where significant changes in optical and ecological properties occur on the scale of meters, the blending of the reflectance signal may result in EDRs that are not representative of true environmental conditions. In a study by Davis et al. (2007), airborne hyperspectral imagery was used to address the spatial resolution necessary to image a harmful algal bloom in Monterey Bay. For optically-deep waters in Monterey Bay, 100 m GSD imaged the essential features including the HAB. An intermediate resolution (300 m) worked well for most conditions and is far more useful than the standard 1 km imagery.

Higher spatial resolution is critical to monitor small-scale phenomena in coastal waters, such as red tides, oil spills, sewage outfall and thermal discharge from the Nuclear Power Station. Some coastal and estuarine ecosystems, such as wetlands or coral reefs, are patchy and small in size, and a spatial resolution of 1 – 30 m would be required for most cases (Klemas et al., 2003). Such high spatial resolution, with appropriate spectral and SNR requirements, is not practical in the current and foreseeable future because spatial resolution competes with frequency of coverage, SNR, and number of bands. In IOCCG Report No. 2 (1999), the spatial and temporal requirements for coastal applications of ocean-colour measurements are discussed. The report recommended imagery with 0.1 to 0.5 km pixels to provide useful scientific information for most bays and estuaries as a realistic goal for the next decade (IOCCG Report No. 2, 1999). At present, MERIS full resolution and MODIS high resolution images already provide this level of spatial resolution. According to the experience of MERIS and MODIS, the preferred spatial resolution for coastal application is around 300 m.

4.3   Regionally-Focused *versus* Global Missions

Most of the geostationary ocean-colour missions proposed to agencies over the past decade were conceived as regionally-focused missions. This was the case, for the proposed (unselected) Special Event Imager and the Hyperspectral Environmental Suite. The underlying logic is that increasing the frequency of observation must be accompanied by an increase of the spatial resolution, which is generally technically

incompatible with the observation of a large portion of the Earth. These missions were oriented towards the monitoring of events rather than towards a basin-scale or even a global vision. This concept still drives most of the existing projects. The underlying idea is that the coastal domain is the only area where rapidly changing phenomena occur which would need a high revisit frequency, however, this is a very restrictive view. It is also desirable to observe the open ocean from a GEO orbit, for two main reasons:

1. There is a diurnal variability in the open ocean, whatever the trophic state, and this variability is not only important *per se* (to increase fundamental knowledge), but characterizing these diurnal fluctuations opens the way to determining the productivity of the ocean, at least in some circumstances. This is one of the most important parameters for which we need a dramatic increase in knowledge, compared to what is possible with today's LEO ocean-colour satellites.

2. The GEO observations will permit full daily coverage above the open ocean, which is also required for better understanding and modelling the coupling between the physical and biogeochemical environments. Again, the dual aspect of GEO observations is manifest here (i.e., obtaining information on diurnal variability, when feasible, or obtaining at least one good observation per day).

Therefore, a reasonable goal would be to observe all oceanic and coastal zones present in the entire Earth disk from a longitude that allows maximizing the observed ocean area. The exploratory nature of these missions should also be considered so that restricting their area of interest *a priori* might be counter-productive. The observation area is restricted, however, to acceptable observing geometries. The limits here are set by physical constraints (the marine signal cannot be accurately determined when it represents 1% or less of the total signal) and also by the capabilities of atmospheric correction schemes (anticipating improvements from future ocean-colour sensors in the GEO orbit).

A limit can be set to a total air mass of 5. This corresponds to a nadir view with a sun zenith angle of 80° or to the sun zenith angle and the viewing angle both equal to ~67°. This limit is not arbitrary. It has been set by Ding and Gordon (1994) who recommended 70° in a plane-parallel system. It is also typically above this threshold of a total air mass 5 that current atmospheric correction schemes fail in retrieving the marine signal with the desired accuracy (IOCCG, 2010). An example observation area is shown on Figure 4.3, where important oceanographic areas are indicated (in particular the so-called "large marine ecosystems").

4.4   Geostationary *versus* Geosynchronous Orbits

The geosynchronous orbit is inclined with respect to the equatorial plane, which induces a movement of the satellite around the equator. When the orbit remains
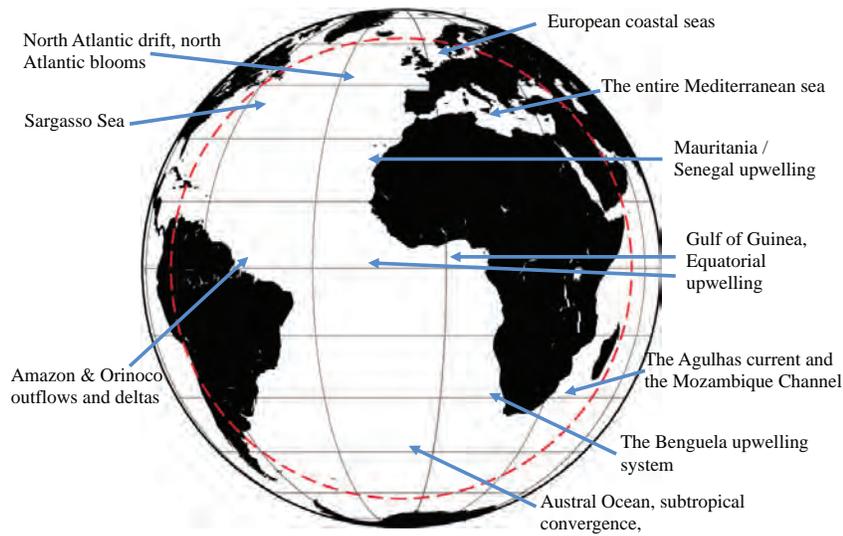
Figure 4.3 Envelope of a typical observation area above the Atlantic Ocean, Africa and Europe, showing some of the large marine ecosystems and other areas of high oceanographic interest. The dashed red circle corresponds roughly to an air mass of 5 for the equinox.

circular, the satellite ground track describes a figure-of-eight (a lemniscate) during the sidereal day. The inclination represents the highest north and south sub-satellite latitudes. The pass of the satellite at a given point shifts each day within a one year period, as depicted in Figure 4.4. Many possibilities exist in terms of when (with respect to solar time) the satellite is at the northernmost part of the lemniscate. These parameters can be optimized as follows:

❖ Maximise inclination to observe high latitudes with a zenith angle as low as possible, yet ensure that coverage of the regions opposite the nadir are not lost;

❖ Avoid some geometrical conditions (e.g., sunglint);

❖ Minimise the inclination for lowering the satellite speed, which can lead to more complex image processing if too high.

The advantage of this orbit is that it allows observation of areas at higher latitudes as compared to the geostationary orbit. The 10° inclination chosen here for illustration purposes leads to the patterns shown in Figure 4.5 in terms of air mass and for a satellite longitude of 10°W (total air mass being $[1/\cos(\theta_s) + 1/\cos(\theta_v)]$). The simpler geostationary orbit corresponds to a sub-satellite point on the equator and at a longitude to be optimized according to mission objectives.
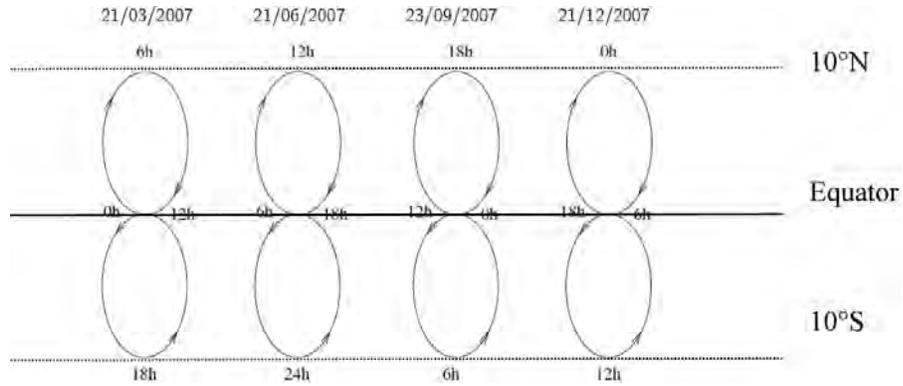
Figure 4.4 Times of satellite pass on an inclined geosynchronous orbit, over the course of a day and the year. Reference time at the top of the figure-of-eight is chosen to be 6:00 am on the vernal equinox. Note that the direction of the satellite displacement can be reversed. Image courtesy of ACRI-ST, Sophia-Antipolis, France.
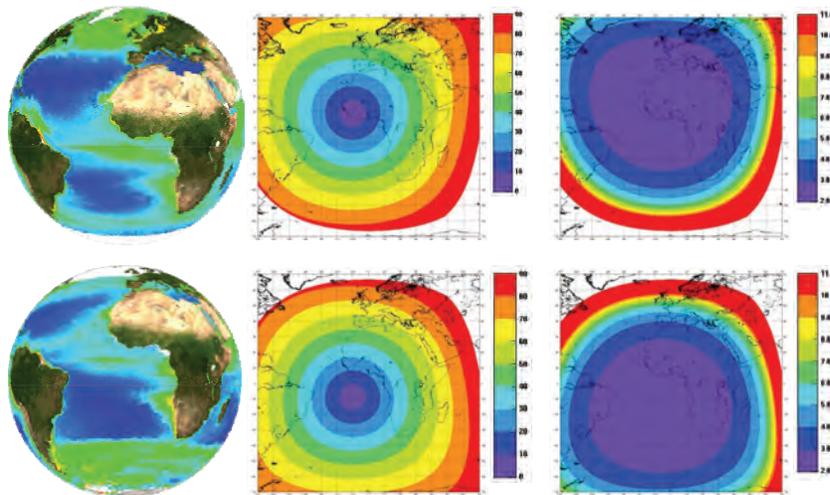

Figure 4.5 Earth view from a geosynchronous orbit at noon, at a position of 10°W, with 10° inclination (top: 21 June; bottom: 21 December). From left to right: climatological Chl distribution from the GlobColour data set, view angle and total air mass. Images courtesy of ACRI-ST, Sophia-Antipolis, France.

Geo-synchronous	21 Mar/21 Sept			21 Jun			21 Dec		
	Q1	Q2	Q3	Q1	Q2	Q3	Q1	Q2	Q3
Latitude 0°	2.15	266 m	8.7	2.25	266 m	9	2.25	266 m	9
Latitude 40°	2.60	281 m	7.8	2.36	270 m	9.3	3.49	303 m	3.7
Latitude 60°	4.75	566 m	0.9	3.80	466 m	3.4	13	775 m	0
Geostationary									
Latitude 0°	2.17	300 m	6.2	2.26	300 m	6.4	2.26	300 m	6.5
Latitude 40°	2.97	466 m	7.8	2.72	466 m	9.2	3.87	466 m	2.3
Latitude 60°	5.1	852 m	0	4.38	852 m	1.64	11.3	852 m	0

Table 4.1 Comparison of geosynchronous and geostationary performances in terms of minimal air mass (Q1), pixel size (Q2) and number of clear acquisitions during one day (Q3) over the course of a year, for three latitudes (0°, 40°, 60°). The colour highlights the performance as satisfactory (green), acceptable (orange) or non acceptable (red).

When dealing with passive radiometry, solar and viewing geometries are key drivers for the performance. From a geostationary perspective, both evolve strongly with latitude as illustrated in Figure 4.5. The viewing zenith angle (θ_v) is constant for every pixel within the observed disk, from zero at the equator, reaching 80° over 60°N latitude. The solar zenith angle (θ_s) varies with the sun elevation over the course of a day and over the year. Both variables merge into the air mass fraction. Standard atmospheric corrections schemes require an air mass lower than ~5 (IOCCG, 2010). A comparison of performances between a geosynchronous orbit with an inclination 30°, and a purely geostationary orbit is presented in Table 4.1 in terms of:

❖ lower air mass during one day (Q1);
❖ lower pixel size during one day (Q2);
❖ number of (clear) acquisitions during one day (assuming 1 h frequency) (Q3) for three latitudes (0°, 20°, 60°) and four seasons.

At 60° latitude, geostationary observations are not feasible whereas geosynchronous observations are possible from March to September. At 40° latitude, geosynchronous observations are better than geostationary observations for all criteria. At 0° latitude, geostationary and geosynchronous observations are equivalent. The advantage of the geosynchronous orbit in terms of viewing conditions is compensated by a reduction of acquisition time compared to the permanent observation from the GEO due to the time spent along the lemniscate. Also there is a drift of about 1° per day in longitude with respect to the sun. Therefore, if the satellite initially reaches its maximum latitude at noon, it will be at the minimum latitude 6 months later.

At initial orbit injection, it is possible to select any time of day for the node crossing and, therefore, the time of passage across the target region (e.g., Europe). However, the time of day will not be constant as the Sun rotates with respect to the
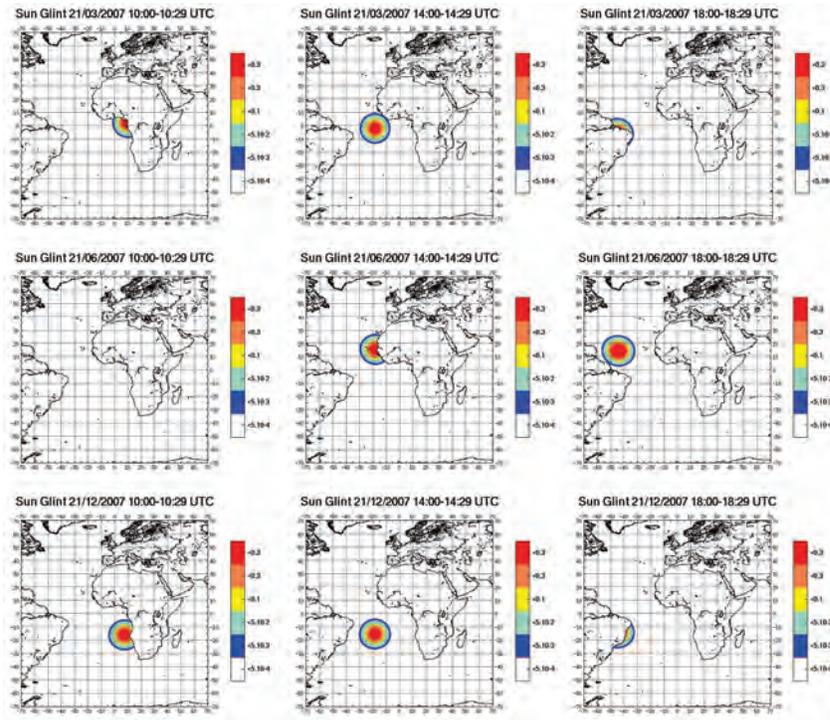
Figure 4.6 Sunglint patterns (reflectance higher than $5.E^{-4}$) from a GEO sensor at 10°W and 10° inclination, simulated with a wind speed of 3 m s^{-1} for three time periods (10:00, 14:00 and 18:00 UTC, left to right) and days in the year (21 March, 21 June, 21 December, top to bottom). Increasing the wind speed would enlarge the patch but decrease the intensity. Image courtesy of ACRI-ST, Sophia-Antipolis, France.

orbit node since the orbit node is fixed inertially. Therefore, throughout the year, the local time of passage over the target region will vary through 24 hours. As a result of the variation of the local time of the node crossing, it is not possible to provide coverage of a given area (e.g., Europe) with a single satellite. More than one satellite is thus required to meet the mission requirements of year round, daytime coverage.

4.5   Sunglint Patterns and Avoidance

The specular reflection of the solar radiation at the sea surface is one of the biggest causes of data loss in ocean-colour missions. In the MERIS mission for instance, the western part of the tracks is often impacted by sunglint and lost for further data exploitation. Although the use of algorithms may correct for sun-glint to some extent (e.g., MERIS POLYMER algorithm, Steinmetz et al. 2011), it is recommended that such situations be avoided for a proper retrieval of the marine signal. Secondary objectives might require sunglint observations in order to study certain patterns

such as oil slicks (Hu et al., 2009) and internal waves (Jackson, 2007).

Characterisation of the sunglint pattern is thus an important issue for GEO ocean-colour missions. Simulations using the Cox and Munk isotropic model (1954), with typical wind speeds, show that a geostationary orbit is very advantageous to avoid sunglint (Figure 4.6): the patch is restricted to a small area, moving from east to west around the equator. In this specific example, the patch never impacts European coasts, for instance, and there is always a sufficiently long time period without sunglint for other regions.

4.6   LEO/GEO Synergy for Ocean-Colour Sensors

4.6.1   Complementarity in terms of oceanographic phenomena

Dickey et al. (2006) documented the time-space continuum of oceanographic processes. Figure 4.7 illustrates this concept and also shows that space and time scales are coupled. Multiple instruments and platforms are therefore required to sample the ocean comprehensively at a given epoch, and a continuum of these observation tools is needed to embed observations in a long-term vision (the "climate" ellipse on the top right corner of Figure 4.7). Another consequence stemming from the analysis of scales is that increasing the frequency of observations should accompany an increase in spatial resolution. For instance, there would be no justification for observing the ocean once a week at meter-scale or making low-resolution observations every hour. Technical and programmatic trade-offs are, however, inescapable when designing observation missions.

The superimposed orange and green boxes on Figure 4.7 show the sampling domains of typical LEO and GEO ocean-colour satellites, respectively, when considering data from one entire mission (e.g., the 5–10 years provided by missions such as SeaWiFS or MERIS). When data from successive missions are merged, the upper limit of these boxes (time scale) move toward the centennial scale. If data from appropriately positioned GEO sensors are merged, the right side of the green box moves towards the global scale. The dashed line represents the domains accessible through merging of GEO and LEO observations over decades. This figure is a first demonstration of the complementarity between LEO and GEO observations of ocean-colour radiometry.

4.6.2   Coverage synergy

Differences in geometry and revisit time between the GEO and LEO orbits offers the possibility of two types of synergy: when both LEO and GEO sensors observe the same target at the exact same time there is a possibility of cross-calibration; or if only one instrument can see the target during the day they add complementary coverage. The maps in Figure 4.8 show these modes for the solstices and equinoxes
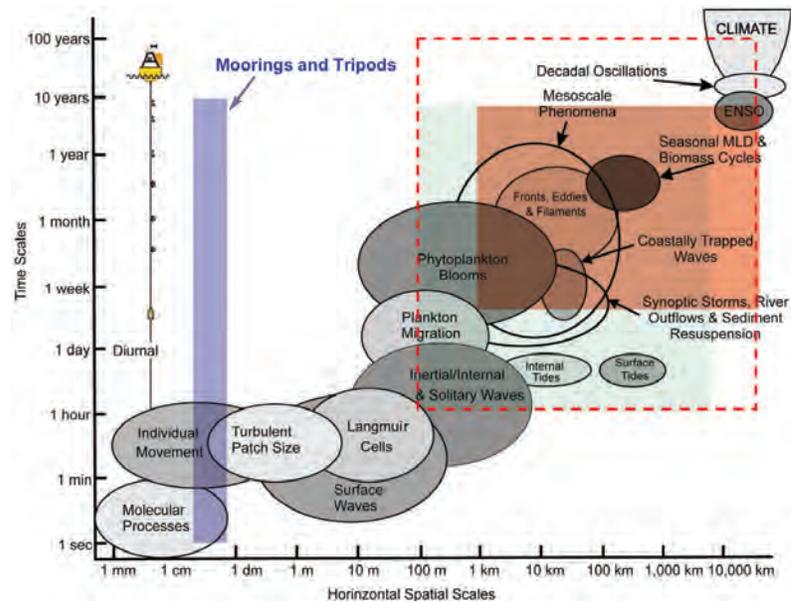
Figure 4.7 Time scales vs. horizontal space scales diagram illustrating physical and biological processes overlain with sampling domains of various platforms: moorings and tripods (blue), typical LEO (orange area) and GEO (green area) ocean-colour satellites. The red dashed frame indicates merged LEO and GEO data over decades. Adapted from Dickey et al. (2006).

in 2007 (note the observed area is constrained by the MSG area because of the use of the MSG cloud product for 2007). It can be seen that in fall and winter in the northern hemisphere, the regions not seen by the GEO can be observed by Sentinel-3, whereas for most of the other regions and times of the year, the GEO fills many gaps.

4.6.3 Improvement of spatial coverage

A coverage performance analysis is presented here to illustrate the synergy between an ocean-colour sensor on a geosynchronous orbit and several LEO sensors. The combination includes several LEO sensors that would fly by 2018, to illustrate both the added-value and the synergy of GEO observations with other ocean-colour missions. The following three limitations can impact the availability of ocean-colour observations and have been taken into consideration:

- ❖ cloud coverage, taken from the full 2007 SEVIRI observations (cloud mask each 15 min);
- ❖ the air mass fraction is limited to a value of 5;
- ❖ the sunglint patch, defined by a glint reflectance of 5x 10^{-4} (Cox and Munk, 1954 model).
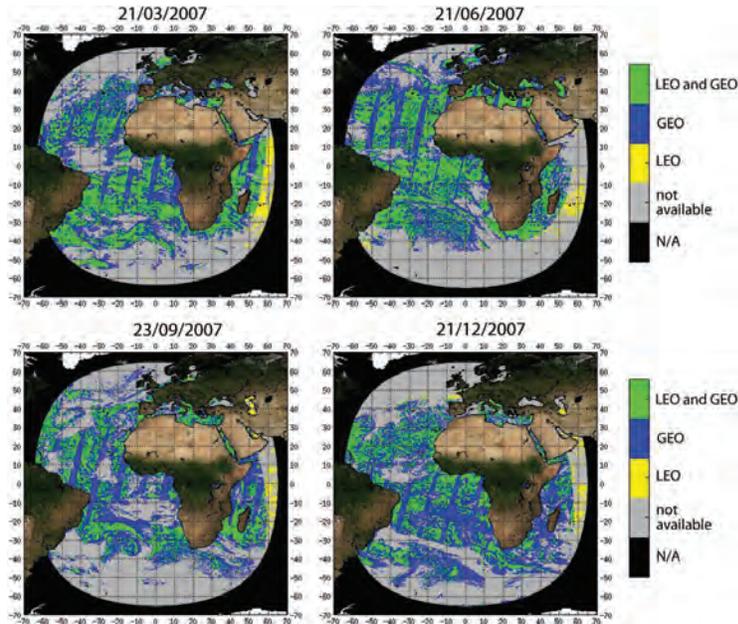
Figure 4.8 Synergy map between the Sentinel 3A-3B constellation and a geostationary mission at 10°W with 10° inclination at the solstices and equinox. Colour bar represents pixels available for LEO and GEO missions during the day. Image courtesy of ACRI-ST, Sophia-Antipolis, France.
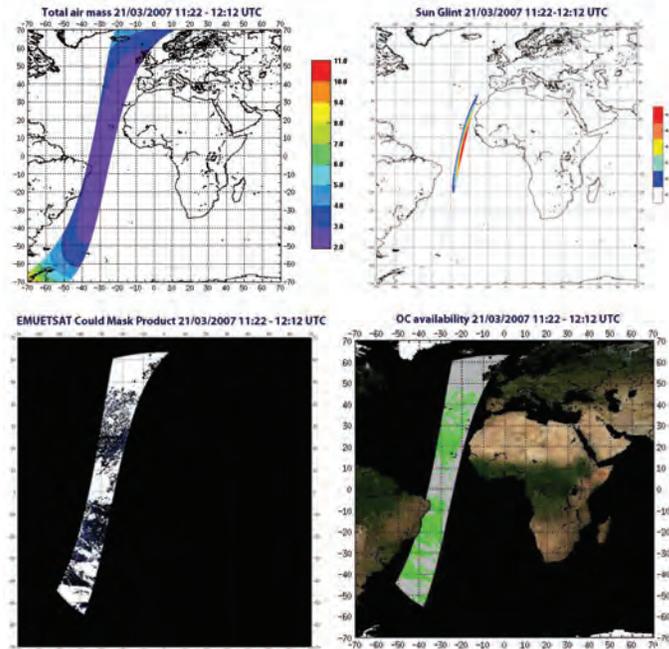

Figure 4.9 Example of coverage performance for a Sentinel-3A track: determination of the available pixels (bottom right, in green) using the air mass fraction (top left), sunglint patch (top right) and cloud cover (bottom left). Image courtesy of ACRI-ST, Sophia-Antipolis, France.

These constraints allow us to assemble the punctual availability of ocean-colour data for a given sensor at a given time, as illustrated in Figure 4.9 (example of a Sentinel-3 track). For these examples, we considered the future Sentinel-3A and Sentinel-3B LEO constellation plus a GEO satellite situated at 10° W with an inclination of 10°, and a 1-hour revisit. Figure 4.10 depicts the coverage performance, as a percentage of observable days in a month. A percentage of 50%, means that at least one usable clear observation is available for half of the days in the month. These simulations clearly demonstrate the enhanced coverage by a GEO mission, thanks to its full disk swath as well as high revisit frequency. For instance, while the LEO constellation can image most of the regions less than 40% of the month, the GEO mission can obtain usable images for at least 60% of the month, and over 90% around the tropics. This is true for the whole year. In summer, the Mediterranean Sea, the Mozambique Channel and a large part of the Atlantic would be observed almost every day. Even in winter, the Mediterranean Sea would be observed more than 50% of the time, compared to < 30% with the LEO constellation. An interesting feature is that because of the large swath and the glint avoidance most of the day, the GEO sensor provides more uniform coverage at daily and monthly scales compared to the LEO sensors.

4.6.4 Improvement of temporal coverage

Figure 4.11 provides an overview of the achievable number of observations per day, taking into account the constraints mentioned above for clouds, air mass, and sunglint and using the previous configuration. Clearly the LEO missions can only observe a target once per day, at the most (except at very high latitudes). On average, with a GEO mission, most of the regions would be observed at least four times per day and up to eight times per day for the Mediterranean Sea and the Equator in summer (Figure 4.11). The right panels in Figure 4.11 show that there are always some days with more than 8 observations. Again, those numbers could be improved if we consider an optimal acquisition scenario. In addition, it should be noted that the current estimates are slightly degraded because the mean is computed over all days, some of which are never cloud free.

4.6.5 Cross calibration

Cross calibration is a powerful option to transfer calibration from one LEO mission to another, thus progressively homogenizing observations across missions. Vicarious calibration of LEO sensors using *in situ* sites out of the view of the GEO sensor could be transferred to the GEO sensor. Conversely, the GEO sensor can be programmed on occasion so that its observations can be used as a reference to intercalibrate several LEO sensors (simultaneous data acquisition over many different targets).
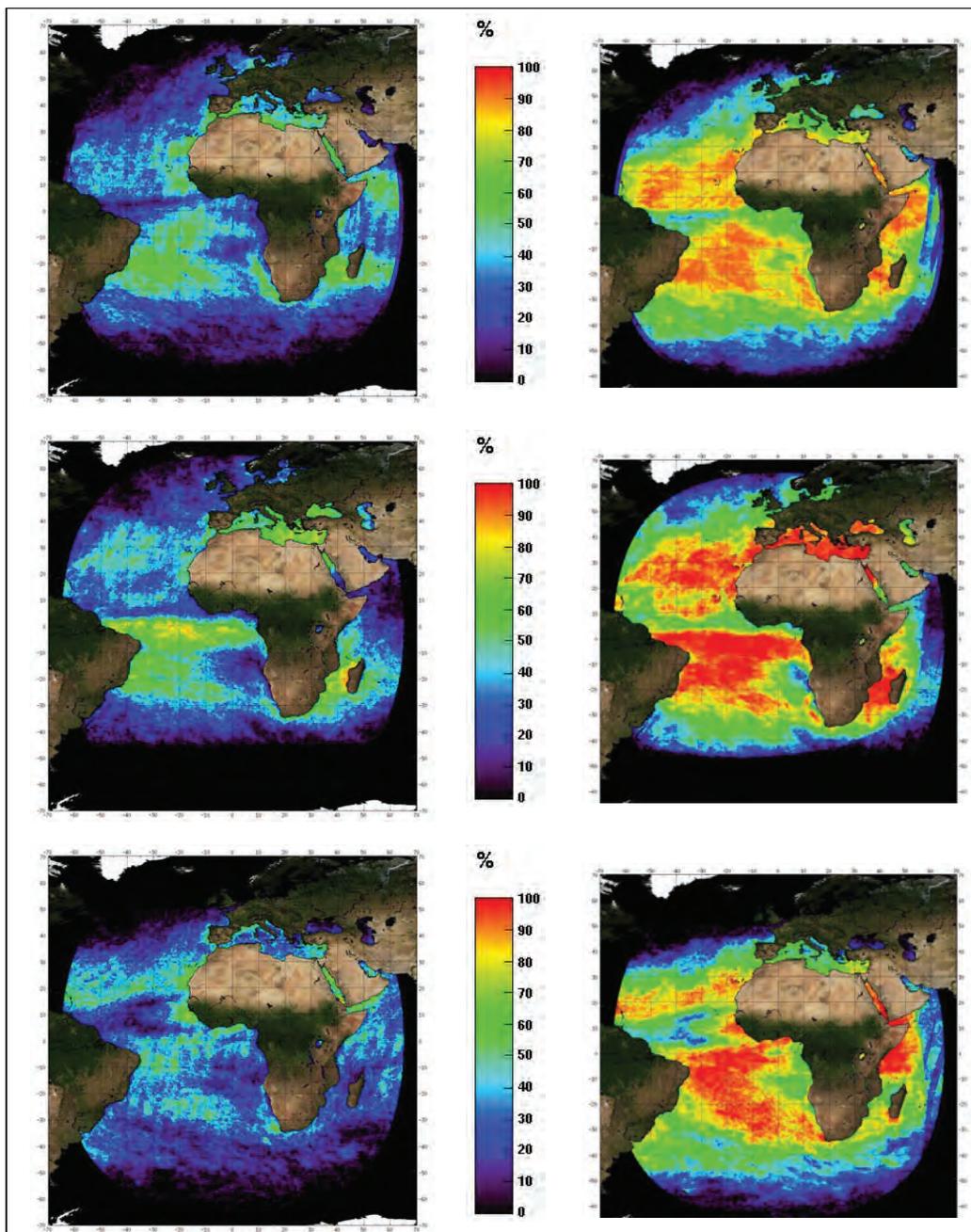
Figure 4.10 Coverage performance of a two-LEO-sensor constellation (left) and the same constellation complemented by a geostationary sensor (right) for March, June and December (top to bottom). The availability represents the percentage of days in the month that a pixel can be observed (i.e., at least one clear observation in the day). See text for the constraints applied. The observation area is constrained by the MSG observation area. Image courtesy of ACRI-ST, Sophia-Antipolis, France.
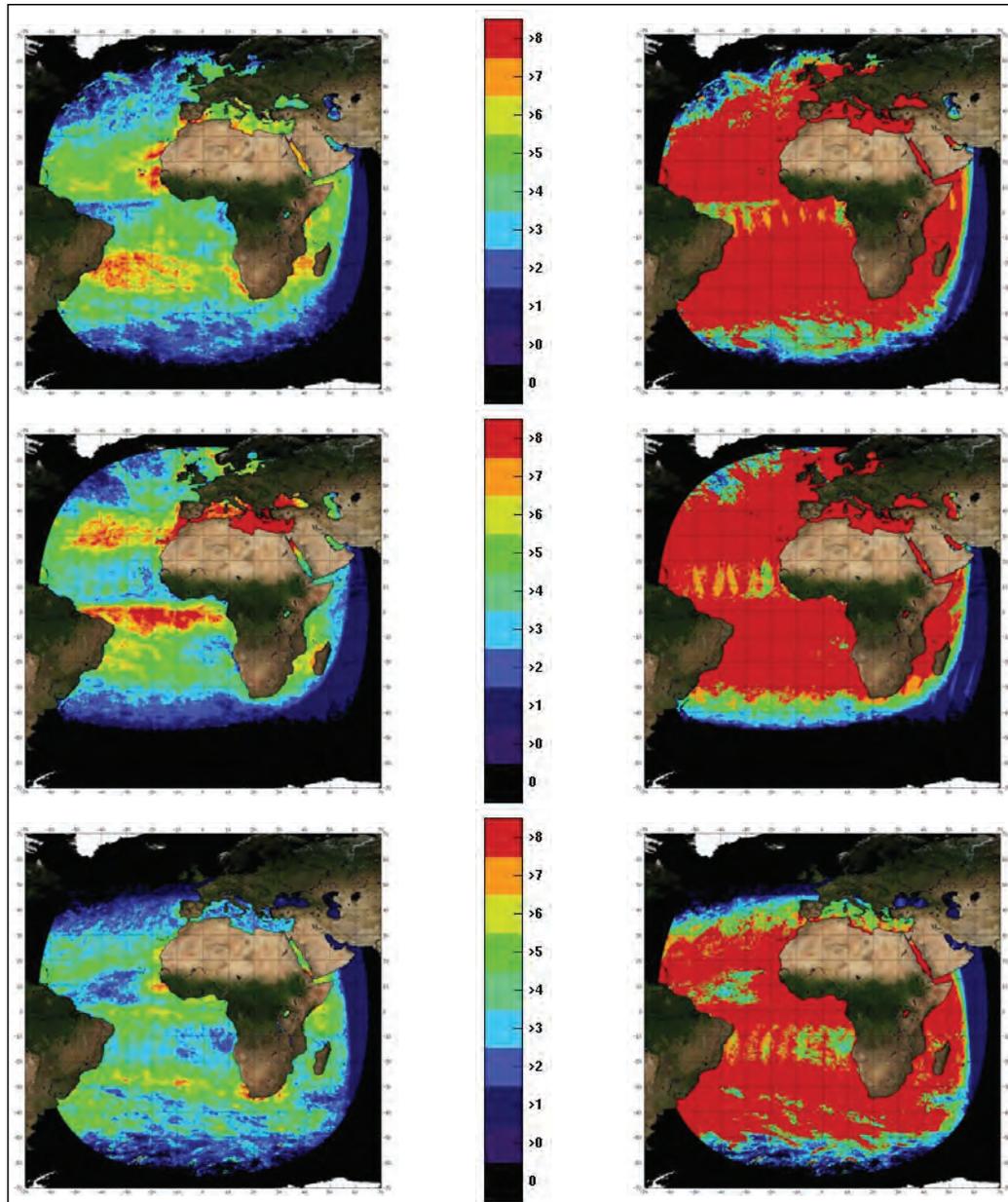
Figure 4.11 Mean (left) and max (right) number of daily available observations, for a two-LEO-sensor constellation complemented by a geostationary sensor in March, June and December (top to bottom). The observation area is constrained by the MSG observation area. Image courtesy of ACRI-ST, Sophia-Antipolis, France.
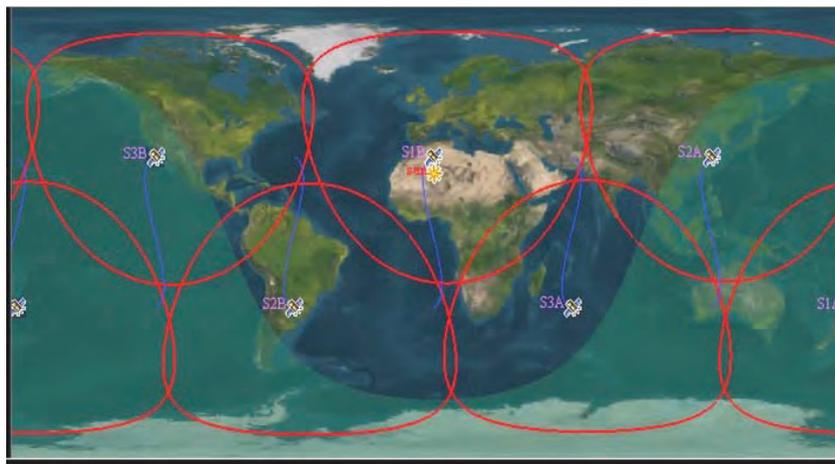
Figure 4.12 Coverage that could be obtained with 6 geosynchronous satellites, each with a 30° inclination, targeting different longitudes.

4.6.6 Synergy among GEO ocean-colour missions

Several GEO ocean-colour instruments are under development for launch in the 2020 time frame, including GEO-CAPE (NASA) and GOCI-II (South Korea). It is thus foreseeable that several geostationary or geosynchronous missions could provide a near-global coverage in the future. Figure 4.12 is an extreme illustration of this idea, using 6 satellites in geosynchronous orbits with an inclination of 30°. Although this is not attainable at present, the aim here is to show the potential of such missions when combined.

4.6.7 Synergy between ocean colour, SST and altimetry

One of the central issues that the biogeochemical community is currently facing, is understanding and modelling biophysical interactions at the sub-mesoscale level. The sub-mesoscale is a key biogeochemical regime since it covers biophysical interactions occurring on the timescale of a plankton bloom (~days). Moreover, this scale is the resolution that is expected on next generation global circulation models - indeed, modelling the climatic processes occurring at the scale of a few km has been recognized as the "The next big climate challenge" in a Nature editorial on 15 May 2008 (http://www.nature.com/nature/journal/v453/n7193/pdf/453257a.pdf).

A necessary step for addressing the sub-mesoscale structure of ocean biogeo-chemistry is developing the capacity to observe it. As a synoptic, global-coverage complement to *in situ* data, altimetry and SST data already cover the mesoscale regime, and future satellite missions will soon provide direct, synoptic observations of sub-mesoscale physics (notably, wide swath altimeter missions). When combined with recently developed theoretical diagnostics, remotely-sensed altimetry and sea

surface temperature observations can be integrated, and relevant biophysical information extracted (e.g., Lehahn et al. 2007; Isern-Fontanet et al. 2008; d'Ovidio et al., 2009). Nevertheless, the presence of clouds currently limits the sub-mesoscale comparison of physical fields and chlorophyll filaments to episodic cases, sparse and unpredictable in space and time. A GEO ocean-colour mission can remove this key obstacle for the integration of physical and biological observations at the timescale of a bloom. In particular, by resolving the chlorophyll variability on individual water filaments detected from altimetry and sea surface temperature images, the effect of horizontal and vertical fluxes can be observed during the development of phytoplankton patches. The concomitant use of altimetry, sea surface temperature, and ocean-colour data will lead, for the first time, to the quantification of biophysical processes, which, until now, have only been examined in numerical studies. When used to validate and improve the biophysical module in the spatio-temporal scales expected in next generation global circulation models, this information will, in turn, reduce the error in modelling global biogeochemical cycles and bring better predictive skills.

4.6.8 An example with the planned MTG mission

Planning for the Meteosat Third Generation (MTG) geostationary mission (available in the 2015 time frame) includes requirements for a mission for High Resolution Fast Imagery (HRFI), with the objective of supporting nowcasting and very short term forecasting of clouds, as well as a mission for Full Disk High Spectral Resolution Imagery (FDHSI) with the objective of supporting nowcasting and very short term atmospheric forecasting, numerical weather prediction at regional and global scales, and climate monitoring. HRFI is designed to acquire data with high temporal resolution (2 minutes), spatial resolution of 500 – 1000 m and a limited number of spectral channels (4 in total). FDHSI is designed to acquire data for a full disk, typically with a temporal resolution of 10 minutes, a spatial resolution of 1 – 2 km and 8 VIS/NIR channels from 0.4 μm to 2.2 μm and 8 infrared channels from 3.8μm to 13.3μm. As an evolution of the Meteosat Second Generation SEVIRI sensor, which has already been shown to be usable for estimation of total suspended matter (TSM) in turbid waters (Neukermans et al., 2009), FDHSI is the MTG instrument offering the most synergy for an ocean-colour sensor.

The spectral and radiometric resolutions of FDHSI are too limited for the estimation of ocean-colour parameters such as chlorophyll-a concentration. At best, FDHSI could provide estimates of TSM and possibly the diffuse attenuation coefficient of PAR, but with reduced accuracy compared to a dedicated ocean-colour sensor, and only for turbid water regions where the marine reflectance signal is sufficiently strong. Exploitation of Level-2 FDHSI atmospheric parameters is likely to provide the main synergistic advantage to ocean-colour sensors since FDHSI benefits from improved spectral resolution in the NIR/SWIR (1.3 - 2.2 μm) as well

as a much higher temporal resolution, allowing identification of rapidly varying atmospheric conditions. Comparison of ocean-colour derived and FDHSI products such as aerosol optical depth, aerosol particle size/Angström exponent and daily PAR can be implemented easily, and will allow suspect data to be flagged.

Use of FDHSI aerosol products in the atmospheric correction of ocean-colour observations may provide improvements, but will also require research on algorithm development since such synergy has not been attempted previously - difficulties are expected with spatial and temporal co-location and with radiometric calibrations. A further obvious synergy is the use of FDHSI cloud products. Finally, the SST products to be generated from MTG will be complementary to chlorophyll a-related products to be generated from ocean-colour missions for use in ecosystem and primary production models.

4.7   Can GEO Missions be Seen as Operational Missions?

The primary focus of the initial geostationary ocean-colour sensors deployed will be research and development (R&D), and they will serve as pathfinders in this context. Even so, data from these R&D sensors can, and certainly will, be used to support user-driven applications (e.g., monitoring harmful algal blooms, water quality), much as the operational use of ocean-colour data from existing LEO research sensors is now commonplace. For example, NOAA presently utilizes ocean-colour data from NASA's MODIS-Aqua sensor operationally, with these data included in products such as the NOAA Harmful Algal Bloom Operational Forecast System (HAB-OFS) Bulletin (`http://tidesandcurrents.noaa.gov/hab/bulletins.html`). The HAB-OFS bulletins provide information on potential or confirmed harmful bloom events, chlorophyll levels, and forecasted wind conditions, as well as forecasts for potential human impacts associated with confirmed harmful blooms, spatial bloom extents, movement, intensification and the potential for bloom formation. Likewise, data from MERIS and other ocean-colour sensors have been successfully utilized for operational monitoring under the Global Monitoring for Environment and Security (GMES) initiative, e.g., the Marine & Coastal Environmental Information Services (MARCOAST), as well as in support of other user-driven initiatives and applications, e.g., the Chlorophyll Globally Integrated Network (ChloroGIN) Project (`http://www.chlorogin.org/`). The availability of geostationary ocean-colour data would benefit the HAB-OFS bulletins significantly as well as other operational products and monitoring efforts, particularly by helping to mitigate frequent coastal cloud cover and monitor dynamic features. In the coming decade, partnerships between R&D and operational agencies, coupled with free, open and timely data access under the data sharing principles of the Global Earth Observing System of Systems (GEOSS), will facilitate user-driven, operational leveraging of R&D-focused GEO ocean-colour data streams (analogous to what is being done with LEO data, as described above). Somewhat longer term,

it is anticipated that eventually there will be operational geostationary mission(s) with ocean-colour sensors, as is currently the case for sea surface temperature (e.g., GOES-12, MTSAT, MSG), and soon will be for LEO ocean-colour sensors (e.g., VIIRS on JPSS, OLCI on Sentinel-3). Geostationary ocean-colour sensors such as GOCI will help clarify and address the various engineering and technical challenges that need to be overcome for accurate GEO ocean-colour observations, leading to their eventual technological and measurement maturity and subsequent operational implementation.

4.8 Algorithm Considerations for Geostationary Ocean Colour Observations

Considerable experience has been built up over the last ten years based on processing of ocean-colour imagery from polar orbiting sensors such as SeaWiFS, MODIS and MERIS. Various reviews have been made on the state of the art for such processing algorithms in general, and for specific aspects such as atmospheric correction (IOCCG Report No. 10, 2010), chlorophyll-a or inherent optical property retrieval (IOCCG Report No. 5, 2006), and the generation of multi-temporal composite products (IOCCG Report No. 4, 2004). This experience also applies in the case of ocean-colour observations from a geostationary orbit. The purpose of this section is to consider specific issues for algorithms for geostationary sensors, what new problems may be encountered, what existing problems will be more critical, and specifically, what benefits can be extracted from a satellite in geostationary orbit.

Whereas polar orbiting sensors provide imaging of any site at a typical frequency of once per day, and with a sun and viewing geometry that cannot be controlled by the data user, geostationary sensors could give imaging at a typical frequency of once per hour, or even once every few minutes, and provide a range of sun zenith and azimuth angles over the day. The potential for improving both the quantity and the quality of ocean-colour products is thus remarkable. The other important difference of the geostationary orbit compared to polar orbits is the viewing geometry, which is above the equator (or close to the equator in the case of geosynchronous orbits). At high latitudes or longitudes far from the sub-satellite longitude, much higher viewing zenith angles occur with geostationary orbits than typical polar orbits, which also increases the uncertainty from atmospheric correction. This will constrain the high latitude limit for the use of products from geostationary orbits (see next section). The viewing geometry will also impact areas affected by sunglint.

4.8.1 Atmospheric correction

The main challenge for atmospheric correction of GEO observations will be to provide accurate marine reflectances under grazing incidences, either when looking

at the edge of the observation area or when looking at any place of this area when the sun elevation is low. Current atmospheric correction schemes (e.g., Gordon, 1997; Antoine and Morel, 1999) are based on various assumptions, including the plane-parallel assumption. Ding and Gordon (1994) showed that the accuracy of radiative transfer computations under this assumption remain valid as long as the sun zenith angle is less than 70°. This represents a large portion of the area observed by a GEO sensor.

The GEO configuration includes larger angles near the edge of the target area or everywhere within this area when the sun elevation is low. Therefore, spherical shell radiative transfer computations might be needed to increase the observational capabilities. The accuracy of such corrections for spherical atmospheres remains to be determined. A tradeoff is necessary, however, between the increased complexity of such computations compared with classical ones, and the gain in coverage. In fact, the latter could be quite limited because the area at the edge of the target for which $60° < \theta < 80°$, is quite small. The issue here is more related to the increase of the temporal window that is usable within the dusk-to-dawn cycle. On the positive side, the fixed position of the target area in the GEO configuration may allow the use of first-guess climatological information about aerosols to help the atmospheric correction process.

Box 6: The GOCI Sunglint Correction

The objective of this algorithm is to identify if sunglint is a problem for the estimation of ocean-colour products by the GOCI instrument, and to propose and validate an alternative solution for the atmospheric correction algorithm in the presence of sunglint. Atmospheric correction is usually done by estimating an aerosol model, optical thickness and type, from the spectral dependence of the top-of-atmosphere (TOA) radiances measured in NIR channels (Gordon and Wang, 1994). Once the aerosol model has been determined, the atmospheric scattering is accurately computed at shorter wavelengths by a radiative transfer (RT) code and subtracted from the TOA radiances to obtain the ocean-colour signal. When the measurements are affected by sunglint, this atmospheric correction scheme fails to estimate the aerosol model, and thus to deliver an accurate atmospheric correction. Sunglint has no spectral dependence and this causes a bias towards larger particles in the retrieval of aerosol properties. The atmospheric correction is also biased because the coupling between molecular scattering and sunglint is not taken into account. The sunglint intensity can be predicted from the wind speed, and corrected with a reasonable accuracy.

Most of the ocean-colour instruments on a low altitude polar orbit are affected by sunglint that significantly reduces the spatial coverage of ocean-colour retrievals between the tropics. This is also the case for a geostationary instrument like GOCI for which the glitter pattern is a large spot centred on the Equator at the Equinox and a little further north (~10°N) at the summer solstice. If the problem is flagged for a glitter value > 0.005, this would affect the GOCI retrieval up to 35°N during the spring and summer seasons. The sunglint correction algorithm (SGCA) applied to GOCI is based on the spectral matching of the GOCI observed TOA radiances at 7 wavelengths by an ocean atmosphere reflectance model that depends on five tuneable variables. The algorithm works pixel by pixel. The input is L1B GOCI data at eight wavelengths, and the output is five parameters, three of which describe the atmospheric scattering, and two (Chl and backscattering coefficient (b_{bp}), describe the marine reflectance. The L2 output parameters include these five coefficients plus the above-water reflectance $R_w(0+)$ or water-leaving radiances L_w.
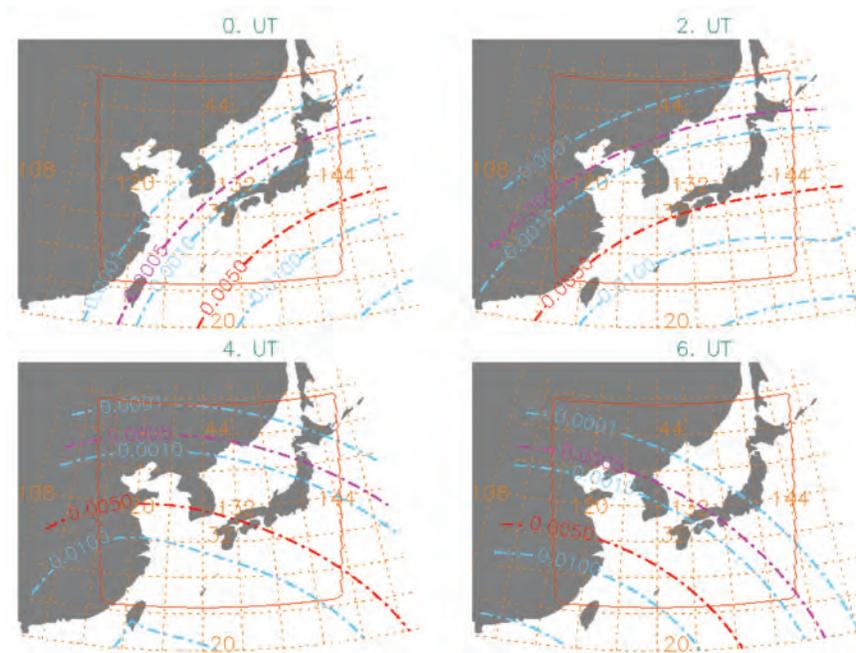
Simulated sunglint reflectance for GOCI viewing geometry on 21 June (summer solstice, where the sunglint migrates maximally to the north), for 0:00, 2:00, 4:00 and 6:00(UTC) at a wind speed of 10m/s. Image courtesy of P.Y. Deschamps.

The input GOCI L1 radiances are converted into reflectance by normalization to the solar extraterrestrial spectral irradiance. The correction for gaseous absorption and molecular scattering and the cloud mask processing is performed for the rough sunglint estimation in clear pixels. The derived reflectance is fitted by the models using an iterative, least-square minimization scheme that determines the five variables, C0, C1, C2, Chl, and b_{bs}, applied pixel by pixel. The L2 output parameters of SGCA are thus C0, C1, and C2 that represent aerosol and glitter-corrected R_w and/or L_w, marine reflectance or water-leaving radiances.

4.8.2 Modification of radiative transfer models

Currently, the radiative transfer (RT) models used to generate the atmospheric correction look-up tables assume the atmosphere is a plane-parallel medium (PPM model). However, the atmosphere surrounding the Earth is actually a spherical shell medium (SSM model). Adams and Kattawar (1978) showed that, for a simple one-layer Rayleigh-scattering medium with a totally absorbing lower boundary, there could be significant differences between the PPM model and SSM model for large solar zenith angles and/or large viewing angles. Ding and Gordon (1994) used the backward Monte Carlo technique to solve the radiative transfer equation in a two layer spherical shell atmosphere with a Fresnel-reflecting ocean surface (smooth or rough) at its lower boundary, and found that for solar zenith angles less than 70° there was no significant difference of performance between the PPM and the SSM models. However, for solar zenith angles larger than 70°, the difference between the PPM and the SSM models is significant (Ding and Gordon, 1994). This means that
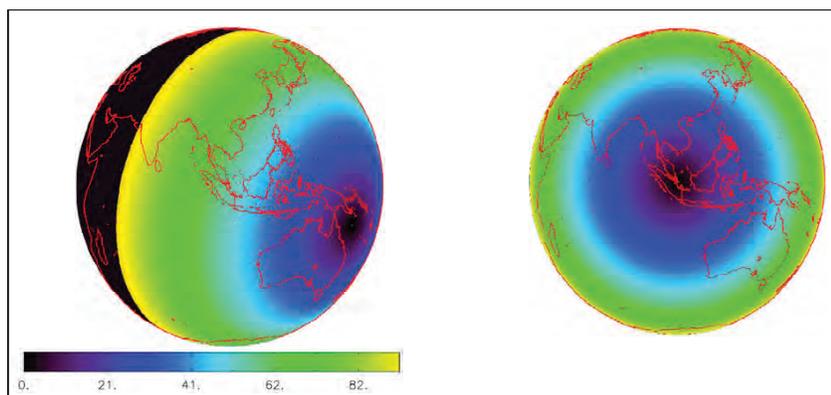
Figure 4.13 Distribution of the solar zenith angle (left) and sensor viewing angle (right) from the geostationary meteorological satellite FY-2C (located above the Equator at longitude 104.50°E) at time of 2008-02-02 00:30 GMT. Image credit: Xianqiang He, SOED, China.

Earth-curvature effects should be considered when the solar zenith angle and/or viewing zenith angle are large.

Geostationary ocean-colour sensors scan multiple times during daylight hours. At dawn and dusk, the solar zenith angle may be larger than 70° (Figure 4.13, left). The viewing zenith angle is also very large at the edges (Figure 4.13, right). Therefore, under such circumstances, it necessary to use the SSM radiative transfer model to generate the look-up tables for atmospheric correction. Up to now, there is no SSM vector radiative transfer model for the coupled atmosphere-ocean system. Ding and Gordon's model is a scalar SSM RT model, and it should be modified to a vector SSM RT model because polarization consideration is important for the exact calculation of the atmospheric scattering (Gordon et al., 1988). Other existing PPM RT models also need be modified to vector SSM RT models so they can be used to generate the atmospheric correction look-up tables for geostationary ocean-colour sensors.

4.8.2.1 Bidirectional reflectance distribution function issues

The anisotropy of the light field emerging from the ocean is well known in open ocean Case-1 waters. It has been modelled for such waters as a function of the inherent optical properties and the illumination conditions at the sea surface (Morel and Gentili, 1991; 1993; Morel et al., 2002). These models have been partly validated against *in situ* measurements (Morel et al., 1995; Voss and Morel, 2005; Voss et al., 2007), and they can be used to derive fully-normalized radiometric quantities from ocean-colour measurements (e.g., Morel and Gentili, 1996), which is necessary in view of data merging from multiple missions. There are no observations or models for coastal Case-2 waters.

In the configuration of GEO observations, anisotropy can be considered from

two points of view. The first is similar to the LEO approach, where the anisotropy has to be accounted for to derive fully normalized water-leaving radiances, i.e., the radiances that would be measured at nadir with the sun at zenith. The second approach would benefit from the availability of observations of the same target under various sun elevations, from dawn to dusk. Provided that the atmospheric correction is accurately performed over a sufficient range of this angle, the BRDF of the surface would be obtained.

4.8.3   Exploiting temporal coherency

One advantage of the high temporal frequency that can be achieved from the GEO orbit is the possibility to exploit temporal coherency of the ocean and/or atmosphere system to constrain retrieval algorithms. Current ocean-colour processing chains generally treat each pixel independently, ignoring its spatial and temporal neighbours. However, in nature, geophysical parameters are highly correlated especially at short time and space scales. If this extra information can be exploited by processing algorithms, the quality or quality control of products could be significantly improved. Processing of measurements in many fields of science involves identification and removal of "spikes" or "outliers". With high frequency geostationary data similar techniques could be applied to ocean-colour measurements as already suggested for LEO ocean-colour data by Sirjacobs et al. (2011, see Figure 7 of their paper for an example of automated outlier detection).

Going further than *a posteriori* outlier analysis of ocean-colour products, information on temporal coherency could also be integrated into the retrieval procedure to better constrain algorithms. Two key problems for ocean colour are: 1) the large uncertainties from atmospheric correction and 2) the possibility that remotely-sensed reflectance spectra may have low sensitivity to the target parameters (e.g., chlorophyll-a retrieval in waters with high yellow substance absorption) or may even correspond equally well to very different combinations of optically active substances creating a complex inversion problem (Defoin-Platel and Chami, 2007). For both problems there may be insufficient spectral information in a single pixel to provide a unique and robust retrieval. On the other hand, if there is knowledge about, say, the chlorophyll concentration 15 minutes before and after the measurement being processed, this information could provide a first guess for an iterative retrieval, i.e., a way of distinguishing between multiple solutions or, more generally, to provide a constraint to the spectral inversion problem.

With the exception of a few fast oceanic processes which could be specifically targeted by a geostationary ocean-colour mission, a geostationary sensor will generally be viewing a relatively constant marine target through a foreground of rapidly-changing atmospheric conditions. Wind-driven variations of aerosol concentration are particularly important. Viewing of the same surface target through different atmospheric conditions has already been proposed for geostationary remote sensing

of aerosols over land by Knapp et al. (2005). Similarly, viewing of the same target for different sun-sea atmospheric path lengths could enable atmospheric effects to be better quantified in a similar way to the dual-view ATSR approach for sea surface temperature (Mutlow et al., 1994) or the multidirectional viewing achieved by POLDER (Herman et al., 2005).

4.8.4 Cloud clearing, daily compositing

Ocean-colour imaging requires sunlight and cloud-free scenes. One advantage of geostationary imaging is the ability to wait until an area is cloud free, rather than sampling at a fixed time, as set by the orbit for polar orbiting ocean-colour imagers such as MERIS and MODIS (Figure 4.14). The capability to obtain frequent cloud-free imagery will be an important asset to monitor water quality because surface currents can alter phytoplankton and sediment distributions near the coast, and also since phytoplankton growth rates can exceed a doubling per day, they can rapidly alter water quality. Monitoring of water quality parameters from satellite, particularly from coastal regions susceptible to harmful algal blooms, is improved by the capability to access imagery on any given day. The frequent image acquisition available from a geostationary satellite will improve the chances of obtaining a cloud-free image and allow imagery collected at different times of the day in various sub-regions to be combined to generate daily cloud-free coastal ocean-colour scenes for the entire region.
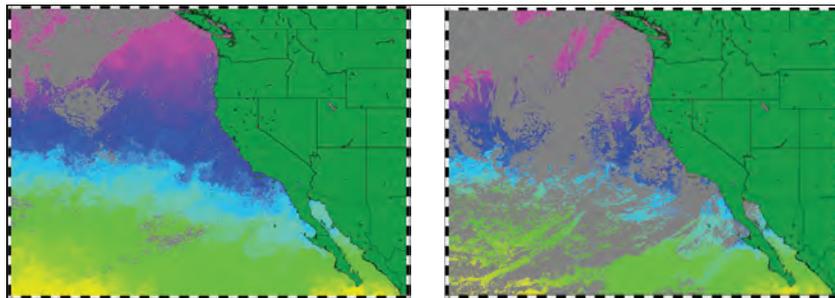

Figure 4.14   Left: three-day composite of GOES SST. Right: three day composite of AVHRR SST for the same period. The more frequent sampling from GOES has effectively cleared the clouds from the eastern North Pacific (Images from NOAA CoastWatch).

Despite their simple optical properties and many decades of experience in detecting clouds in remote sensing data, imperfect masking of clouds remains a significant source of bad ocean-colour data. Sub-pixel scale clouds, cloud edges, thin clouds and cirrus are specific cases where errors may occur (Robinson et al., 2008). Traditionally, polar orbiting ocean-colour sensors use the single reflectance threshold at the NIR band to detect clouds, such as 865 nm for SeaWiFS and 869 nm for MODIS. Such a simple method generally works well over the open oceans

where Case-1 waters and maritime aerosols are usually the case. However, in coastal regions, there are often cases with significant ocean contributions at the NIR wavelengths from the turbid waters. In addition, aerosols are likely to be dominated by small particles (large Angström exponent). In these cases, unless improved algorithms are used (Nordkvist et al., 2009) the cloud-masking scheme using the NIR reflectance threshold often mistakenly identifies these scenes as clouds, leading to significant loss of coverage in coastal regions (Wang and Shi, 2006).

For a geostationary ocean-colour sensor, because of the variation of the geometry between sun and sensor with the different observation times in the same day, operational cloud detection methods will need further development. Another issue is the daily compositing of the multiple temporal images obtained by one or more geostationary ocean-colour sensors. Daily compositing can increase the chances of finding clear skies due to changing cloud patterns. Several studies have been undertaken to merge data from different polar orbiting ocean-colour sensors. For example, large improvements in coverage frequency (daily to four-day) can be expected by combining ocean-colour data from the SeaWiFS and MODIS missions. Results indicated 40 to 70% increase in global coverage over SeaWiFS alone, and > 100% in low latitudes. IOCCG Report 6 (2007) presents a comprehensive discussion of the different merging methods, including the random error-correcting type methods, bias-correcting type methods, bio-optical methods and numerical model-based methods. Primarily, these methods can be used to merge geostationary ocean-colour sensor data, but the diurnal variation problem should be considered. For polar orbiting ocean-colour sensors, it ignores the reality of diurnal variation due to the absence of sufficient sampling frequency. For example, chlorophyll concentration increases during the daytime as a result of photosynthesis but geostationary ocean-colour sensors can resolve this diurnal variation directly. Therefore, suitable methods for the daily compositing of the geostationary ocean-colour data should be developed.

4.9 Summary of Requirements for GEO Ocean-Colour Missions

Generic requirements reviewed in this report are summarized in Table 4.2. When appropriate, three levels are used, otherwise a unique value is given when there is no possible trade-off. **Goal** represents the value which, if exceeded, would not yield significant improvements in mission performance; **Threshold** is the value below which the observation would not yield any significant benefit for the mission; and **Breakthrough** is an intermediate value between "threshold" and "goal" that, if achieved, would result in a significant improvement for the mission. The breakthrough level is expected to be more appropriate than the "goal" from a cost-benefit point of view.

Parameter	Goal	Breakthrough	Threshold	Comments
Orbit	Geosynchronous (inclination depending on mission goals)		Geo-stationary	
Type of Coverage	Complete Earth disk (oceans, coastal zones, land)	Complete Earth disk (oceans, coastal zones)	Selected areas of interest	
Revisit	30 min	1 hour	avg. 1 h	
Accessibility to specific revisit areas	15 min		none	
Resolution (Nadir GSD)	100 m	250 m	500 m	Aggregation might be acceptable for some bands
Imager bands	20 (See Table 3.1)	16	10	
Temporal co-registration for one scene	< 1 minute			For acquisition of a given point in all bands
Out of band integrated signal	< 1 %			
SNR	See Table 3.1			
Solar calibration	On-board devices (sun-illuminated diffusers)			
Temporal stability	0.1 % over the mission (moon observation)			
Vicarious calibration	Based on fixed-sites			Mandatory element for success of any OC mission
Pre-launch absolute radiometric accuracy	2 % in radiance, w.r.t. lab standard	N/A	4 %	
Relative accuracy between bands	1 %			
Polarisation sensitivity	1 %			
Stray light	Accurate modelling of instrument stray light			
Modulation Transfer Function (MTF)	0.3	0.2	0.15	
Clouds	Clouds to be observed	Degraded SNR for clouds	No data required	
Geolocation	1\4 pixel	1\2 pixel	1 pixel	
Latency	NRT	1 hour	1 day	Time between data acquisition and L1B availability
Lifetime	10 years	7 years	5 years	

Table 4.2   Summary of requirements for an OC sensor on a GEO orbit that would provide observations useful for the domains identified in Chapter 2.

Chapter 5

General Summary and Recommendations

Numerous scientific and applied domains have been identified in this report that would benefit from ocean-colour observations from a geostationary or geosynchronous orbit. There is now a body of studies that support the development of such missions. Since the successful launch of the GOCI instrument, the question is no longer the feasibility of such missions but rather which schedule can possibly be put in place at the international level for several GEO ocean-colour missions to be launched in the coming decade (2011-2020). Many agencies are engaged in such developments (see Appendix A).

Many options are possible for the design of missions capable of providing ocean-colour observations from a geostationary or geosynchronous orbit at the desired radiometric accuracy, spatial and spectral resolution and, above all, revisit time. It is out of the scope of this report to review technological solutions, but within scope to discern possible mission scenarios and sensor requirements to fulfil the mission objectives.

GEO ocean-colour missions can be focused on limited areas, with high spatial resolution to support monitoring applications and services in coastal areas. Other types of missions would observe the entire Earth disk not only to provide data for operational applications, but also for advanced scientific investigations in both coastal zones and the open ocean. In any case, the spatial resolution should be within the 100 – 500m range at nadir. Higher resolutions are not necessarily required for scientific purposes, and would be difficult to achieve high SNR. Depending on the mission specific goals, either a purely geostationary orbit (sub-satellite point at the Equator) or an inclined geosynchronous orbit can be chosen. The later allows higher latitudes to be observed in better conditions. When the goal is to observe the entire disk from such orbits, however, two satellites are needed to ensure the same revisit frequency over the full disk.

Spectral requirements have been summarised, which are not specific to the GEO orbit, and which come in a variety of band sets adapted to specific mission goals. In particular, the trade off between multispectral and hyperspectral observations cannot be resolved, because these two options have important consequences on sensor design and cost. Wherever feasible, continuity with contemporaneous ocean-colour missions in a low Earth orbit should be ensured. SWIR bands are required for accurate atmospheric correction above turbid Case-2 waters, which is a focus of

possible GEO ocean-colour missions.

Radiometric characteristics have to ensure high SNR typical of ocean-colour requirements. This is particularly important in the GEO configuration, to maximize the temporal window within the dusk-to-dawn cycle for which the signal can be meaningfully interpreted. On board accurate calibration units should exist, based on sun illuminated diffuser(s) with a means to monitor their degradation during the lifetime of the mission. In addition, Moon viewing capabilities for monitoring of instrument degradation should be enforced. As for any ocean-colour sensor, pre-flight instrument characterization must be carried out as accurately and comprehensively as possible. In particular, an accurate modelling of the instrument stray light has to be considered in the Level-1B ground processor. Polarization sensitivity should be maintained below 1%.

In this report, ocean colour from a geostationary orbit has been considered from the point of view of ocean observations. Launching sensors in a GEO orbit is expensive, and the question of adapting mission characteristics so they can serve other purposes (e.g., observations of land vegetation) will inevitably be raised when designing such missions. The goal and success of the ocean-colour mission should not be jeopardized, however, by unrealistic compromises (in particular, a high radiometric accuracy has to be preserved; IOCCG 1998). In the case of a multi-purpose missions, the dynamic range of the sensor must avoid saturation above highly turbid waters or clouds, and still remain adapted for ocean colour. Another dichotomy may exist between ocean-colour GEO missions that would be either purely science-driven or more application-driven i.e., operational missions. Combining both aspects is, however, recommended to better share investment among agencies with different focuses.

Interpretation of satellite ocean-colour observations still requires improvements in our understanding of how the various optically-significant quantities combine in forming the water reflectance. This requirement is not specific to ocean colour from a geostationary orbit, although this peculiar configuration adds to the difficulty of retrieving accurately the spectrum of water-leaving radiances and deriving geophysical quantities. These difficulties have been identified in this report. They stem mainly from the geometry under which the TOA signal is recorded and from the focus on coastal zones that many of the planned GEO ocean-colour missions propose. Therefore, the recommendations are:

❖ to maintain and possibly augment the effort towards better understanding optics in optically-complex waters (in particular the bidirectionality of reflectance, which is still undocumented in these waters);

❖ to better document and interpret diurnal changes in optical properties (both inherent and apparent optical properties), and assess accessibility of these changes from satellite;

❖ to improve atmospheric correction for low sun elevations and high viewing angles (which may require spherical shell atmosphere modelling to be further

 developed and used) and;
  ❖ to support studies that would benefit from the spatial or temporal coherence of observations to better constrain or verify inversion algorithms.

Another requirement, which is more generic and not GEO-specific, is to maintain existing calibration/validation sites that will allow the GEO ocean-colour observations to be properly vicariously calibrated and connected to time series of low-Earth orbiting sensors. Studies to be supported also include the cross-calibration of GEO and LEO ocean-colour observations.

Concerted efforts should be made to ensure maximum compatibility across missions. Compatibility can be at the level of the instruments themselves (joint developments allowing cost reduction) or at the level of processing algorithms (to facilitate data merging) or even at the level of longitude selections to provide overlap between observation areas (to facilitate cross calibration). The network of existing geostationary meteorological satellites (e.g., GOES series, MSG and MTG, MTSAT) show that coordination is required and is possible to meet global coverage requirements. A coordinated multi-national network of geostationary ocean-colour satellites is therefore a tangible goal, feasible in the 2025 horizon.

International Context

The following sections summarize current plans of space agencies with an interest in launching ocean-colour sensors on geostationary platforms. Note that this is a rapidly evolving arena - the information below is the situation as of April 2012.

A.1   NASA (USA)

Over the past several years, NASA has initiated planning efforts and science and engineering studies for a geostationary ocean-colour mission. A planning document on NASA's ocean biology and biogeochemistry research (NASA, 2006) presents a description for a geostationary ocean-colour mission. This planning document describes the mission science and a preliminary set of instrument requirements for a geostationary hyperspectral imaging radiometer to study coastal ocean processes. The considerations for ocean-colour retrievals in coastal waters entails significant improvements in current ocean-colour sensor capabilities, which include: high frequency sampling each day, higher spatial and spectral resolution, broad spectral coverage including UV-VIS-NIR and SWIR bands, high SNR and dynamic range, cloud avoidance, minimal polarization sensitivity (< 0.2%) or change, minimal stray light with narrow FOV optics and low scatter gratings (< 0.1%), no image striping or image latency, solar and lunar on-orbit calibration. Details on the proposed instrument requirements are described in the NASA planning document (2006; http://oceancolor.gsfc.nasa.gov/DOCS/). The authors recommended that NASA (or in partnership with other U.S. federal agencies or international space agencies) contribute a regional sensor to a broader international effort to provide global coverage of the coastal oceans from geostationary orbit. If international coordination is not possible, then a single geostationary sensor with a precessing orbit to study short duration processes in temperate and tropical waters was recommended.

The U.S. National Research Council (NRC), at the request of NASA, NOAA and the U.S. Geological Survey, conducted an Earth Science Decadal Survey (DS) review to assist these agencies in planning the next generation of Earth Science satellite missions. The final report recommended 17 missions including a mission called GEO-CAPE (Geostationary Coastal and Air Pollution Events) focused on measurements of tropospheric trace gases, aerosols, and coastal ocean colour from geostationary orbit (NRC, 2007). The NRC placed GEO-CAPE within the second tier of mission

79

launches which NASA plans to launch after 2020. With respect to the coastal ocean-colour sensor on GEO-CAPE, the NRC recommended a UV-VIS-IR (350-1050 nm) hyperspectral radiometer capable of scanning coastal waters of North and South America between 50°N and 45°S multiple times per day at 250 m spatial resolution. In preparation for the release of the NRC report, NASA conducted a series of mission planning and engineering studies in 2006. In August 2008, NASA convened a workshop on the GEO-CAPE mission to refine the scientific goals, objectives and requirements for this mission and define the necessary investments to advance the mission concept for a Phase A mission start. The workshop report is posted at `http://geo-cape.larc.nasa.gov/documents.html`.

NASA assembled formal Atmospheric and Ocean Science Working Groups (SWGs) between August 2008 and April 2009 for GEO-CAPE pre-phase-A mission formulation to develop a science traceability matrix to define science objectives as well as measurement, instrument and mission requirements for coastal ocean ecosystem research and applications. A working meeting of the SWGs was convened in September 2009 to discuss GEO-CAPE mission science objectives and requirements. The agenda and presentations given at this meeting are posted at `http://geo-cape.larc.nasa.gov/events-SEP2009SWGM.html`. In March 2010, NASA convened a working meeting of the GEO-CAPE ocean and atmospheric science working groups. During this meeting, draft GEO-CAPE atmospheric and coastal ocean ecosystems dynamics Science Traceability Matrices (STM) were endorsed by voice consensus as a sufficient, although not immutable, starting point for preliminary mission planning work. As living documents, the STMs are expected to further evolve pending the outcome of ongoing science pre-formulation studies. In May 2011, an open workshop was held to report recent progress to the science and instrumentation communities. The agenda and presentations are available at `http://geo-cape.larc.nasa.gov/events-MAY2011CW.html`. The primary outcomes of this workshop were: (1) identification of opportunities for international synergy if GEO-CAPE is launched in the 2018 timeframe; (2) agreement that the Atmosphere and Ocean science objectives can be met by launching instrumentation on either a single dedicated spacecraft or on separate platforms; and (3) agreement that the possibility of launching the instrument suite on commercial spacecraft as hosted payloads should be explored.

The science working groups proposed the following set of science questions traceable to the NRC Decadal Survey (2007) and NASA's Ocean Biology and Biogeochemistry Program long-term planning document (NASA, 2006) that GEO-CAPE can address:

❖ How do short-term coastal and open ocean processes interact with and influence larger scale physical, biogeochemical and ecosystem dynamics?

❖ How are variations in exchanges across the land-ocean interface related to changes within the watershed, and how do such exchanges influence coastal and open ocean biogeochemistry and ecosystem dynamics?

❖ How are the productivity and biodiversity of coastal ecosystems changing, and how do these changes relate to natural and anthropogenic forcing, including local to regional impacts of climate variability?

❖ How do airborne-derived fluxes from precipitation, fog and episodic events such as fires, dust storms and volcanoes affect the ecology and biogeochemistry of coastal and open ocean ecosystems?

❖ How do episodic hazards, contaminant loadings, and alterations of habitats impact the biology and ecology of the coastal zone?

The oceans STM was presented to the ocean-colour community at the NASA Ocean Colour Research Team meeting in May 2010 (`http://oceancolor.gsfc.nasa.gov/ MEETINGS/OCRT_May2010/`). This presentation also describes a preliminary instrument design study conducted in January 2010 for a GEO-CAPE ocean-colour sensor. An update on the status of GEO-CAPE activities was presented at the NASA OCRT meeting in April 2012, which included the latest version of the oceans science traceability matrix (Figure A.1). Currently, NASA is funding science and engineering studies for the Tier 2 Earth Science Decadal Survey missions including GEO-CAPE. The publication of a NASA technical memorandum is planned for summer 2012 that describes the GEO-CAPE ocean colour mission science and instrument requirements as well as past, current and planned mission activities.

A.2   NOAA (USA)

Current ocean-colour sensors, for example MODIS and VIIRS, are well suited for sampling the open ocean. However, coastal environments are quite heterogeneous, typically characterized by dynamic, episodic and/or ephemeral processes and phenomena, with waters that are spatially and optically more complex and require more frequent sampling and higher spatial resolution sensors with additional spectral channels. To address these issues, NOAA considered including a Coastal Waters imaging capability (HES-CW) as part of the Hyperspectral Environment Suite (HES) on the next generation Geostationary Operational Environmental Satellite (GOES-R). From 2004 to 2006 NOAA supported field experiments and engineering design studies for HES-CW. These studies confirmed that the key advantage for NOAA of a geostationary imager is frequency of revisit. Coastal waters are highly dynamic, e.g., tides, diurnal winds, river runoff, upwelling and storm winds drive currents from one to several knots. Three hour or better sampling is required to resolve these features, and to track HAB events, pollutant and pathogen-laden storm water runoff, oil spills or other features of concern for coastal environmental management. Spatial sampling of 300 m and the MERIS (or better) set of channels including channels in the SWIR were also required to image complex coastal waters. In the fall of 2006, due to budget and engineering concerns, NOAA dropped HES, including HES-CW, from GOES-R. While there are still strong user requirements for coastal waters imaging

GEO-CAPE Oceans STM Draft v.4.1 – Feb. 1, 2012

Science Focus	Science Questions	Approach	Measurement Requirements	Instrument Requirements	Platform Requirem. Requirem	Ancillary Data Requirem
Short-Term Processes	**1** How do short-term coastal and open ocean processes interact with and influence larger scale physical, biogeochemical and ecosystem dynamics? (OBB 1)	GEO-CAPE will observe coastal regions at sufficient temporal and spatial scales to resolve near-shore processes, tides, coastal fronts, and eddies, and track carbon pools and pollutants. Two complementary operational modes will be employed: (1) survey mode for evaluation of diurnal to interannual variability of constituents, rate measurements and hazards for estuarine and continental shelf and slope regions with linkages to open-ocean processes at appropriate spatial scales, and (2) targeted, high-frequency sampling for observing episodic events including evaluating the effects of diurnal variability on upper ocean constituents, assessing the rates of biological processes and coastal hazards. *Measurement objectives for both modes include:*	**Maps to Science Question** ◢ Product uncertainty TBD	**Spectral Range:** Hyperspectral UV-VIS-NIR bands 345–1050 nm; 2 SWIR • **#**Threshold: 1245 & 1640 nm • Baseline: 340–1100 nm; 3 SWIR bands 1245, 1640, 2135 nm	Geostationary orbit at 95° longitude to permit sub-hourly observations of coastal waters adjacent to the continental U.S., North, Central and South America	**Measurement Requirements** (1) Ozone (2) Total water vapor (3) Surface wind velocity (4) Surface barometric pressure (5) Vicarious calibration – coastal & ocean (6) Full prelaunch characterization (7) Cloud cover
Land-Ocean Exchange	**2** How are variations in exchanges across the land-ocean interface related to changes within the watershed, and how do such changes influence coastal and open ocean biogeochemistry and ecosystem dynamics? (OBB 1 & 2)	3 4 2 *Targeted Events:* (a) Quantify dissolved and particulate carbon pools and related rate measurements such as export production, respiration, and photochemical oxidation of dissolved organic matter.	**Temporal Resolution:** *Targeted Events:* • Threshold: ≤1 hour • Baseline: ≤0.5 hour *Survey Coastal U.S.:* • Threshold: ≤3 hours • Baseline: ≤1 hour *Regions of Special Interest (RSI): Threshold: ≥1 RSI 3 scans/day*	**Spectral Sampling & Resolution:** • Threshold: UV-VIS-NIR: ≤2 & ≤5nm; 400-450nm: ≤0.4 & ≤0.8nm (for NO₂); nadir)**#**: SWIR resolution: ≤20–40 nm; SWIR: ≤20–50 nm	Storage and download of full spatial data and spectral data.	**Science Requirements** (1) SST (2) SSH (3) PAR (4) UV solar irradiance (5) MLD (6) Air/Sea pCO2 (7) pH
Impacts of Climate Change & Human Activity	**3** How are the productivity and biodiversity of coastal ecosystems changing, and how do these changes relate to natural and anthropogenic forcing, including local to regional impacts of climate variability? (OBB 1, 2 & 3)	1 2 3 4 5 (b) Quantify phytoplankton properties: biomass, pigments, functional groups (size/taxonomy/Harmful Algal Blooms (HABs)), daily primary productivity using bio-optical models, vertical migration, and chlorophyll fluorescence. 1 2 3 4 5 (c) Measure the inherent optical properties of coastal ecosystems: absorption and scattering of particles, phytoplankton and detritus, CDOM absorption. 3 4 (d) Estimate upper ocean particle characteristics including particle abundance and particle size distribution. 5 (e) Detect, quantify and track hazards including HABs and petroleum-derived hydrocarbons.	*Other coastal and large inland bodies of water within ocean color FOR:* • Baseline: multiple RSI 3 scans/day **Spatial Resol. (nadir):** • **#**Descope: ≤500 x 500 m • **#**Threshold: ≤375 x 375 m • Baseline: ≤250 x 250 m **Field of Regard for Ocean Color Retrievals:** 5 2 3 60°N to 60°S; 155°W to 35°W	**Signal-to-Noise Ratio (SNR) at Ltyp(70° SZA):** • Threshold: ≥1000:1 for 10 nm FWHM (350-800 nm); ≥600:1 for 40 nm FWHM in NIR; ≥250:1, ≥180:1 at 1:00:1 for the 1245 & 1640 nm (20 & 40 nm FWHM); ≥500:1 NO₂ band • **#**Baseline: ≥1500:1 for 10 nm (350-800 nm); NIR, SWIR and NO₂ bands same as threshold; ≥100:1 for the 2135nm (50nm FWHM) **Scanning area per unit time:** Threshold: ≥25,000 km²/min; Baseline: ≥50,000 km²/min **Field of Regard:** • Full disk: 20.8° E-W and 19° N-S imaging capability from nadir for Lunar & Solar Calibrations		(8) Ocean circulation (9) Tidal & other coastal currents (10) Aerosol deposition (11) run-off (12) Wet deposition in coastal zone (13) Wave height & surface wind speed
Impacts of Airborne-Derived Fluxes	**4** How do the airborne-derived fluxes from precipitation, fog and episodic events such as fires, dust storms & volcanoes significantly affect the ecology and biogeochemistry of coastal and open ocean ecosystems? (OBB 1 & 2)	GEO-CAPE observations will be integrated with field measurements, models and other satellite data: (1) to derive coastal carbon budgets and determine whether coastal ecosystems are sources or sinks of carbon to the atmosphere, 2 3 (2) to quantify the responses of coastal ecosystems and biogeochemical cycles to river discharge, land use change, airborne-derived fluxes, hazards and climate change, and	**#Error** (as % of nadir pixel) **Pointing Knowledge LOS** **Pointing Accuracy LOS** **Pointing Stability LOS** **Geolocation Reconstr.** **Non-saturating detector array(s) at Lmax** **On-board Calibration:** • Lunar: Threshold: minimum monthly; Baseline: same as threshold • Solar: Threshold: none; Baseline: daily **Polarization Sensitivity:** <1.0%	(table) Threshol / Baselin: <50% / <10%; <100% / <25%; <50% / <10%; #<100% / <10%		**Science Requirements** Conduct high frequency field measurements and modeling to validate GEO-CAPE retrievals from river mouths to beyond the edge of the continental margin.
Episodic Events & Hazards	**5** How do episodic hazards, contaminant loadings, and alterations of habitats impact the biology and ecology of the coastal zone? (OBB 4)	(3) to enhance management decisions with improved information on the coastal ocean, such as Chesapeake Bay & Integrated Ecosystem Assessment (IEA), protection of water quality, and mitigation of harmful algal blooms, oxygen minimum zones, and ocean acidification. 3 5	RSI examples: Amazon & Orinoco River plumes, Peruvian upwelling, Cariaco Basin, Bay of Fundy, Rio Plata, etc. TBD) **Intelligent Payload Module:** Near Real-Time satellite data download from other sensors (GOES, etc.) for on-board autonomous decision making - **Baseline**. **Solar Zenith Angle Sensitivity:** Threshold: ≤70°; Baseline: ≤75°	**Relative Radiometric Precision:** • Threshold: ≤1% through mission lifetime • Baseline: ≤0.5% through mission lifetime **Mission lifetime:** 3 years; Goal: 5 years **Pre-launch characterization:** to achieve radiometric precision above on orbit	**Validation Requirements**	

 # Requirements under review for further discussion

GEO-CAPE Science Questions are traceable to NASA's OBB Advanced Planning Document. .....

* Coastal coverage within field-of-view (FOV) includes major estuaries and rivers such as Chesapeake Bay & Lake Pontchartrain/Mississippi River delta; e.g., the Chesapeake Bay coverage region would span west to east from Washington D.C. to several hundred kilometers offshore (total width of 375 km threshold).

Figure A.1 Science traceability matrix for the NASA GEO-CAPE mission.

capability, there are presently no specific plans in place at this time to meet those requirements. That said, NOAA scientists are actively involved in pre-formulation activities for NASA's GEO-CAPE mission as described above. NOAA scientists have also been actively working on improving ocean colour products in coastal regions, including the operational delivery of SWIR-based ocean colour data for U.S. coastal regions. As is presently the case with data from NASA's MODIS sensor and VIIRS on Suomi NPP, it is envisioned that data from GEO-CAPE and other R&D GEO missions implemented in the future could be utilized operationally by NOAA to support its coastal user needs and applications.

A.3   KIOST (Korea)

A.3.1   GOCI current status

GOCI (Geostationary Ocean Color Imager) is the world's first ocean-colour imager in a geostationary orbit. GOCI was successfully launched at the Kourou Space Center in French Guiana on 27 June 2010 (Korea Standard Time) as the main payload of the Communication, Ocean and Meteorological Satellite (COMS). The first GOCI image acquisition test was successfully performed on 13 July 2010. The GOCI in-orbit test campaign was scheduled for six months for in-orbit performance validation and operational testing for the ground segments in KARI and KIOST. The Korea Ocean Satellite Centre (KOSC, in KIOST `http://kosc.kordi.re.kr`) has been successfully disseminating GOCI data since 20 April 2011 (see Figure A.2).

A.3.2   GOCI-II mission, user requirements and concept design

In late 2011, KORDI (now called KIOST) started to develop the next generation geostationary ocean-colour imager, GOCI-II, which is scheduled to be launched in 2018. Major mission differences between GOCI and GOCI-II are full disk coverage to monitor long-term ocean environment and climate change, and higher ground resolution (< 250 m) in local area coverage to effectively monitor coastal waters. The following mission requirements of GOCI-II were developed by the Korean ocean-colour expert community, organized by KIOST.

❖ Succession and expansion of the GOCI mission:
  ❖ to reduce the damage caused by disasters and catastrophes in the ocean,
  ❖ to provide real time ocean environment monitoring, and
  ❖ to monitor oil spills, tidal waves and the spread of harmful algal blooms (red tides).
❖ Global area (full disk) observation with moderate spatial resolution (~1,000 m):
  ❖ to establish an ocean observation system to monitor long-term climate change, and
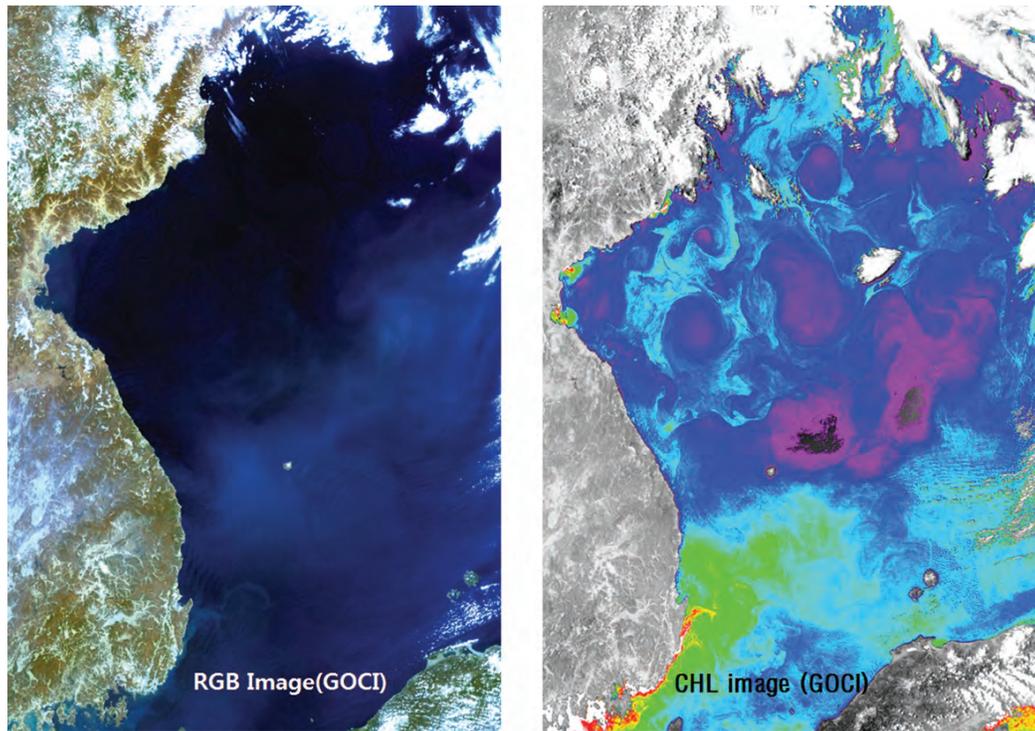
Figure A.2 RGB (left) and Chlorophyll (right) images captured by GOCI in the East (Japan) Sea on 30 March 2011. The physical dynamics of surface water movement (eddies) are clearly visible in fine detail in the Chlorophyll image.

❖ to provide ocean environment monitoring to detect variations in marine ecosystems
❖ User selectable local area observation with high spatial resolution (< 250m):
  ❖ to monitor the fresh water environment for the drift and spread of polluting materials,
  ❖ to monitor pollution of coastal waters, and
  ❖ to search for fishing grounds and monitor aquaculture environments in coastal waters.

To satisfy the GOCI-II user requirements, state-of-the-art electronic-optics technologies are necessary to develop GOCI-II. A complicated FOV selectable optical system or full disk scanning optical system is required to adapt the functions of coverage selection (between full disk and local area), and movable local area. High spatial resolution (< 250 m) for local area observation in the geostationary orbit is one of the most challenging requirements in the design process. The solution of GOCI-II is to equip a state-of-the-art, low-noise FPA detector with small pixel size (< 7 μm; GOCI is 14μm) and to fabricate the optical system with a large aperture (~30 cm; GOCI is 14 cm). As a result of the GOCI-II concept study, all user requirements are achievable with state-of-the-art technologies and fall within the development

	GOCI-II	GOCI
Temporal resolution	1 hour intervals	1 hour intervals
	8 times/day during daylight hours	8 times/day during daylight hours
Spatial resolution	< 250 m in local area mode	
	1,000 m in full disk mode	500 m
Spatial coverage	2,500 km in local area mode	
	12,500 km in full disk mode	2,500 km in local area mode
Spectral resolution	10 to ~40 nm	10 to ~40 nm
Spectral bands	15 bands	8 bands
	(1 UV, 9 visible, 2 NIR and 3 SWIR)	(6 visible, 2 NIR)
SNR	1,500	1,000

Table A.1 Comparison of GOCI-II and GOCI main technical requirements.

time frame for GOCI-II.

GOCI-II will have 15 spectral bands (GOCI has 8 bands) for phytoplankton fluorescence signal (FLH) and enhanced atmospheric correction accuracy. Table A.2 below shows the specifications of the 15 bands (8 of which are common to the heritage GOCI instrument) as well as some of the primary applications.

A.4   ESA (European Union)

The European Space Agency (ESA) is currently developing two identical Sentinel-3 satellites as part of the Global Monitoring for Environment and Security (GMES) programme. The pair of Sentinel-3 satellites will monitor ocean and land surfaces routinely to generate valuable information for the European Union Marine Core Service as well as the Land Monitoring Core Service, with the first launch in 2013. The OLCI (Ocean Land Colour Imager) instrument on board Sentinel-3 will continue the role of Envisat's MERIS instrument but with enhanced performance, in particular regarding the coverage. The mean revisit time over the sea (after sunglint masking and assuming cloud free conditions) will be better than 2 days. The instrument will acquire 21 channels in the visible and NIR and transmit the full resolution data (300 m) continuously.

ESA has started investigating a mission for real-time monitoring through high resolution imaging from a geostationary orbit, named Geo-Oculus with the following objectives:

Primary Mission Objectives:

- ❖ algal bloom detection and monitoring,
- ❖ water quality monitoring with respect to European regulations,
- ❖ disaster monitoring, and
- ❖ fire monitoring.

Band	Heritage	Band Center (nm)	Band width (nm)	Primary Application
1	GOCI-II	380	20	CDOM, atmospheric correction for strong absorbing aerosols
2	GOCI-B1	412	20	yellow substance and turbidity
3	GOCI-B2	443	20	chlorophyll absorption maximum
4	GOCI-B3	490	20	chlorophyll and other pigments
5	GOCI-II	520	20	red tides
6	GOCI-B4	555	20	turbidity, suspended sediment
7	GOCI-II	625	20	suspended sediments
8	GOCI-B5	660	10	baseline of fluorescence signal, chlorophyll, suspended sediment
9	GOCI-B6	681	10	atmospheric correction and fluorescence signal
10	GOCI-B7	745	20	atmospheric correction and baseline of fluorescence signal
11	GOCI-II	765	20	aerosol properties, atmospheric properties TBD
12	GOCI-B8	865	40	aerosol optical thickness, vegetation, water vapor reference over the ocean TBD
13 to 15	GOCI-II	3-SWIR (TBD)	40 nm	Atmospheric correction for turbid waters

Table A.2 Specifications of the 15 GOCI-II spectral bands (TBD, 8 of which are common to the heritage GOCI instrument) as well as some of the primary applications.

Secondary Mission Objectives:

❖ oil slick environmental information, and
❖ monitoring of erosion and sediment transport on the European shoreline.

The observations will be based on a system with satellite agility and the capability to access the whole of Europe with a resolution ranging from 20 m to 100 m. The mission plan would take into account the actual weather conditions. It has been shown that effective coverage of European coastal waters would be more than doubled compared to LEO based observations. ESA is planning to continue the Geo-Oculus assessment after the consolidation of the mission requirements (from the "HR GEO User Consultation Workshop" in 2010).

ESA is also currently supporting a variety of activities aimed at verifying and quantifying marine reflectances obtained after atmospheric correction of TOA radiances measured by MERIS on Envisat. An important project is BOUSSOLE, an optical buoy located in Case-1 waters in the middle of the Ligurian Sea. BOUSSOLE provides data that can be used to study the calibration of MERIS and quality control the atmospheric correction algorithms. It complements the NOAA optical buoy MOBY, by providing measurements obtained with essentially the same protocols, providing data under different illumination geometries and different atmospheric

aerosol conditions. In addition, ESA supports the network of Ocean-Colour Aeronet stations (AAOT in the Adriatic sea, Palgruden Lighthouse in Lake Wanern, Sweden) and one land-based AERONET station (Sagres, Portugal) to characterize the aerosol properties in the region of Cape Saint-Vincent, which is famous for the purity of its skies. ESA also supports the evaluation of optical measurements made with small optical buoys (TACCS systems, multispectral and hyperspectral) or above-water TriOS Ramses systems mounted on small ships, in coastal waters. Emphasis is on traceability of calibration, stray light issues and tilt correction. In addition, ESA supports the collection of inherent optical properties of waters in various coastal areas of Europe, with the goal of developing regional bio-optical algorithms for the ultimate inversion of marine reflectance to provide products suitable for practical monitoring of coastal waters. All current activities are generic and can be applied to all present and future ocean-colour sensors. Within the framework of the GMES Service Element Programme ESA has initiated the MARCOAST (Marine & Coastal Environmental Information Services) project with the aim of establishing a durable network of marine and coastal information services. MARCOAST is delivering a portfolio of water quality and algal bloom information services on a systematic basis to operational regional, National and European organisations responsible for monitoring coastal environmental conditions.

A.5   CNES (France)

Up until now, the major contribution of CNES in observing the oceans from space has been dedicated to physical oceanography through altimetry (TOPEX-JASON series, SARAL, Sentinel-3, HY-2A) and innovative cooperation in the field of physical oceanography (SMOS, CFOSAT, SWOT). CNES has also supported a number of initiatives towards developing ocean-colour observations, both through POLDER on ADEOS-I and II satellites, as well as supporting the establishment of the IOCCG in 1996, and supporting French research activities such as the BOUSSOLE validation site, *in-situ* instrumentation and campaigns. In recent years CNES has been contributing to the development of the ocean colour community in France through its participation in a Scientific Interest Group on Ocean Colour (GIS-COOC). CNES also participates in ESA missions such as MERIS on Envisat and OLCI on Sentinel-3.

After more than 20 years, ocean-colour remote sensing is now transitioning from research to applications with growing attention devoted to coastal areas. This implies a significant increase in requirements in terms of resolution (spatial and temporal). Providing one useful observation per day (or at least, every two days) is the minimal threshold requirement, the ultimate goal being to monitor diurnal cycles of various phenomena. State-of-the-art models of the ocean (MERCATOR) will soon be ready to include biology at least in a pre-operational configuration, and this also requires daily observations. Clearly, none of the current single satellite missions

can meet this requirement. Although very attractive in principle, constellations of LEO satellites are still a challenge for space agencies. This is why cooperation at the agency level is critical for developing "virtual" constellations among partners. This is also why CNES is interested in the GEO approach. A Phase 0 study was conducted in 2008 regarding the GEO/LEO trade-off as well as research and development (R&D) studies on aerosol retrieval and development of tools preparing for the processing of GEO observations.

A scientific proposal entitled "Ocean Colour Advanced Permanent Imager" (OCAPI) was submitted to the CNES "Appel á idées" (call for ideas), assessed by the CNES scientific advisory committee and recommended in March 2009. Consequently a Phase-0 study for a GEO ocean-colour mission was started and continued until mid-2012. Since cooperation among the various space agencies is even more complicated with GEO than for LEO missions, the role of a coordinating body is essential. CNES Headquarters therefore participates in the CEOS "Virtual Constellation" for Ocean-Colour Radiometry (OCR-VC), established by the IOCCG in the context of the Committee on Earth Observation Satellites (CEOS) and the Group on Earth Observations (GEO).

A.6 ISRO (India)

The Indian Space Research Organsiation (ISRO) is planning to launch a High Resolution-GEO mission called GISAT, which is a multi-spectral, multi-resolution mission capable of imaging the full, or part of, the Earth disk from a geostationary platform with following four basic instruments:

- ❖ high resolution, multi-spectral VNIR (HRMX-VNIR),
- ❖ hyperspectral (HySI-VNIR),
- ❖ hyperspectral (HySI-SWIR),
- ❖ high resolution multi-spectral TIR (HRMX-TIR).

Sections A.6.1 to A.6.4 below provide details of the individual instruments while Table A.4 provides summary details of this proposed GISAT mission.

A.6.1 High resolution multi-spectral VNIR imager (HRMX-VNIR)

This instrument will image in the visible and near infrared bands. The band characteristics will be similar to the IRS series of payloads with a resolution of ~50 m (see Table A.3 for details of proposed bands).

A.6.2 Hyperspectral Imager (HySI-VNIR)

This instrument will have hyperspectral imaging capabilities with 60 bands in the 400 to 870 nm range which will be used for ocean-colour imaging. The footprint at nadir (GIFOV) will be around 350 m.

Centre wavelength (nm)	Bandwidth (nm)
485	70
555	70
650	60
815	90

Table A.3 Band specifications for the high resolution multi-spectral VNIR imager.

A.6.3   Hyperspectral SWIR Imager (HySI-SWIR)

This instrument will provide hyperspectral data of the Earth in the short wave infrared (SWIR) bands. It will have 150 bands in range 1000 to 2500 nm with a footprint at nadir (GIFOV) of 200 m.

A.6.4   High resolution multi-spectral TIR Imager (HRMX-TIR)

High resolution multi-spectral thermal infrared (TIR) imaging will be carried out in the following three bands: 8.2 – 9.2 μm, 10.3 – 11.3 μm and 11.5 – 12.5 μm. The footprint at nadir (GIFOV) will be 1.5 km x 1.5 km.

Sensor	Number of Bands	Spectral range (μm)	Band-width (nm)	Spatial Resolution (m)
High resolution multi-spectral VNIR imager (HRMX-VNIR)	4	0.45 - 0.52 0.52 - 0.59 0.62 - 0.68 0.77 - 0.86	70 70 60 90	50
Hyperspectral (HySI-VNIR) imager	60	0.40 - 0.87	~8	350
Hyperspectral (HySI-SWIR) imager	150	1.0 - 2.5	~20	200
High resolution multi-spectral TIR imager (HRMX-TIR)	3	8.2 - 9.2 10.3 - 11.3 11.5 - 12.5		1500

Table A.4 Summary details of the four instruments on ISRO's planned GISAT mission.

A.7   JAXA (Japan)

JAXA launched the Advanced Earth Observation Satellite (ADEOS) carrying the Ocean Color and Temperature Scanner (OCTS) in 1996, and ADEOS-II carrying the Global Imager (GLI) in 2002. Each of these sensors collected global ocean-colour radiometry data for about 8 months, with a 1 km resolution. GLI also provided 250 m spatial

resolution radiometry with coarse spectral resolution. The Advanced Visible and Near Infrared Radiometer type 2 (AVNIR-2) on the Advanced Land Observing Satellite (ALOS), was launched on 2006 and operated for about 5 years, also providing coarse spectral radiometry data with a high resolution of 10 m.

JAXA is now planning to launch the second generation GLI instrument (SGLI) onboard the Global Change Observation Mission for Climate (GCOM-C). This sensor will include ten wavelengths of 250 m resolution from near-ultraviolet to short wave-infrared and two thermal channels. The possible time schedule of the first launch is in 2015. A geostationary ocean-colour sensor was one of candidates for a future geostationary mission. However, the atmospheric hyperspectral observation is the current first priority. The Japanese ocean-colour community will contribute towards the validation of GOCI as principle investigators and co-investigators of the mission.

A.8   CNSA (China)

Regarding dedicated ocean remote sensing satellites, the China National Space Administration (CNSA) has established a blueprint for three series of sun-synchronous ocean satellites to be launched before 2020, including the Ocean Colour Satellite series (HY-1 Series), Ocean Dynamic Satellite series (HY-2 Series) and Ocean Watch & Monitor Satellite series (HY-3 Series). Currently, there is no formal plan to launch a special GEO ocean-colour satellite, but there is interest from some scientists to propose a GEO ocean-colour remote sensing satellite program.

The HY-1 series is the ocean-colour and temperature satellite. HY-1A was launched on 15 May 2002 and failed in 2004, and HY-1B was launched on 11 April 2007, and is still in orbit providing routine products. The HY-1C/D (AM/PM) should be launched in the 2014 time frame after which two HY-1 satellites (AM/PM) will be launched every 3 – 4 years up to 2020. There are two sensors on board the HY-1A/B: one is the COCTS (Chinese Ocean-Colour and Temperature Sensor) with 1.1 km spatial resolution, and the other is the CZI (Coastal Zone Imager, the CCD camera) with 300 m spatial resolution. The HY-2 series is the dynamic ocean satellite for ocean surface wind, wave field, as well as the topography, sea level and gravity monitoring. HY-2A was launched on 16 August 2011 with a payload of a radar altimeter, microwave scatter meter and microwave radiometer. The third series, HY-3, will be a comprehensive and operational satellite constellation combining the functions of ocean-colour radiometry and dynamic monitoring, especially for observing coastal regions with high spatial resolution. The HY-3A satellite is scheduled for launch in 2015.

Besides the special ocean remote sensing satellite series, the meteorological satellite series (FY) can also be used for ocean monitoring, including ocean-colour observations. The meteorological satellite series (FY) are the most sophisticated

satellites in China with four satellite series planned. FY-1 and FY-3 are the polar orbiting satellites, and FY-2 and FY-4 are the GEO satellite series. The World Meteorological Organization has accepted the FY-1, FY-2 and FY-3 satellites into the international operational meteorological satellite network. Currently, the FY-1 series is operating its fourth satellite (FY-1D), carrying a visible and infrared radiometer.

The FY-3A mission was launched on 27 May 2008 carrying 11 sensors, one of which, MERSI (Medium Resolution Spectra Imager), is similar to ESA's MERIS sensor, and is capable of monitoring ocean colour with a spatial resolution of 250 m. The FY-3 series represents China's new generation of polar orbiting meteorological satellites with 9 planned operational satellites, which will be launched every 2 years from 2013.

FY-2 is the first generation of the GEO meteorological series with 7 satellites (FY-2A,B,C,D,E,F,G). FY-2A/B is the experimental GEO satellites with FY-2A launched on 10 June 10 1997, and FY-2B on 25 June 2000. The operational satellites with a 5 channel VISSR (Visible and near-Infrared Spin Scanner Radiometer) include FY-2C (18 October 2004), FY-2D (8 December 2006) and FY-2E (23 December 2008). Currently, FY-2C,D,E are operational with an observation frequency of 15 minutes. FY-4 is the next generation of GEO meteorological satellites, which is at the pre-phase A stage and is scheduled to be launched after 2012. The major payloads in consideration include a multi-channel scan imaging radiometer, infrared sounder, atmosphere vertical sounder, lightning mapping sensor, solar X-ray imager and space environment monitor suite, amongst others, to integrate the optical and microwave sensing ability. For the imaging radiometer, 12 channels will be considered (similar to MSG and GOES-R) with a high spatial resolution (e.g., 100 m), more frequent observations (15 minutes over China), and ~300 x 300 km swath.

Theoretically, the GEO meteorological satellites FY-2/4 can be used for coastal ocean-colour applications using the visible and near-infrared radiometer, although the radiometric performance is not sufficient for the open ocean. In the future, there will be less distinction between oceanic and meteorological satellites in China, since the onboard sensors have become more and more sophisticated and allow for comprehensive applications.

Appendix B

Acronyms and Abbreviations

AAOT	Acqua Alta Oceanographic Tower (AERONET platform in Adriatic Sea)
ACRI-ST	Independent R&D company based in Sophia-Antipolis, France
ADC	Analog to Digital Converter
ADEOS	Advanced Earth Observation Satellite (Japan)
AERONET	Aerosol Robotic Network
ALOS	Advanced Land Observing Satellite (Japan)
AOD	Aerosol Optical Depth
ATSR	Along Track Scanning Radiometer
AVHRR	Advanced Very High Resolution Radiometer (NOAA)
AVNIR	Advanced Visible and Near Infrared Radiometer (Japan)
BOUSSOLE	Buoy for the acquisition of a long-term optical series (Mediterranean Sea)
BRDF	Bidirectional Reflectance Distribution Function
CCD	Charge-Coupled Device
CDOM	Coloured Dissolved Organic Matter
CEOS	Committee on Earth Observation Satellites
CFOSAT	Chinese-French Oceanic Satellite
ChloroGIN	Chlorophyll Globally Integrated Network
CMOS	Complementary Metal Oxide Semiconductor
CNES	Centre National d'Etudes Spatiales
CNRS	Centre National de la Recherche Scientifique
CNSA	China National Space Administration
COCTS	Chinese Ocean-Colour and Temperature Sensor
COMS	Communication, Ocean and Meteorological Satellite (Korea)
CSA	Chinese Space Agency
CZCS	Coastal Zone Color Scanner
CZI	Coastal Zone Imager (China)
DIC	Dissolved Inorganic Carbon
DN	Digital Number
DOC	Dissolved Organic Carbon
EDR	Environmental Data Record
Envisat	Environmental Satellite (ESA)
ESA	European Space Agency

FDHSI	Full Disk High Spectral Resolution Imagery
FLH	Fluorescence Line Height
FOV	Field-of-View
FPA	Focal Plane Array
FSLE	Finite Size Lyapunov Exponent
FY	Chinese meteorological satellite series
GCOM-C	Global Change Observation Mission for Climate (Japan)
GEO	Used for geostationary in this report
GEO	The intergovernmental Group on Earth Observations
GEO-CAPE	Geostationary Coastal and Air Pollution Events mission (NASA)
GIFOV	Ground Instantaneous Field-of-View
GISAT	High Resolution GEO Imager (India)
GIS-COOC	Groupement d'Intérêt Scientifique - COlour of the OCean
GLI	Global Imager (Japan)
GMES	Global Monitoring for Environment and Security (EU)
GOCI	Geostationary Ocean Colour Imager (Korea)
GOES	Geostationary Operational Environmental Satellite
GOOS	Global Ocean Observing System
GSD	Ground Sample Distance
GSFC	Goddard Space Flight Center (NASA)
HAB	Harmful Algal Bloom
HAB-OFS	Harmful Algal Bloom Operational Forecast System (NOAA)
HES	Hyperspectral Environment Suite (NOAA)
HRFI	High Resolution Fast Imagery
HY	Chinese Ocean Colour Satellite Series
IEU	Instrument Electronics Unit
IGBP	International Geosphere-Biosphere Programme
INSAT	Indian National Satellite
IOCCG	International Ocean-Colour Coordinating Group
IRS	Indian Remote Sensing satellite series
ISRO	Indian Space Research Organization
JASON	Satellite mission to monitor global ocean circulation
JAXA	Japan Aerospace Exploration Agency
JPSS	Joint Polar Satellite System (NOAA)
KARI	Korea Aerospace Research Institute
KIOST	Korea Institute of Ocean Science and Technology
LEO	Low-Earth Orbiting
LOV	Laboratoire d'Océanographie de Villefranche
MARCOAST	Marine & Coastal Environmental Information Services (ESA)
MBR	Maximum Band Ratio
MERCATOR	An ocean model (France)

MERIS	Medium Resolution Imaging Spectrometer (ESA)
MERSI	Medium Resolution Spectra Imager (China)
Meteosat	Series of geostationary meteorological satellites
MLI	Multi Layer Insulation
MOBY	Marine Optical Buoy
MODIS	Moderate Resolution Imaging Spectroradiometer (NASA)
MSG	Meteosat Second Generation
MTG	Meteosat Third Generation
MTSAT	Multi-functional Transport Satellite
MUMM	Management Unit of the North Sea Mathematical Models
NASA	National Aeronautics & Space Administration
NIR	Near-Infrared
NIST	National Institute of Standards and Technology (USA)
nL_w	normalized water-leaving radiance
NOAA	National Oceanographic and Atmospheric Administration
NPL	National Physical Laboratory (UK)
NRC	National Research Council (USA)
OC	Ocean Colour
OCAPI	Ocean Colour Advanced Permanent Imager (CNES)
Oceansat	Indian satellite carrying the OCM instrument
OCM	Ocean Colour Monitor (India)
OCR	Ocean Colour Radiometry
OCR-VC	Ocean Colour Radiometry - Virtual Constellation
OCTS	Ocean Color and Temperature Scanner (Japan)
OLCI	Ocean and Land Colour Imager (ESA)
OMI	Ozone Monitoring Instrument
OSU	Oregon State University
PAR	Photosynthetically Active Radiation
PIP	Payload Interface Plate
POC	Particulate Organic Matter
POLDER	Polarization and Directionality of the Earth's Reflectances (CNES)
PP	Primary Production
PPM	Plane-Parallel Medium
R&D	Research and Development
ROLO	Robotic Lunar Observatory model (USGS)
RT	radiative transfer
SARAL	Satellite with ARgos and ALtika (cooperative mission between CNES and ISRO)
SeaPRISM	SeaWiFS Photometer Revision for Incident Surface Measurements
SeaWiFS	Sea-viewing Wide Field-of-view Sensor (NASA)
Sentinel-3	Third series of "Sentinel" (ESA satellites)
SEVIRI	Spinning Enhanced Visible and Infrared Imager

SGLI	Second Generation Global Imager (Japan)
SGCA	Sunglint Correction Algorithm
SGLI	Second generation GLI instrument (Japan)
SMOS	Soil Moisture and Ocean Salinity mission (ESA)
SNR	Signal-to-Noise Ratio
SPM	Suspended Particulate Matter
SPOT	High-resolution, optical imaging Earth observation satellite system
SSM	Spherical Shell Medium
SST	Sea Surface Temperature
STM	Science Traceability Matrix
SWIR	Short Wave Infrared
SWOT	Surface Water Ocean Topography
TACCS	Tethered Attenuation Coefficient Chain Sensor
TIR	Thermal Infrared
TOA	Top of Atmosphere
USGS	U.S. Geological Survey
TMA	Three-Mirror Anastigmat (telescope)
TSM	Total Suspended Matter
UTC	Coordinated Universal Time
UV	Ultra Violet
VIIRS	Visible Infrared Imager Radiometer Suite
VISSR	Visible and near-Infrared Spin Scanner Radiometer
VNIR	Visible and Near Infra-Red
VIS	Visible

Appendix C

References

Adams CN and Kattawar GW (1978) Radiative transfer in spherical shell atmospheres I. Rayleigh scattering. ICARUS, 35,139-151

Ahmad Z, McClain CR, Herman JR, Franz BA, Kwiatkowska EJ, Robinson WD, Bucsela EJ and Tzortziou M (2007) Atmospheric correction for NO_2 absorption in retrieving water-leaving reflectances from the SeaWiFS and MODIS measurements. Appl. Opt. 46, 6504-6512

Allan TD (Ed.) (1983) Satellite Microwave Remote Sensing, John Wiley and Sons, Toronto 526 pp

Antoine D and Morel A (1999) A multiple scattering algorithm for atmospheric correction of remotely sensed ocean color (MERIS instrument): principle and implementation for atmospheres carrying absorbing aerosols. Int. J. Remote Sens. 20, 1875-1916

Antoine D and Nobileau D (2006) Recent increase of Saharan dust transport over the Mediterranean Sea, as revealed from ocean color satellite (SeaWiFS) observations. J. Geophys. Res. Atmos. 111, D12214, doi:10.1029/2005JD006795

Antoine D, Chami DM, Claustre H, D'Ortenzio F, Morel A, Bécu G, Gentili B, Louis F, Ras J, Roussier E, Scott AJ, Tailliez D, Hooker SB, Guevel P, Desté JF, Dempsey C and Adams D (2006) BOUSSOLE: a joint CNRS-INSU, ESA, CNES and NASA ocean color calibration and validation activity. NASA Technical Memorandum, 2006-214147, 61 pp

Antoine D, Siegel DA, Kostadinov T, Maritorena S, Nelson NB, Gentili B, Vellucci V and Guillocheau N (2011) Variability in optical particle backscattering in contrasting bio-optical oceanic regimes. Limnol. Oceanogr. 56(3), 955-973

Barnes RA, Eplee RE, Patt FS, Kieffer HH, Stone TC, Meister G, Butler JJ, and McClain CR (2004) Comparison of SeaWiFS measurements of the Moon with the U.S. Geological Survey lunar model. Appl. Optics 43, 5838-5854

Behrenfeld MJ, O'Malley RT, Siegel DA, McClain CR, Sarmiento JL, Feldman GC, Milligan AJ, Falkowski PG, Letelier RM, Boss ES (2006) Climate-driven trends in contemporary ocean productivity. Nature, 444(7120), 752-5

Beusen AHW, Dekkers ALM, Bouwman AF, Ludwig W and Harrison J (2005) Estimation of global river transport of sediments and associated particulate C, N, and P. Global Biogeochem. Cycles, 19, GB4S05, doi:10.1029/2005GB002453

Bignami F, Bohm E, D'Acunzo E, D'Archino R, Salusti E (2008) On the dynamics of surface cold filaments in the Mediterranean Sea. J. Mar. Syst. 74, 429-442

Bissett WP, Arnone R, Davis CO, Dickey T, Dye D, Kohler DDR and Gould R (2004) From meters to kilometers - a look at ocean colour scales of variability, spatial coherence, and the need for fine scale remote sensing in coastal ocean optics. Oceanogr. 17(2), 32-43

Boucher O, and Tanré D (2000) Estimation of the aerosol perturbation to the Earth's radiative budget over oceans using POLDER satellite aerosol retrievals. Geophys. Res. Lett. 27, 1103-1106

Brasseur P, Gruber N, Barciela R, Brander K, Doron M, El Moussaoui A, Hobday A, Huret M, Krémeur AS, Lehodey P, Matear R, Moulin C, Murtugudde R, Senina I and Svendsen E (2009) Integrating biogeochemistry and ecology into ocean data assimilation systems. Oceanogr. 22(3), 206-215

Brown SW, Flora SJ, Feinholz ME, Yarbrough MA, Houlihan T et al. (2007) The marine optical buoy (MOBY) radiometric calibration and uncertainty budget for ocean color satellite sensor vicarious calibration. Proc. SPIE, 6744, 67441M; doi:10.1117/12.737400

Carmillet V, Brankart JM, Brasseur P, Drange H, Evensen G and Verron J (2001) A Singular Evolutive Extended Kalman filter to assimilate ocean colour data in a coupled physical-biochemical model

of the North Atlantic ocean. Ocean Modelling, 3, 167-192

Chauhan OS, Menezes AAA, Jayakumar S, Malik MA, Pradhan Y, Rajawat AS, Nayak SR, Badekar G, Almeida C, Talaulikar M, Ramanamurthy MV and Subramanian BR (2007) Influence of the macro tidal environment on the source to sink pathways of suspended flux in the Gulf of Kachchh, India: evidence from the Ocean Colour Monitor (IRS-P4). Int. J. Remote Sens. 28(15), 3323-3339

Chauhan P, Mohan M, Matondkar P, Kumari B, and Nayak S (2002) Surface chlorophyll-a estimation using IRS-P4 OCM data in the Arabian Sea. Int. J. Remote Sens. 23(8), 1663-1676

Chiapello I, Goloub P, Tanré D, Herman J, Torres O, and March and A (2000) Aerosol detection by TOMS and POLDER over oceanic regions. J. Geophys. Res. 105, 7133-714

Clarke GL, Ewing GC and Lorenzen CJ (1970) Spectra of backscattered light from the sea obtained from aircraft as a measure of chlorophyll concentration. Science, 167, 1119-1121

Claustre H, Bricaud A, Babin M, Bruyant F, Guillou L, Le Gall F, Marie D and Partensky F (2002) Diel variations in *Prochlorococcus* optical properties. Limnol. Oceanogr. 47, 1637-1647

Claustre H, Morel A, Babin M, Cailliau C, Marie D, Marty JC, Tailliez D, and Vaulot D (1999) Variability in particle attenuation and chlorophyll fluorescence in the Tropical Pacific: Scales, patterns, and biogeochemical implications. J. Geophys. Res. 104, 3401-3422

Claustre H, Huot Y, Obernosterer I, Gentili B, Tailliez D and Lewis M (2008) Gross community production and metabolic balance in the South Pacific Gyre, using a non intrusive bio-optical method. Biogeosci. 5, 463-474

Cox C and Munk W (1954) Statistics of the sea surface derived from sun glitter. J. Mar. Res. 13, 198-227

Dall'Olmo G, Westberry TK, Behrenfeld MJ, Boss E and Slade WH (2009) Significant contribution of large particles to optical backscattering in the open ocean. Biogeosci. 6, 947-967

Davis CO, Kavanaugh M, Letelier R, Bissett WP and Kohler D (2007) Spatial and spectral resolution considerations for imaging coastal waters. Proc. SPIE 6680, 66800P, 1-12 Frouin RJ and Lee, ZP (Eds), doi: 10.1117/12.734288

Defoin-Platel M, and Chami M (2007) How ambiguous is the inverse problem of ocean color in coastal waters. J. Geophys. Res. 112(C03004): doi10.1029/2006JC003847

Dekker AG, Malthus TJ and Hoogenboom HJ (1995) In: Advances in Environmental Remote Sensing, John Wiley & Sons Ltd, England pp. 123-142

Del Castillo CE and Miller RL (2008) On the use of ocean color remote sensing to measure the transport of dissolved organic carbon by the Mississippi River Plume. Remote Sens. Environ. 112, 836-844

Deschamps PY, Bréon FM, Leroy M, Podaire A, Bricaud A, Bureiz JC and Seze G (1994) The POLDER mission: instrument characteristics and scientific objectives. IEEE Trans. Geosci. Remote Sens. 32, 598-615

Deuzé JL, Goloub P, Herman M, Marchand A, Perry G, Tanré D, Susana S (2000). Estimate of the aerosols properties over the ocean with POLDER. J. Geophys. Res. 105, 15329-15346

Deuzé, JL, Herman M, Goloub P, Tanré D, Marchand A (1999). Characterization of aerosols over ocean from POLDER/ADEOS-1. Geophys. Res. Lett. 26, 1421-1424

Dickey T, Lewis M, and Chang G (2006) Optical oceanography: recent advances and future directions using global remote sensing and *in situ* observations. Rev. Geophys. 44, RG1001, doi:10.1029/2003RG000148

Ding K and Gordon HR (1994) Atmospheric correction of ocean-color sensors: effects of the Earth's curvature. Applied Optics, 33(30), 7096-7106

D'Ovidio F, Isern-Fontanet J, López C, García-Ladona E, Hernández-García E (2009) Comparison between Eulerian diagnostics and the finite-size Lyapunov exponent computed from altimetry in the Algerian Basin. Deep Sea Res. I, 56, 15-31

Doxaran D, Froidefond JM, Castaing P and Babin M (2009) Dynamics of the turbidity maximum zone in a macrotidal estuary (the Gironde, France): Observations from field and MODIS satellite data. Est. Coast. Shelf Sci. 81, 321-332

Dubuisson P, Frouin R, Duforêt L, Dessailly D, Voss K and Antoine D (2009) Estimating aerosol altitude from reflectance measurements in the O_2 A-band. Remote Sens. Environ., 113, 1899-1911

Duforêt-Gaurier L, Loisel H, Dessailly D, Nordkvist K and Alvain S (2010) Estimates of particulate organic carbon over the euphotic depth from *in situ* measurements. Application to satellite data over the global ocean. Deep-Sea Res. I, 57, 351-367

Faugeras B, Lévy M, Mémery L, Verron J, Blum J, Charpentier I (2003) Can biogeochemical fluxes be recovered from nitrate and chlorophyll data? A case study assimilating data in the Northwestern Mediterranean Sea at the JGOFS-DYFAMED station. J. Mar. Syst. 40-41, 99-125

Field CB, Behrenfeld MJ, Randerson JT, Falkowski PG (1998) Primary production of the biosphere: Integrating terrestrial and oceanic components. Science, 281(5374), 237-240

Frankignoulle M, Abril G, Borges A, Bourge I, Canon C, Delille B, Libert E, and Théate J-M (1998) Carbon dioxide emission from European estuaries. Science, 282, 434-436

Franz BA, Bailey SW, Werdell PJ and McClain CR (2007) Sensor-independent approach to the vicarious calibration of satellite ocean colour radiometry. Appl. Opt. 46, 5068-5082

Gao B-C, Montes MJ, Ahmad Z and Davis CO (2000) An atmospheric correction algorithm for hyper-spectral remote sensing of ocean colour from space. Appl. Opt. 39(6), 887-896

GEO (2007) GEO Inland and Nearshore Coastal Water Quality Remote Sensing Workshop, 27 - 29 March 2007, Geneva, Switzerland 1-32 (http://www.igcp565.org/library/reports/GEO%20Water%20Quality%20report.pdf)

Gernez P, Antoine D and Huot Y (2011) Diel cycles of the particulate beam attenuation coefficient under varying trophic conditions in the northwestern Mediterranean Sea: observations and modelling. Limnol. Oceanogr. 56, 17-36

Gordon HR (1997) Atmospheric correction of ocean color imagery in the Earth observing system era. J. Geophys. Res. 102D, 17081-1710

Gordon HR and Wang M (1994) Retrieval of water-leaving radiance and aerosol optical thickness over the oceans with SeaWiFS: a preliminary algorithm. Appl. Opt. 33, 443-452

Gordon HR, Brown JW, Evans RH (1988) Exact Rayleigh scattering calculations for use with the Nimbus-7 Coastal Zone Colour Scanner. Appl. Opt. 27(5), 862-871

Gordon HR (1987) Calibration requirements and methodology for remote sensors viewing the ocean in the visible. Remote Sens. Environ. 22, 103-126

Gordon HR (1988) Ocean color remote sensing systems: radiometric requirements, SPIE symposium, Orlando, 4 April 1988

He, XQ, Pan DL, and Mao ZH (2004) Atmospheric correction of SeaWiFS imagery for turbid coastal and inland waters. Acta Oceanologica Sinica, 23, 609-615

Hedges JI (1992) Global biogeochemical cycles: progress and problems. Mar. Chem. 39, 67-93

Herman J, Cede A, Spinei E, Mount G, Tzortziou M, Abuhassan N (2009) NO$_2$ column amounts from ground-based Pandora and MFDOAS spectrometers using the direct-sun DOAS technique: Inter-comparisons and application to OMI validation. J. Geophys. Res. Atmos. 114, doi:10.1029/2009JD011848

Herman M, Deuze JL, Marchant A, Roger B, Lallart P (2005) Aerosol remote sensing from POLDER/ADEOS over the ocean: Improved retrieval using a nonspherical particle model. J. Geophys. Res. 110, D10S02, doi:10.1029/2004JD004798

Holden H and LeDrew E (1998) Critical literature review of the issues surrounding remote sensing of coral reef ecosystems. Prog. Phys. Geog. 190-221

Hooker SB, Esaias WE, Feldman GC, Gregg WW and McClain CR (1992) An Overview of SeaWiFS and Ocean Color. NASA Tech. Memo. 104566, Vol. 1, Hooker SB and Firestone ER, Eds. NASA Goddard Space Flight Center, Greenbelt, Maryland

Hovis WA, Clark DK, Anderson F, Austin RW, Wilson WH, Baker ET, Ball D, Gordon HR, Mueller JL, El Sayed SZ, Sturm B, Wrigley RC and Yentsch CS (1980) Nimbus-7 Coastal Zone Color Scanner: system description and initial imagery. Science, 210, 60-63

Hu C, Li X, Pichel WG, and Muller-Karger FE (2009) Detection of natural oil slicks in the NW Gulf of Mexico using MODIS imagery. Geophys. Res. Lett. 36, L01604, doi:10.1029/2008GL036119

IGOS (2006) A Coastal Theme for the IGOS Partnership - For the Monitoring of our Environment from Space and from Earth. UNESCO, Paris, IOC Information document No. 1220, 1-60

IOCCG (1998) Minimum Requirements for an Operational Ocean-Colour Sensor for the Open Ocean. Morel, A (ed.), Reports of the International Ocean-Colour Coordinating Group, No. 1, IOCCG, Dartmouth, Canada

IOCCG (1999) Status and Plans for Satellite Ocean-Colour Missions: Considerations for Complementary Missions. Yoder JA (ed.), Reports of the International Ocean-Colour Coordinating Group, No. 2,

IOCCG, Dartmouth, Canada

IOCCG (2000) Remote Sensing of Ocean Colour in Coastal and Other Optically-Complex Waters. Sathyendranath S (ed.), Reports of the International Ocean-Colour Coordinating Group, No. 3, IOCCG, Dartmouth, Canada

IOCCG (2004) Guide to the Creation and Use of Ocean-Colour, Level-3, Binned Data Products. Antoine D (ed.), Reports of the International Ocean-Colour Coordinating Group, No. 4, IOCCG, Dartmouth, Canada

IOCCG (2006) Remote Sensing of Inherent Optical Properties: Fundamentals, Tests of Algorithms, and Applications. Lee Z-P (ed.), Reports of the International Ocean-Colour Coordinating Group, No. 5, IOCCG, Dartmouth, Canada

IOCCG (2007) Ocean-Colour Data Merging. Gregg W (ed.), Reports of the International Ocean-Colour Coordinating Group, No. 6, IOCCG, Dartmouth, Canada

IOCCG (2008) Why Ocean Colour? The Societal Benefits of Ocean-Colour Technology. Platt T, Hoepffner N, Stuart V and Brown C (eds.), Reports of the International Ocean-Colour Coordinating Group, No. 7, IOCCG, Dartmouth, Canada

IOCCG (2009) Remote Sensing in Fisheries and Aquaculture. Forget M-H, Stuart V and Platt T (eds.), Reports of the International Ocean-Colour Coordinating Group, No. 8, IOCCG, Dartmouth, Canada

IOCCG (2010) Atmospheric Correction for Remotely-Sensed Ocean-Colour Products. Wang M (ed.), Reports of the International Ocean-Colour Coordinating Group, No. 10, IOCCG, Dartmouth, Canada

Isern-Fontanet, Lapeyre JG, Klein P, Chapron B and Hecht MW (2008) Three-dimensional reconstruction of oceanic mesoscale currents from surface information. J. Geophys. Res. 113, C09005, doi:10.1029/2007JC004692

Jackson C (2007) Internal wave detection using the Moderate Resolution Imaging Spectroradiometer (MODIS). J. Geophys. Res. 112, C11012, doi:10.1029/2007JC004220

Jamet C, Moulin C, and Thiria S (2004) Monitoring aerosol optical properties over the Mediterranean from SeaWiFS images using a neural network inversion. Geophys. Res. Lett. 31, 10.129/2004GL019951

Karl DM, Hebel DV, Bjorkman K and Letelier RM (1998) The role of dissolved organic matter release in the productivity of the oligotrophic North Pacific Ocean. Limnol. Oceanogr. 43, 1270-1286

Kaufman YJ, Koren I, Remer L, Tanré D, Ginoux P and Fan S (2005) Dust transport and deposition observed from the Terra-Moderate Resolution Imaging Spectroradiometer (MODIS) spacecraft over the Atlantic Ocean. J. Geophys. Res. 110, 10.129/2003JD004436

Kaufman YJ, D Tanré and O Boucher (2002) A satellite view of aerosols in the climate system. Nature, 419, 215-223

Kaufman YJ, Tanré D, Gordon HR, Nakalima T, Lenoble J, Frouin R, Grassl H, Herman BM, King MD and Teillet PM (1997), Passive remote sensing of tropospheric aerosol and atmospheric correction of the aerosol effect. J. Geophys. Res. 102, 16815-16830

Kieffer HH (1997) Photometric stability of the lunar surface. Icarus, 130, 323-327

Kieffer HH, Stone TC (2005) The spectral irradiance of the Moon. Astronomical Journal, 129, 2887-2901

King MD, Kaufman YJ, Tanré D and Nakajima T (1999) Remote sensing of tropospheric aerosols from space: past, present, future. Bull. Am. Meteorol. Soc. 80, 2229-2259

Klemas V, Field, R, and Weatherbee O (2003) Uses and limitations of remote sensing for coastal zone management. Proc. Coastal Zone 03, Baltimore, Maryland, July 13-17, 2003. p 1-3

Knapp KE, Frouin R, Kondragunta S and Prados AI (2005) Towards aerosol optical depth retrievals over land from GOES visible radiances: Determining surface reflectance. Int. J. Remote Sens. 26(18), 4097-4116

Knaeps E, Raymaekers D, Sterckx S, Ruddick K and Dogliotti A (2012) In-situ evidence of non-zero reflectance in the OLCI 1020 nm band for a turbid estuary. Remote Sens. Environ. doi: 10.1016/j.rse.2011.07.025.

Lee ZP and Carder K (2002) Effects of spectral-band number on retrievals of water column and bottom properties from ocean-colour data. Appl. Opt. 41, pp. 2191-2201

Lee ZP, Carder KL, Arnone R and He M (2007a) Determination of primary spectral bands for remote sensing of aquatic environments. Sensors, 7, 3428-3441

Lee ZP, Casey B, Arnone R, Weidemann A, Parsons R, Montes MJ, Gao BC, Goode W, Davis CO and Dye J (2007b) Water and bottom properties of a coastal environment derived from Hyperion data measured from the EO-1 spacecraft platform. J. Appl. Remote Sens. 1, 011502

Lehahn Y, d'Ovidio F, Lévy M and Heitzel E (2007) Stirring of the Northeast Atlantic spring bloom: a lagrangian analysis based on multi-satellite data. J. Geophys. Res. 112, C08005, doi: 10.1029/2006JC003927

Lévy M (2008) The modulation of biological production by oceanic mesoscale turbulence. Lect. Notes Phys. 744, 219-261, DOI 10.1007/978-3-540-75215-8_9

McClain CR, Feldman GC and Hooker SB (2004) An overview of the SeaWiFS project and strategies for producing a climate research quality global ocean bio-optical time series. Deep-Sea Res. II , 51(1), 5-42

McClain CR, Ainsworth EJ, Barnes RA, Eplee RE, Patt FS, Robinson WD, Wang M, Bailey SW (2000) SeaWiFS Postlaunch Calibration and Validation Analyses, Part 1, NASA Tech. Memo. 2000-206892, Vol.9. Hooker SB, Firestone ER (Eds), NASA Goddard Space Flight Center, 82 pp

Morel A (1991) Light and marine photosynthesis: A spectral model with geochemical and climatological implications. Prog. Oceanogr. 26, 263-306

Morel A, Antoine D and Gentili B (2002) Bidirectional reflectance of oceanic waters: Accounting for Raman emission and varying particle phase function. Appl. Opt. 41, 6289-6306

Morel A and Gentili B (1991) Diffuse reflectance of oceanic waters: its dependence on sun angle as influenced by molecular scattering contribution. Appl. Opt. 30, 4427-4438

Morel A and Gentili B (1993) Diffuse reflectance of oceanic waters. 2. Bidirectional aspects. Appl. Opt. 32, 6864-6872

Morel A and Gentili B (1996) Diffuse reflectance of oceanic waters. 3. Implication of bidirectionality for the remote-sensing problem. Appl. Opt. 35, 4850-4862

Morel A, Voss KJ and Gentili B (1995) Bidirectional reflectance of oceanic waters: A comparison of modeled and measured upward radiance fields. J. Geophys. Res. 100, 13,143-13,150

Moulin C, Gordon HR, Banzon VF and Evans RH (2001) Assessment of Saharan dust absorption in the visible from SeaWiFS imagery. J. Geophys. Res. 106, 18239-18249

Mutlow CT, Zavody AM, Barton IL and Llewellyn-Jones DT (1994) Sea surface temperature measurements by the along track scanning radiometer on the ERS-1 satellite: early results. J. Geophys. Res. 99, 22575- 22588

NASA (2006) Earth's Living Ocean: The Unseen World. An advanced plan for NASA's Ocean Biology and Biogeochemistry Research. http://oceancolor.gsfc.nasa.gov/DOCS/OBB_Report_5.12.2008.pdf

Natvik L-J and Evensen G (2003) Assimilation of ocean colour data into a biochemical model of the North Atlantic: Part 1. Data assimilation experiments. J. Mar. Sys. 40-41, 127-153

Nerger L and Gregg W (2008) Improving assimilation of SeaWiFS data by the application of bias correction with a local SEIK filter. J. Mar Syst. 73, 87-102

Neukermans G, Ruddick K, Bernard E, Ramon D, Nechad B and Deschamps PY (2009) Mapping total suspended matter from geostationary satellites: a feasibility study with SEVIRI in the Southern North Sea. Opt. Express, 17(16), 14029-14052

Nobileau D and Antoine D (2005) Detection of blue-absorbing aerosols using nearinfrared and visible (ocean color) remote sensing observations. Remote Sens. Environ. 95, 368-387

Nordkvist K, Loisel H and Gaurier LD (2009) Cloud masking of SeaWiFS images over coastal waters using spectral variability. Opt. Express 17(15), 12246-12258

NRC (2007) Earth Science and Applications from Space: National Imperatives for the Next Decade and Beyond. The National Academies Press, Washington, D.C.

O'Reilly JE, Maritorena S, Mitchell BG, Siegel DA, Carder KL, Garver SA, Kahru M, and McClain CR (1998) Ocean color chlorophyll algorithms for SeaWiFS. J. Geophys. Res. 103, 24937-24953

O'Reilly JE, Maritorena S, Siegel DA, O'Brien, MC, Toole D, Mitchell BG, et al. (2000). Ocean color chlorophyll-a algorithms for SeaWiFS, OC2, and OC4: version 4. SeaWiFS postlaunch calibration and validation analyses, Part 3, NASA/TM 206892, 11, 9-23

Preusker R, Fischer J, Albert P, Bennartz R, Schuller L (2007) Cloud-top pressure retrieval using the oxygen A-band in the IRS-3 MOS instrument. Int. J. Remote Sens. 28, 1957-1967

Rajawat AS, Gupta M, Pradhan Y, Thomaskutty AV and Nayak S (2005) Coastal processes along the Indian coast-Case studies based on synergistic use of IRS-P4 OCM and IRS-1C/1D data. Indian J. Mar. Sci. 34(4), 459-472

Ramachandran S and Wang M (2011) Near-real-time ocean color data processing using ancillary data from the Global Forecast System model. IEEE Trans. Geosci. Remote Sens. 49(4), 1485-1495

Ramakrishnan R and Rajawat AS (2008) Sediment dynamics in Gulf of Kachchh, In the proceedings of National symposium on Advances in Remote Sensing technology and applications with special emphasis on microwave remote sensing, ISRS Symposium Dec. 18-20, Ahemadabad, India

Rast M and Bézy JL (1995) The ESA medium resolution imaging spectrometer (MERIS): requirements to its mission and performance of its system, in RSS95, In: Remote Sensing in Action, Proceedings of the 21st Annual Conf. Remote Sensing Soc. 11-14 September, 1995, University of Southampton, Curran PJ & Robertson YC (eds), Taylor and Francis, p. 125-132

Rast M, Bézy JL and Bruzzi, S. (1999) The ESA Medium Resolution Imaging Spectrometer MERIS: a review of the instrument and its mission. Int. J. Remote Sens. 20, 1681-1702

Remer LA, Kaufman YJ, Tanré D, Mattoo S, Chu DA, Martins JV, Li RR, Ichoku C, Levy RC, Kleidman RG, Eck TF, Vermote E and Holben BN (2005), The MODIS Aerosol Algorithm, Products and Validation. J. Atm. Sci. Special Section. 62, 947-973

Robinson IS, Antoine D, Darecki M, Gorringe P, Pettersson L, Ruddick K, Santoleri R, Siegel H, Vincent P, Wernand MR, Westbrook G, Zibordi G (2008) Remote Sensing of Shelf Sea Ecosystems: State of the Art and Perspectives. Connolly N (ed.), Position paper 12 of the Marine board of the European Science Foundation.

Ruddick KG, Ovidio F, Rijkeboer M (2000) Atmospheric correction of SeaWiFS imagery for turbid coastal and inland waters. Appl. Opt. 39(6), 897-912

Sabine CL, Heimann M, Artaxo P, Bakker D, Chen C-TA, Field CB, Gruber N, LeQuéré C, Prinn RG, Richey JE, Lankao PR, Sathaye J and Valentini R (2004) Current status and past trends of the global carbon cycle in SCOPE 62, The Global Carbon Cycle: Integrating Humans, Climate, and the Natural World. Field CB and Raupach MR (eds.), Island Press, Washington D.C. 17-44

Salomonson VV, Barnes WL, Maymon PW, Montgomery HE and Ostrow X (1989) MODIS: advanced facility instrument for studies of the earth as a system. IEEE Trans. Geosci. Remote Sens. 27, 145-152

Sandwell WT and Smith WHF (1997) Marine gravity anomaly from Geosat and ERS-1 satellite altimetry. J. Geophys. Res. 102:10039-10054

Schlunz B and Schneider RR (2000) Transport of terrestrial organic carbon to the oceans by rivers: re-estimating flux and burial rates. Int. J. Earth Sci. 88, 599-606

Shi W and Wang M (2009) An assessment of the black ocean pixel assumption for MODIS SWIR bands. Remote Sens. Environ. 113, 1587-1597

Simis SGH, Peters SWM and Gons HJ (2005) Remote sensing of the cyanobacterial pigment phycocyanin in turbid inland water. Limnol. Oceangr. 50(1), 237-245

Siegel DA, Dickey TD, Washburn L, Hamilton MK and Mitchell BG (1989) Optical determination of particulate abundance and production variations in the oligotrophic ocean. Deep Sea Res. 36, 211-222

Simon E and Bertino L (2009) Application of the Gaussian anamorphosis to assimilation in a 3-D coupled physical ecosystem model of the North Atlantic with the EnKF: a twin experiment. Ocean Sci. Discuss. 6, 617-652

Sirjacobs D, Alvera-Azcárate A, Barth A, Lacroix G, Park Y, Nechad B, Ruddick K and Beckers J-M (2011) Cloud filling of ocean color and sea surface temperature remote sensing products over the southern North Sea by the Data Interpolating Empirical Orthogonal Functions methodology. J. Sea Res. 65, 114-130

Stegman PM (2004b) Characterization of aerosols over the North Atlantic ocean from SeaWiFS. Deep-Sea Res. II, 51, 913-925.

Stegman PM (2004a) Remote sensing of aerosols with ocean colour sensors: then and now. Int. J. Remote Sens. 25, 1409-1413

Stegman PM and Tindale NW (1999) Global distribution of aerosols over the open ocean as derived from the coastal zone color scanner. Global Biogeochem. Cycles, 13, 383-397

Steinmetz F, Deschamps PY, Ramon D (2011) Atmospheric correction in presence of sun glint: application to MERIS. Opt. Express, 19(10), 9783-800. doi: 10.1364/OE.19.009783

Stone TC, Kieffer HH and Grant IF (2005) Potential for calibration of geostationary meteorological satellite imagers using the Moon. Proceedings of SPIE, 5882, OP1-8

Stramski D and Reynolds RA Diel (1993) Variations in the optical properties of a marine diatom. Limnol. Oceanogr. 38, 1347-1364

Taylor LG, Boss E, Brickley P, Swift D, Zaneveld R and Strutton P (2006) Long term measurements of physical and optical properties with profiling floats. Ocean Optics XVIII, Conference poster, Montreal, Quebec

Voss K and Morel A (2005) Bidirectional reflectance function for oceanic waters with varying chlorophyll concentration: Measurements versus predictions. Limnol. Oceanogr. 50, 698-705

Voss K, Morel A and Antoine D (2007) Detailed validation of the bidirectional effect in various Case 1 waters for application to Ocean Color imagery. Biogeosci. 4, 781-789

Wang M and Shi W (2005) Estimation of ocean contribution at the MODIS near-infrared wavelengths along the east coast of the U.S.: Two case studies. Geophys. Res. Lett. 32, L13606, doi:10.1029/2005GL022917

Wang M and Shi W (2006) Cloud masking for ocean colour data processing in the coastal regions. IEEE Trans. Geosci. Remote Sens. 44(1), 3196-3105

Wang M and Shi W (2007) The NIR-SWIR combined atmospheric correction approach for MODIS ocean color data processing. Opt. Express, 15(24), 15722-15733, doi:10.1364/OE.15.015722.

Wang M and Shi W (2008) Satellite observed blue-green algae blooms in China's Lake Taihu. EOS Trans. AGU, 89(22), 201-202, doi:10.1029/2008EO220001

Wang M and Shi W (2011) Water property monitoring and assessment for China's inland Lake Taihu from MODIS-Aqua measurements. Remote Sens. Environ. 115, 841-854.

Wang M, Bailey S and McClain CR (2000) SeaWiFS provides unique global aerosol optical property data. EOS Trans. AGU, 81, 197-202

Wang M, Knobelspiesse KD and McClain CR (2005) Study of the Sea-Viewing Wide Field-of-View Sensor (SeaWiFS) aerosol optical property data over ocean in combination with the ocean color products. J. Geophys. Res. 110, 10.129/2004JD004950

Wang M, Son S and Shi W (2009) Evaluation of MODIS SWIR and NIR-SWIR atmospheric correction algorithms using SeaBASS data. Remote Sens. Environ. 113, 635-644

Wang DP, Vieira MEC, Salat J, Tintoré J and La Violette PE (1988) A shelf/slope frontal filament off the north east Spanish coast. J. Mar. Res. 46, 321-332